Fall 2011

Application of polymers in nucleic acid delivery

Dahai Jiang
University of Iowa

APPLICATION OF POLYMERS IN NUCLEIC ACID DELIVERY

by

Dahai Jiang

An Abstract

Of a thesis submitted in partial fulfillment
of the requirements for the Doctor of
Philosophy degree in Pharmacy
in the Graduate College of
The University of Iowa

December 2011

Thesis Supervisor: Associate Professor Aliasger K. Salem

ABSTRACT

Gene therapy and immunotherapy are powerful techniques in the treatment of many life threatening diseases. The major challenge in these therapies is to seek a safe and efficient delivery carrier for gene and antigen materials. Carriers are designed to protect these molecules from degradation, improve their stability and facilitate the delivery of them to the site of action. This research study aims to develop appropriate carriers for small interferencing RNA (siRNA), DNA, antigen and ajuvant respectively.

In the case of siRNA, material encompassing mannose, polyethylene glycol (PEG) and polyethylenimine (PEI) was investigated. Two structures were assembled: in one construct, mannose was conjugated to PEI directly (Mannose-PEI-PEG) whilst in a second construct; the mannose was conjugated to PEI via a PEG spacer (PEI-PEG-mannose). Confocal microscopy images suggested a faster escape and release of siRNA into the perinuclear region when siRNA was complexed with mannose-PEG-PEI. Mannosylation and PEGylation generated significant toxicity reduction compared to unmodified PEI alone. Real-time polymerase chain reaction (RT-PCR) results showed a significant decrease on mRNA knockdown when using modified PEIs. It was found that PEI-PEG-mannose was a stronger candidate for siRNA delivery because it displays lower toxicity, higher uptake efficiency and higher relative knockdown efficiencies.

In the case of pDNA delivery, dextran was introduced to reduce the toxicity generated by PEI. PEI 2000 was more effective than PEI 800 in condensing DNA and inducing transfection when incorporated with dextran. The toxicity of dextran-PEI was greatly reduced when compared to unmodified PEI. Dextran-PEI was able to generate significantly higher transfection efficiencies than PEI alone in the presence of serum. An

improved stability of complexes in serum by dextran-PEI was noticed along with a faster release of complexes to the perinuclear region of cells after endocytosis. These observations help to account for the higher efficiency of dextran-PEI in gene transfer.

In our final study on vaccines, we utilized cationic polyamidoamine (PAMAM) dendrimer polymers to modify biodegradable particles for enhanced delivery of antigens and adjuvants. Vaccines were formulated by loading CpG oligonucleotide (CpG ODN) and ovalbumin (OVA) into biodegradable microparticles. In one group, OVA and CpG were conjugated together and then loaded into the PLGA microparticles. In other groups, CpG was loaded into the particles and OVA bound to the surface and finally particles were prepared that were loaded with OVA and surface modified with cationic PAMAM dendrimers to electrostatically bind CpG ODN. The microparticles were able to provide sustained release of antigen and adjuvants over 14 day's course. The up regulation of CD86 and H2Kb indicated strong activation of DC and therefore strong induction of CD8+ T-cells. MHC II markers were not as significantly affected. Particles loaded with OVA and surface bound CpG ODN ((OVA)-CpG) showed the highest cytotoxic CD8+ T cell response, suggesting that formulation is optimal for vaccine applications.These observations were further supported by IgG1 and IgG2a antibody levels in mice sera.

Abstract Approved: _____
Thesis Supervisor

_____
Title and Department

_____
Date

APPLICATION OF POLYMERS IN NUCLEIC ACID DELIVERY

by

Dahai Jiang

A thesis submitted in partial fulfillment
of the requirements for the Doctor of
Philosophy degree in Pharmacy
in the Graduate College of
The University of Iowa

December 2011

Thesis Supervisor: Associate Professor Aliasger K. Salem

Graduate College
The University of Iowa
Iowa City, Iowa

CERTIFICATE OF APPROVAL

_____

PH.D. THESIS

_____

This is to certify that the Ph.D. thesis of

Dahai Jiang

has been approved by the Examining Committee
for the thesis requirement for the Doctor of Philosophy
degree in Pharmacy at the December 2011 graduation.

Thesis Committee: _____
Aliasger K. Salem, Thesis Supervisor

_____
Mickey Wells

_____
Gary Milavetz

_____
Liu Hong

_____
Mahfoud Assem

To my parents

ACKNOWLEDGMENTS

I would like to convey my thanks to those people who made this thesis possible.

First I would like to express my gratitude to my advisor Dr. Aliasger K. Salem for his generous support, wholehearted help and thoughtful guidance throughout the Ph.D. candidature.

I would like to thank the many people who have ever worked with me in the lab. I am grateful to Aiman Abbas, Janjira Intra, Jessica Graham, Yogita Krishnamachari, Megan Pearce, Caitlin Lemke, Sean Geary, Vijaya Joshi, Sheetal D'mello, Amaraporn Wongrakpanich, and Denison Kuruvilla.

I am also grateful to my former colleagues in Singapore for timely assistance and critical information provided. I would like to thank Yupeng Ren, Cheng Li, Min Huang, Yun Mo, Wenxia Zhang, Hong Wu, Chunxia Wang and Weiqiang Chen.

I am indebted to my alumni and colleagues for providing kind help, encouragement, company and advice. Zhuming Sun in Texas, Jin Xu in Tenessee, Guodong Zhu in Georgia, Bin Zhu in Arkansas, deserve special mention.

Lastly and most notably, I would like to thank my parents, Zhizhong Jiang and Fengyin Tao. To them I dedicate this thesis.

.

ABSTRACT

Gene therapy and immunotherapy are powerful techniques in the treatment of many life threatening diseases. The major challenge in these therapies is to seek a safe and efficient delivery carrier for gene and antigen materials. Carriers are designed to protect these molecules from degradation, improve their stability and facilitate the delivery of them to the site of action. This research study aims to develop appropriate carriers for small interferencing RNA (siRNA), DNA, antigen and ajuvant respectively.

In the case of siRNA, material encompassing mannose, polyethylene glycol (PEG) and polyethylenimine (PEI) was investigated. Two structures were assembled: in one construct, mannose was conjugated to PEI directly (Mannose-PEI-PEG) whilst in a second construct; the mannose was conjugated to PEI via a PEG spacer (PEI-PEG-mannose). Confocal microscopy images suggested a faster escape and release of siRNA into the perinuclear region when siRNA was complexed with mannose-PEG-PEI. Mannosylation and PEGylation generated significant toxicity reduction compared to unmodified PEI alone. Real-time polymerase chain reaction (RT-PCR) results showed a significant decrease on mRNA knockdown when using modified PEIs. It was found that PEI-PEG-mannose was a stronger candidate for siRNA delivery because it displays lower toxicity, higher uptake efficiency and higher relative knockdown efficiencies.

In the case of pDNA delivery, dextran was introduced to reduce the toxicity generated by PEI. PEI 2000 was more effective than PEI 800 in condensing DNA and inducing transfection when incorporated with dextran. The toxicity of dextran-PEI was greatly reduced when compared to unmodified PEI. Dextran-PEI was able to generate significantly higher transfection efficiencies than PEI alone in the presence of serum. An

improved stability of complexes in serum by dextran-PEI was noticed along with a faster release of complexes to the perinuclear region of cells after endocytosis. These observations help to account for the higher efficiency of dextran-PEI in gene transfer.

In our final study on vaccines, we utilized cationic polyamidoamine (PAMAM) dendrimer polymers to modify biodegradable particles for enhanced delivery of antigens and adjuvants. Vaccines were formulated by loading CpG oligonucleotide (CpG ODN) and ovalbumin (OVA) into biodegradable microparticles. In one group, OVA and CpG were conjugated together and then loaded into the PLGA microparticles. In other groups, CpG was loaded into the particles and OVA bound to the surface and finally particles were prepared that were loaded with OVA and surface modified with cationic PAMAM dendrimers to electrostatically bind CpG ODN. The microparticles were able to provide sustained release of antigen and adjuvants over 14 day's course. The up regulation of CD86 and H2Kb indicated strong activation of DC and therefore strong induction of CD8+ T-cells. MHC II markers were not as significantly affected. Particles loaded with OVA and surface bound CpG ODN ((OVA)-CpG) showed the highest cytotoxic CD8+ T cell response, suggesting that formulation is optimal for vaccine applications.These observations were further supported by IgG1 and IgG2a antibody levels in mice sera.

TABLE OF CONTENTS

LIST OF TABLES

LIST OF FIGURES

CHAPTER 1: BACKGROUND INTRODUCTION

Gene therapy

Gene therapy is a promising technique in the treatment of life-threatening diseases such as cystic fibrosis[1,2], adenosine deaminase deficiency (ADA deficiency)[3,4], HIV infection[5] and cancer[6]. Many diseases, especially genetic disorders, are closely associated with the absence of specific proteins or enzymes. Hence, the relief of symptoms associated with these diseases if a gene encoding the protein or enzyme was successfully delivered to the patient. In 1990, a four year old girl with severe combined immune deficiency (SCID) caused by ADA deficiency was the first successful case cured by gene therapy[7]. In subsequent years, gene therapies have been applied to other targets such as metastatic melanoma[8], myeloid cells[9], organ transplant rejection[10] and retinal diseases[11] with satisfying results. However, gene therapy is not completely risk free. Four of nine patients receiving gene therapy against ADA-SCID developed leukemia-like conditions[12,13]. Besides, the death of a patient in a clinical trial for crosslinked SCID (X-linked SCID) further reminded the public of the safety concerns associated with gene therapy[14]. Improving safety and efficacy of gene therapies is a critical direction for researchers because the ultimate goal is to apply new therapies in the clinic.

The materials used in gene therapy are usually nucleic acids. These nucleic acids, whether DNA or RNA, are large in size, susceptible to degradation, and anionic in nature. Because of these features, direct delivery of gene materials to pathological sites is extremely challenging in practice. Exogenous assistance is indispensible to facilitate successful delivery of gene materials and thus the effectiveness of gene therapy. Physical

manipulations such as direct injection[15], gene gun[16] and electroporation[17] have been reported to ease the gene transfer process. These physical methods increase the permeability of cell membrane directly or indirectly to facilitate the transportation of DNA into cells.

Viral vectors used in gene delivery

In addition to physical methods, both viral and non-viral delivery methods were also investigated. Viral vectors aim to take advantage of the natural capability of viruses to transport their genetic material into host cells. After million years of evolution, viruses have adapted to allow for efficient infection and replication in mammalian cells. Adenoviruses are representative viral vectors that were selected for evaluation in clinical trials. One primary reason is that adenovirus infections with symptoms such as cold, tonsillitis and bronchitis are commonly seen in adults so they have moderately less safety concerns than other viruses.

The human adenoviruses are non-enveloped double stranded DNA viruses. They contain a linear genome of 36 kb[18]. The interaction between the virus fiber protein and the specific host cell receptor on the surface initiates attachment of the virus to the cell [19]. After binding to the cell surface, adenoviruses are internalized via receptor mediated endocytosis into clathrin-coated pits. Escape from the endosome to the cytoplasm before enzymatic degradation is essential for subsequent replication. The pH in the lumen of the endosome is maintained at 5 by H^+ATPase[20]. The dramatic pH change from the neutral to the acidic region induces conformational changes in the adenovirus capsid and results in rupture of the endosomal vesicle membrane[20,21].

Recombinant adenoviruses are replication deficient and simply serve as efficient vehicles for exogenous gene transfer[22]. There are several major benefits associated with the use of adenovirus based vectors. They are able to infect both replicating and differentiated cells, which is clinically important because target cells may not be actively dividing. The transfection efficiency is generally very high. Unlike retroviruses, adenovirus genomes do not integrate into the host genome and only induce transient expression of the foreign gene. However, one drawback is that adenoviruses can cause inflammatory responses which eliminate infected cells by effector cells, cytokines and chemokines[23]. The production of neutralizing antibodies also interferes with the efficacy of the adenovirus vector, especially with patients receiving repeated treatments. Another drawback is that hepatic toxicity has been observed following administration of adenovirus based vectors[24]. In general, though, adenoviruses are the most intensively studied viral vectors and have shown an excellent safety record. Several other viral vectors such as adeno-associated viruses[25], lentiviruses[26] and retroviruses[27] are also under studies.

The main concern regarding the use of viral vectors in clinical trials is safety issues including the risk of mutation and inflammatory responses[28,29]. Other drawbacks of viral vectors such as limited gene carrying capacity and the high cost of manufacturing are often noted as well.

Non-viral vectors used in gene delivery

Non-viral vectors are less likely to cause the aforementioned problems[30,31]. Compared to viral vectors, non-viral vectors are more amenable to manufacturing, not limited by cargo size, and raise much less inflammatory or carcinogenic concerns, but

often more toxic. Most studies evaluating non-viral carriers focus on cationic polymers and lipids[32-35].

Cationic lipsomes are made with lipids and gene materials. These lipids consist of a cationic head for DNA binding and a hydrophobic chain for membrane fusion to deliver genes into cells. Liposomes are double layer spheres in structure, with the lumen inside and surface outside loaded with genetic material. By this way, cationic liposomes can protect genes from degradation and promote surface adhesion to cells by electrostatic interaction. In most cases, helper lipids such as dioleoylphosphatidylethanolamine (DOPE) are included in formulations to increase transfection efficiency. DOPE can form bilayer liposomes when used with other cationic lipids. However, DOPE adopts non-bilayer formation at neutral pH, suggesting the possibility of cell membrane destabilization upon contact with cationic liposomes, thus allowing for cytoplasmic delivery.

Cationic polymers interact with DNA by electrostatic forces, and condense DNA into particulate complexes at appropriate nitrogen/phosphate (N/P) ratios. The complexes formed with polymers and DNA should carry a net positive charge, which enable charge interactions between complexes and the cell membrane. The positively charged complexes can induce endocytosis and transport foreign genes into endosomes/lysosomes. Because there is no hydrophobic fragment in the structure of cationic polymer, it is unlikely that polyplexes destabilize the endosomal membrane and escape into cytoplasm. As exemplified by the case poly-L-lysine, low transfection efficiency was usually observed without the assistance of endosomalytic agents such as deactivated adenovirus and chloroquine. Other polymers such as polyethyleneimine can act as a proton sponge

and induce the swelling and rupture of endosomes by themselves. After dissembly of complexes and rupture of endosomes/lysosomes, gene materials are then released into the cytoplasm and eventually reach the nuclei. Commonly used cationic polymers in gene delivery include but are not restricted to poly-L-lysine, chitosan, polyamidoamine and polyethyleneimine.

Polyethyleneimine (PEI)

Several cationic polymers have been developed and tested as gene carriers over the past decades[35-41]. Among them, PEI is one of the most efficient and well studied materials. PEI is a synthetic polymer composed of ethylene imine monomers. The chemical structure of PEI can be linear or branched. Linear PEI consists of two amine types: primary and secondary, whereas branched PEI contains all three amines including tertiary amines. PEI has even been used in waste water treatment during pulp manufacture[42]. Since the 1990s, PEI has been used as a gene carrier because of its polycationic characteristics[43-47]. PEI is able to condense naked DNA and form polyplexes at appropriate N/P ratios. Both linear and branched PEI showed high transfection efficiencies in gene delivery studies[48]. It has been observed that linear PEI is more efficient than branched PEI *in vivo* because the reduced complexation allows for more efficient dissociation of complexes[49]. Branched PEI, however, showes higher transfection efficiencies *in vitro* because of its stronger condensation properties[50].

The superior transfection efficiency of PEI is believed to be at least partially explained by the proton sponge effect[51,52]. The proton sponge effect describes the phenomena of endosomes/lysosomes and rupture after endocytosis of PEI/DNA complexes. The secondary amines in PEI has a pKa of 5.5[53], they constitute a buffering

system along with primary amines and tertiary amines in endosomes. It was observed that the uptake of PEI/DNA polyplexes was followed with an influx of counter-ions such as chloride that results in swelling of the endosomes[54]. The osmotic pressure difference could be the primary reason for endosomal rupture.

Toxicity of PEI

Although PEI is highly efficient in transfection, toxicity is one of the major drawbacks of using PEI in biomedical applications. The mechanism for toxicity induced by PEI is not fully understood yet, but it is believed that the charge interaction between PEI and the cell membrane plays an important role in toxicity development at the cellular level[55]. Cell apoptosis was induced by PEI-mediated membrane damage as shown by time-dependent decrease of mitochondrial membrane potential[56]. PEI is also able to interact with serum proteins and cause aggregation that can eventually lead to capillary embolism[49].

The toxicity of PEI is dependent upon its concentration, architecture and molecular weight[57,58]. In general, lower molecular weight (MW) PEI is less toxic than higher MW PEI, and leads to lower transfection efficiencies[59]. Reduced toxicity were observed on conjugate where small size PEI units were assembled into a larger and degradable structure[60]. A previous study has described the conjugation of PEI 800 into 14-30 kDa architectures using 1,3-butanediol diacrylate as the linker. The lowest cytotoxicity was observed on the conjugate with the fastest ester hydrolysis rate[61]. Moreover, the toxicity of PEI can be reduced by chemical modifications such as PEGylation. PEGylation involves that attachment of non-ionic units to PEI and also decrease the charge density of PEI[62].

Modified PEI used in gene delivery

PEI is an excellent choice for a basic building block in the design of gene carriers because of its high efficiency and abundant amino groups are amenable to conjugation[45,46,63-68]. Further improvements in the transfection efficiency generated by PEI can often be achieved after conjugation of a cell binding ligand to PEI, thereby enabling ligand-receptor mediated endocytosis. Modifications on PEI such as PEGylation are also expected to help reduce toxicity, which is another major reason for developing modified PEI as gene carriers.

Transferrin and antiCD3 antibodies were early examples in the construction of modified PEI carriers for gene delivery[69]. The intention was to make use of the transferrin receptors on K562 cells, and CD3 molecules on T cells. Folate receptors are commonly used in targeted delivery, as exemplified by folate-PEI conjugates prepared to deliver a reporter gene pCMV-Luc[70]. Galactose receptor was utilized in hepatocytes targeting in the case of PEI-galactose conjugate[71,72]. Peptide ligands such as epidermal growth factor (EGF) [73] and RGD[74] have also been linked to PEI for receptor mediated target delivery.

In addition to toxicity reduction, PEGylation on PEI can also decrease transfection efficiencies[70]. Therefore, conjugation of PEG and ligands in combination are desirable to achieve high delivery efficiency and keep low toxicity at the same time[70,71,74]. A hydrophilic layer around complexes is formed after PEGylation. This PEG layer is reported to reduce interactions between complexes and opsonin proteins in serum by steric repulsion, making the complexes stealthy to the reticuloendothelial system (RES). A longer circulation half life of complexes is expected when using PEGylated PEI in

comparison to unmodified PEI. A prolonged circulation half life is usually favorable because nonspecific endocytosis by phagocytes is minimized allowing for maximal delivery of complexes to target sites.

RNA interference (RNAi) and small interferencing RNA (siRNA)

RNA interference (RNAi) is a newly discovered technique that holds great potential in gene therapy. RNAi is a natural mechanism found in *Caenorhabditis elegans* where mRNA is destroyed by the complementary sequence double stranded RNA (dsRNA)[75]. This discovery affords the possibility of regulating the expression of a specific gene at the post-transcriptional level. In contrast to traditional gene therapy which introduces exogenous gene materials into the host nuclei, RNAi makes little change to the host genome and is more specific to the target gene. Therefore, it minimizes the safety risk in gene therapy.

The process of RNAi includes multiple steps. dsRNA was first subjected to an enzyme called dicer[76,77], which cleaved dsRNA into siRNA sequences that were about 20 base pairs (bp) in length. SiRNA was further untwisted into two strands by helicase. One of them named the guide strand was incorporated into the RNA induced silencing complex (RISC), which was bound to the target messenger RNA (mRNA) and then initiated degradation of the mRNA[78]. This process led to a significant reduction in the expression level of a specific gene and this was achieved as a direct result of mRNA loss. Biomedical research studies found that dsRNA could be an agonist to TLR3 and induce immune response such as IFN-1 and protein kinase activation[79,80]. Therefore, dsRNA was replaced with siRNA, which is the fragment produced by dicer from dsRNA. The use of

siRNA provides a convenient tool in regulating particular gene expression with reduced adverse side-effects.

siRNA is generally 21-27 bp in length and double stranded RNA. Delivery of siRNA to target cells is required to initiate the RNAi process. In biomedical research, siRNA is usually customized and synthesized to target specific genes. Similar to other nucleic acids, siRNA is relatively large, hydrophilic and anionic. Direct delivery of siRNA unsurprisingly typically results in low gene knockdown efficiencies. Research is therefore currently focused on developing appropriate carriers to facilitate siRNA delivery.

Carriers used in siRNA delivery

An ideal carrier will protect siRNA from enzymatic degradation, induce endocytosis and promote gene silencing. Many ideas and techniques used in siRNA delivery were adopted from previous experiences in plasmid DNA delivery. Both viral and non-viral vectors used in gene delivery have also found their applications in siRNA delivery.

Viral vector such as lentivirus was used to transfer siRNA to induce gene silencing in human CD34+ cells[81], and inhibit influenza virus replication[82]. Following the same concept in gene delivery, polymeric carrier RGD-PEG-PEI was developed to deliver siRNA inhibiting the expression of vascular endothelial growth factor receptor-2 (VEGF R2), and thus interfering with cancer angiogenesis[83]. Other cationic polymers such as polyamindoamine (PAMAM) G5 was conjugated to TAT peptide and used as an siRNA carrier[84]. Liposomes[85] and poly(lactic-co-glycolic acid) (PLGA)[86] have also been utilized for delivery of siRNA.

Polyamidoamine (PAMAM)

Another type of cationic polymer that is receiving more attention in the gene and drug delivery area is the polyamidoamine (PAMAM) dendrimer. The term dendrimer refers to a branched structure constructed with repeating units. PAMAM is a representative cationic dendrimer used in gene delivery[87,88]. The size of PAMAM is marked by layers or generations of repeating units in the structure. Each additional layer of graft adds around 10 angstroms to the size and doubles the surface amino groups on the PAMAM molecule. For example, PAMAM generation 3 (G3) has a MW of 3,256, is 10Å in size and has 32 surface amino groups. PAMAM G4 has a MW 6,909, is 45Å and has 64 surface amino groups. By chemical reactions, PAMAM can be built up layer by layer with increasing generations. Because PAMAM is a sphere-like macromolecule with positive charges distributed on the outmost surface, it affords the possibility of binding negatively charged DNA and facilitating gene transfer. PAMAM can interact with DNA electrostatically and protect DNA from nuclease degradation[89]. Compared to PEI, PAMAM can provide both high transfection efficiencies and degradable structures[90-92]. It has also been reported that PAMAM is a non-immunogenic and biocompatible material[93]. Similar to PEI, PAMAM is toxic but its toxicity is correlated to its size or generation.

Application of PAMAM in gene and drug delivery

Because of the periodic structure of PAMAM, it provides unique capabilities for drug and gene delivery. In 2000, a pioneering study explored the use of PAMAM in gene transfer[94]. PAMAM was able to generate similar transfection efficiencies as PEI and polylysine, but at a lower toxicity. In subsequent years, PAMAM and PAMAM conjugates have been extensively studied for gene transfection[95-97]. As mentioned above,

PAMAM has also found its application in siRNA delivery[84,98-100]. For some drugs with low solubility such as nifedipine, PAMAM is able to increase its solubility[101]. It is believed that the cavity in the dendrimer structure provides space and hydrogen bonding formation to nifedipine so that an improved solubility is observed. A similar result has been found with niclosamide, whose solubility is significantly higher in the presence of PAMAM[102]. A proportional increase in the solubility of sulfamethoxazole was produced by addition of PAMAM G3[103].

PLGA microparticles used in vaccine delivery

PLGA is a co-polymer composed of lactic acid and glycolic acid monomer units. Unlike many other synthetic polymers, PLGA is biodegradable and biocompatible, and the degraded fragments are nontoxic. PLGA has been studied intensively for drug delivery and tissue engineering applications. PLGA can be fabricated into microparticles of defined sizes loaded with drug molecules. Vaccines when formulated as PLGA microparticles are proposed to simulate the natural pathogen and stimulate innate immune responses of the human body. In addition, PLGA microparticles can protect antigens from degradation, enhance the uptake by dendritic cells and provide sustained release over time. In addition, co-delivery of antigen and adjuvants such as Cytosine-phosphodisester-guanine oligodeoxynucleotide (CpG ODN) can trigger significantly greater antigen-specific immune response than delivering antigen alone. Therefore, logical approach to enhancing vaccine induced immune responses is to load antigen and adjuvant into the microparticles. The simulation of intracellular bacteria is supposed to initiate Type 1 helper T cells (Th-1) type responses that can lead to the proliferation of cytotoxic T cells. CpG ODN is able to trigger Th-1 type responses when delivered with

antigen. PLGA microparticles loaded with antigen and CpG are therefore predicted to be able to generate stronger Th-1 type immune responses than delivery of either agent alone. In our studies, we are also interested in whether sequential release of antigen and CpG can be used to optimize the antigen-specific immune response.

Unmethylated cytosine and guanine oligodeoxynucleotides (CpG ODN)

Over years, human beings have developed sophisticated immune mechanisms to fight against invasion of pathogens. Toll-like receptors (TLRs) are important participants in pathogen pattern recognition in the immune system[104]. So far there are ten characterized TLRs in human and each of them is adapted to the recognition of specific ligands[105]. TLR9 recognizes unmethylated cytosine and guanine oligodeoxynucleotides (CpG ODN)[106-108]. The CpG sequence is present in mammalian cells in methylated form. Once CpG ODN is uptaken into endosomes where TLR9 locates[109], the ligand-receptor interaction triggers a complex cytokine cascade, followed by inflammation and antimicrobial reactions. The antigen presenting cells (APCs) that take up CpG also affect other immune cells and induce phagocytosis by macrophage via specific signaling pathways.

Numerous studies on animals have demonstrated that co-delivery of antigen and CpG ODN is able to generate stronger immune responses than antigen alone[110-115], highlighting its potential as a vaccine adjuvant in immunotherapy. For example, fungal infections in mice treated with CpG ODN resulted in significantly higher survival rates[116]. Antibody titers 4 and 6 weeks after administration were significantly higher in mice receiving the HBV vaccine and CpG than vaccine only[117]. Because CpG is a short nucleotide sequence, it also faces similar challenges to delivery as siRNA. An area of

research that requires further investigation is therefore the development of systems that can protect CpG from degradation and facilitate endocytosis of CpG at the same time.

Objectives

The overall objective is to develop a safe and efficient carrier system for nucleotides and antigens.

For siRNA delivery, a tri-component polymer material consisting of mannose, PEG and PEI will be designed, prepared and tested. Mannose will serve as the ligand and mediate cell specific endocytosis. PEG provides steric stabilization and is expected to impart stealth properties to the polymer/siRNA complexes and extend their circulation half-life, reducing non-specific endocytosis by the RES system. PEI is the cationic backbone that allows for electrostatic complexation with siRNA, protects siRNA from degradation and promotes gene knockdown. In this study, we will evaluate the impact of the location of the mannose ligand on the constructs. In the first construct, we have a PEG as a spacer between the PEI and mannose. In the second construct, both PEG and mannose are directly linked to PEI.

For plasmid DNA delivery, dextran will be used to reduce the toxicity of PEI and aggregation of PEI/DNA complexes in serum. A conjugate polymer made with PEI and dextran will be synthesized. PEI will serve as core cationic structure for DNA binding and gene transfer. The dextran-PEI conjugate is expected to provide high transfection efficiencies at lower toxicity levels relative to PEI alone, and show improved stability in serum-present conditions.

For antigen and CpG oligonucleotide delivery, PLGA microparticles loaded with chicken ovalbumin (OVA) and CpG ODN 1826 will be fabricated. OVA serves as a

model antigen in the study to evaluate antigen-specific immune responses. CpG 1826 is used to bind TLR9 receptor and stimulate polarized Th-1 type immune responses. OVA and CpG will be loaded into PLGA microparticles by several methods to determine if sequential release of antigen and adjuvant from microparticles can be used to optimize the immune response.

CHAPTER 2: DEVELOPMENT OF PEI-PEG-MANNOSE TRI-COMPONENT MATERIAL AS siRNA CARRIER

Introduction

As a cationic polymer, PEI is able to electrostatically interact with nucleic acids and form complexes at appropriate nitrogen to phosphate (N/P) ratios. N/P values estimate the relative amounts of cationic polymers and DNA unitsAn N/P value more than 1 is generally required to ensure high efficiency of gene transfer by PEI. Compared to linear PEI, branched PEI shows even higher efficiency among *in vitro* tests. In the structure of branched PEI, the molar ratio of primary amine, secondary amine and tertiary amine is 1:2:1[118]. The pKa of secondary amine in PEI was reported as 5.5[53], which is close to the value of pH 5 in endosomal vesicles[119]. This proximity in pKa values maximizes the buffering capacity of PEI when PEI/DNA complexes were endocytosed. The influx of chloride was observed after endocytosis of PEI/DNA complexes, which initiated swelling and rupture of endosomes at a later stage. This finding provided supporting evidence to the proton sponge hypothesis[54].

The application of PEI is usually limited by its toxicity. Numerous studies have focused on engineering methods to alleviate this weakness. A common approach is to reduce the number of free primary amino groups on PEI and thus decrease the charge density. PEG chains are non-ionic and hydrophilic, and have been employed to shield excessive positive charges of PEI. PEGylation has also been shown to reduce the toxicity of PEI[120]. The other benefit of PEGylating PEI is to reduce non-specific endocytosis by reticuloendothelial system (RES), which filters and remove particles from the

bloodstream by size screening[121]. If the target organ or tissue is other than RES, increasing the circulation half time can significantly increase the efficiency of gene delivery[122]. Because of the filtration of the RES, particles not shielded with PEG can be removed from the bloodstream within seconds to minutes. A minimum MW of 2 kDa of PEG is required to provide appropriate stealth shielding effects on the particles[123]. The toxicity of PEG is negligible compared to PEI.

In this collaborative study with Najung Kim who did biological tests of siRNA, a tri-component material was designed and tested. Our long term interest focuses on modulation of antigen presenting cells (APC) especially dendritic cells and macrophages. A ligand with specificity for these cells was preferred to attempt targeted delivery. A common receptor on macrophages is the one for mannose, whose receptor can also be found on APC and liver cells[124,125]. For this reason, the goal in this study was to build a carrier system consisting of PEI, PEG and mannose and identify the impact of the location of mannose on the construct.

Materials

PEI 25kDa and α-D-mannopyranosylphenyl isothiocyanate (MPITC) were purchased from Sigma-Aldrich (St. Louis, MO, Lot# 047K3786). PEG 2 kDa was purchased from Creative PEGworks (Winston Salem, NC). Sulfuric acid, Dimethyl sulfoxide (DMSO), glacial acetic acid and ethylenediaminetetraacetic acid (EDTA) were purchased from Fisher (Pittsburgh, PA). Bio-Gel P2 was from Bio-Rad (Hercules, CA). Maleic anhydride, toluene, glutaraldhyde 50%, and methanol were also purchased from Sigma (St. Louis, MO). All siRNAs (DS scrambled negative control, RLuc-S1 DS

positive control, Cy-3, NC1 and HPRT) and pDNA (psiCHECK™-2 from Promega, Madison, WI) were kindly provided by Integrated DNA Technologies (Coralville, IA).

Methods

Synthesis of PEI-PEG

PEG 500 mg was dissolved in 10 ml toluene and heated to 100˚C. Maleic anhydride 33 mg was dissolved in 40 ml toluene and slowly added into the PEG solution. The temperature of reaction was increased to 110˚C and refluxed for 12 hrs until all the maleic anhydride was consumed. Toluene was removed using rotary evaporation and the regenerated product was dissolved in 2.5 ml de-ionized (DI) water, followed with purification using a P-2 column. The elution was collected, lyophilized and re-dissolved in 10 ml methanol. A volume of 1 ml methanol solution containing modified PEG was slowly added to the mixture of 50 µl glutaraldehyde 50% w/v solution and 300 µl methanol. The reaction was stopped in 2 hrs and loaded to another P-2 column to remove excessive glutaraldehyde. The elution was immediately added to a 2 ml PEI solution (containing about 150 mg PEI) for overnight conjugation. Finally PEG-PEI was recovered after dialysis for 3 days (MWCO 10,000, Pierce, Rockford, IL) and lyophilized (Labconco FreezeZone 4.5, Kansas City, MO).

Mannosylation on PEI-PEG

PEGylated PEI (prepared as above) was reacted with MPITC solution 80 µl (dissolved in DMSO at 0.125 mg/ml) overnight. The product was recovered similarly after dialysis and lyophilization.

Synthesis of PEI-PEG-mannose

PEG 50 mg was dissolved in 2 ml NaHCO3 buffer (8.516 mg/ml, pH 8.4), then PEG solution was mixed with MPITC solution 80 µl (same as above) for overnight reaction. The resultant mixture was reacted with 50 µl glutaraldehyde (same as above) in 300 µl methanol. The reaction was stopped after 2 hrs and loaded into a P-2 column to remove excessive glutaraldehyde and MPITC. The elution was added to a 2ml PEI solution (containing about 150 mg PEI) for overnight conjugation. Similarly, PEI-PEG-mannose was recovered after dialysis and lyophilization.

^{1}HNMR Spectra

All products were dissolved in 1.0% w/v DCl (Sigma, St. Louis, MO)/D_2O (Cambridge Isotope, Andover, MA) (deuterium chloride diluted using deuterium oxide) at approximately 40 mg/ml and loaded into a Bruker AVANCE 300 MHz NMR spectrometer.

Resorcinol assay

Resorcinol was dissolved in DI at 6 mg/ml and filtered using a 0.45 µm Millipore syringe filter unit. D-(+)-mannose was pre-dried at 100-110˚C overnight before use as a standard. Mannose was prepared at concentrations ranging from 9.0854 to 908.54 µg/ml using 1.0% HAc as a solvent. All products containing mannose were dissolved in HAc at appropriate concentration from 3 to 20 mg/ml. Each test mixture, consisting of 20 µl mannose standard (or sample solution), 20 µl resorcinol solution, 50 µl pristane (Acros Organic, Geel, Belgium) and 100 µl 75% w/v sulfuric acid, was mixed in a 96-well plate's well, gently vortexed for 30 sec, heated at 93˚C for 30 min and cooled down to room temperature for another 30 min. The absorbance was recorded at 480 nm.

Cell culture

Raw264.7 cells (ATCC, Manassas, VA), a murine macrophage cell line that is known to express mannose receptors and typically difficult to transfect, was selected for *in vitro* experiments because macrophages are a potential target for this delivery system. The cells were cultured in Dulbecco's Modified Eagle Medium (DMEM) (Gibco, Grand Island, NY) supplemented with 10% Fetal Bovine Serum (FBS) (Hyclone, Logan, UT), penicillin-streptomycin (100 u penicillin; 100 µg streptomycin/ml, Gibco, Grand Island, NY). The cells were maintained at 37˚C in a humidified, 5% CO2 atmosphere.

Amplification and purification of pDNA

The psiCHECK™-2 (Promega, Madison, WI) is a 6.3 kb pDNA designed to monitor a quantitative measurement of RNAi. It affords two luciferases genes: firefly and renilla. Each gene carries a HSV-TK or SV40 promoter respectively. The firefly reporter gene has been constructed to serve as an intraplasmid standard so that the renilla luciferase signal can be normalized to the firefly luciferase signal. The pDNA was transformed in E.coli DH5α (Invitrogen, San Diego, CA) and amplified in LB broth media at 37˚C overnight on a plate shaker set at 250 rpm. The pDNA was extracted with Wizard Plus Maxipreps DNA Purification System (Promega, Madison, WI) followed by removal of bacterial endotoxin contamination with Endotoxin Removal Kit (MiraCLEAN, Madison, WI) according to the manufacture's guide. Purified pDNA was dissolved in Tri-EDTA buffer and its purity and concentration were determined by UV absorbance at 260/280 nm.

Preparation of PEI-siRNA polyplexes

PEI/siRNA polyplexes were formed at pre-determined N/P ratios (nitrogen in cationic polymer per phosphate in nucleotides), amounts of siRNA and concentrations of polymer solutions. The molar mass of phosphate was used as 325 daltons and nitrogen was 43daltonto calculate N/P ratio. siRNA solution was mixed with polymer solution, vortexed for 20 seconds and incubated for 30 minutes at room temperature before use.

Determination of polyplexes size and zeta potential

siRNA polyplexes solutions were sprayed on silicon wafers using an All-Glass Nebulizer (PELCO, Redding, CA). The silicon wafers were stained with 4% osmium tetraoxide (OsO_4) vapor in the hood overnight and mounted on aluminum stubs using liquid colloidal silver adhesives followed by overnight drying at room temperature. Specimens were observed using SEM (Hitachi S-4800, SN#9131-01). The size of polyplexes was measured using a zetasizer (Malvern Nano ZS, SN#MAL500260). Polyplexes were prepared at a concentration of 1 mg/ml, loaded into a sample cuvette and the scattered light observed at a 173 °angle.

Gel retardation

PEI/siRNA polyplexes were loaded into a 2% agarose gel stained with 0.5 μg/ml Ethidum bromide (EtBr) and run at 60V in Tris-Acetic acid-EDTA (TAE) buffer for 45 min. The bands of gel were visualized on a UV transilluminator (Spectroline, Westbury, NY, SN#1552703). Photos were taken using a digital camera, cropped and resized using ImageJ software (National Health Institute, Bethesda, MD).

Intracellular trafficking

Raw264.7 cells (macrophage) were plated in 8-well chamber slides (Lab-Tek, Rochester, NY) coated using 0.01% w/v poly-L-lysines, at a density of $1.2x10^4$ cells/well and incubated overnight. Lysosomes were stained when cells were incubated using Opti-MEM (reduced serum media)-containing 75 nM Lysotracker Green DND-26 (Molecular Probes, Carlsbad, CA) for 30 min followed with transfection with PEI/Cy-3 labeled siRNA polyplexes in Opti-MEM. At pre-determined time points, cells were washed using PBS and fixed using 4% paraformaldehyde and mounted using DAPI (4',6-diamidino-2-phenylindole)-containing Vectashield mounting medium for nuclear staining (Vector Laboratories, UK). The slides were covered with a coverslip and stored at 4 ℃ in darkness before observation under multiphoton/confocoal microscope (Bio-Rad Radience 2100MP and Zeiss Confocal 710, SN#0186588).

Dual luciferase assay

Raw264.7 cells were seeded in a T25 flask ($6.8x10^6$ cells) on day 0 and incubated overnight. PEI was used to transfect psiCHECK™-2 in Opti-MEM media on day 1 for 4 hrs, then digested using trypsin and transferred to 24-well plates at ($3x10^5$ cells/well). The RLuc-S1 DS positive control siRNA (Integrated DNA Technologies, Coralville, IA), encoding a complementary sequence for renilla luciferase gene in psiCHECK™-2, was transfected using each different polymer in Opti-MEM media on day 2, and cells were incubated for 4 hrs followed by overnight incubation in complete media. On day 3, luciferase gene expression was analyzed using dual luciferase reporter system (Promega, Madison, WI, Lot#0000004492) and Lumat LB 9507 (Berthold Technologies, Bad Wildbad, Germany, ID#81957-52) according to manufacture's userguide. PEI/siRNA and

polymer/siRNA polyplexes were prepared as described above at pre-determined N/P ratios. DS scrambled negative siRNA, non-targeting sequences in human, mouse or rat transcriptome, served as negative control. The renilla luciferase gene expression was normalized to firefly luciferase as internal control expression and expressed as relative gene expression (100% to DS scambled negative transfected with PEI). The data were reported as mean±sd for triplicate samples using Prism software (Graphpad Software Inc, San Diego, CA). Every experiment was repeated at least twice.

Real-time PCR (RT-PCR)

Cells were seeded on 48-well plate ($8x10^4$ cells/well) for endogenous gene knowdown on day 0. NC1 (negative control) and HPRT siRNAs were transfected using each different polymer in Opti-MEM media on day 1 and incubated for 24 hrs. Total RNA was extracted using Promega SV96 total RNA isolation system (Promega, Madison, WI) on day 2 followed with cDNA systhesis and real-time PCR. An amount of 150 ng total RNA was used for reverse transcription with Supercript II reverse transcriptase (Invitrogen, San Diego, CA). cDNA equivalent to 40 ng total RNA was analyzed by real-time PCR in triplicate Immolase polymerase (Bioline, Randolph, MA) on AB7900HT (Applied Biosystems, Carlsbad, CA). The results were reported as mean±sd from triplicate RT-PCR reactions of each triplicate samples using Prism software (GraphPad). Every experiment was repeated at least twice.

Cytotoxicity study

The MTS (3-(4,5-dimethylthiazol-2-yl)-5-(3-carboxymethoxyphenyl)-2-(4-sulfophenyl)-2H-tetrazolium) assay was used to determine the cytotoxicity of tri-component polymer. Following manufacturer's userguide, Raw264.7 cells were seeded to

96-well plates at $5x10^5$ cell/well and incubated overnight. Polymers were dissolved in DMEM media and added to cells, 20 µl MTS solution per 100 µl media was added to each well for further 1-3 hrs incubation at 37 ℃ and 5% CO2 in a humidified incubator. The plate was measured at 490 nm using a UV spectrometer in duplicates. The viability of cells was represented as a percentage to untreated cells and calculated based on a calibration curve.

2.4 Results

^{1}HNMR characterization of tri-component polymer

As listed in Figure 2-1, both PEI-PEG-mannose and PEG-PEI-mannose showed peaks at δ 7.0 (MPITC phenyl-H), δ 3.5 (PEG-CH), and δ 2.6 (PEI-CH), which indicated that all polymers consisted of PEI, PEG and mannose (in MPITC) in the final products. The peak at 7 ppm was relatively weak but confirmed the existence of mannose (in MPITC). Signals at 3.5 ppm and 2.6 ppm were corresponding to the structure of PEG and PEI hydrocarbon chains, respectively. The conjugation ratio was determined based on the peak integration of PEG and PEI. Table 2-1 summarized the results of characterization. In PEI-PEG, the molar ratio of PEI to PEG was 3.704. In PEI-PEG-mannose, this ratio was 1.23. Two PEG-PEI-mannose samples were prepared, and ratios of PEI to PEG were 3.491 and 0.962. The latter one was selected in the following tests because it provided a comparable ratio of PEI/PEG to the PEI-PEG-mannose sample. There was no significant difference between the spectra of PEI-PEG-mannose and PEG-PEI-mannose.

Resorcinol assay in determining mannose content in tri-component polymers

The resorcinol assay is an established method for determining the content of monosaccharides in polymeric structures[126]. The mannose content in our products was

determined using this method after slight modifications for better plate reading on a UV spectrometer. PEI-PEG-mannose was shown to have 0.12 μmol mannose / mg polymer. Two PEG-PEI-mannose samples had 0.81 and 0.19 μmol mannose / mg polymer. Similarly as above, the latter one was selected for the following tests because it had similar mannose content to PEI-PEG-mannose sample. The summary of characterization results were listed in Table 2-1, including PEI/PEG molar ratio derived from peak integration and mannose content derived from resorcinol assay.

Microscopic imagining study of polyplexes formed between polymer and siRNA

A scanning electron microscopy was used to study the surface morphology and shape of the polymer/siRNA polyplexes. The polyplexes without pegylation were spherical or semi-spherical in shape with porous but otherwise smooth surfaces (Figure 2-2 A&C). In contrast, the polyplexes formed with PEGylated material showed coarser surfaces (Figure 2-2 B, D&E). Polyplex sizes were in the range of 60 to 170 nm in diameter. A further checkup using a zetasizer suggested that some of the larger sizes observed by SEM represented clusters of polyplexes formed during the drying process of SEM specimen preparation.

Gel migration of polyplexes

Gel migration was used to confirm the capability of tri-component polymers to condense siRNA into polyplexes. Cationic polymers interact with anionic siRNAs and form complexes. As shown in Figure 2-3, the migration of siRNA on agarose gel was visualized by EtBr under UV light. The formation of polyplexes will retard siRNA from migrating under an electric field. All polymers tested were able to retard the migration of siRNA on agarose gel even at a lower N/P ratio 1. Both PEI-PEG-mannose and PEG-

PEI-mannose showed complete exclusion of EtBr from N/P 1 to 15, suggesting a strong complexation capability with siRNAs.

Endocytosis of tri-component polymers by Raw264.7 cells

The uptake and translocation of polyplexes formed with tri-component polymers and siRNA were visualized using Cy3 florescence labeling. As seen in Figure 2-4, most of the polymer/Cy3-siRNA complexes were internalized into Raw264.7 cells at 2 hrs post-transfection. PEI/siRNA and PEG-PEI/siRNA complexes were taken up by cells and localized in vesicular structures as shown by yellow florescence (the overlapping red and green colors representing lysosomes and siRNA). PEG-PEI-mannose/siRNA was also found in the lysosomes/endosomes. PEI-PEG-mannose/siRNA showed the most uniformed endocytosis distribution among cells. Several images also suggested a strong distribution of polyplexes in the perinuclear region of cytoplasm, as observed by the separation of red and green colors (nuclei in blue).

Real-Time PCR

Endogenous gene knockdown was analyzed using Hypoxanthine-Guanine Phosphoribosyl Transferase (HPRT) siRNA transfection. HPRT is a ubiquitously expressed enzyme and commonly used as a positive control for endogenous gene knockdown experiments. The results of mRNA level were included in Figure 2-5. PEI/siRNA polyplexes resulted in a 68.31% gene expression at N/P 10 and PEG-PEI/siRNA generated a 65.80% remaining expression. Tri-component polymers PEG-PEI-mannose and PEI-PEG-mannose showed a greater reduction to 62.15% and 61.19%, respectively. Mannose-PEI generated a 95.48% gene expression at N/P 10, suggesting a

decrease after mannosylation on PEI. Although PEGylation and mannosylation did generate enhanced knockdown at the mRNA levels, these differences were not significant.

Dual luciferase assay: the influence of PEGylation and mannosylation on knockdown efficiency of PEI

A reporter encoding two luciferase's was used to evaluate the capability of the tri-component delivery system. Raw264.7 cells were transfected with siRNA only against renilla luciferase mRNA, and using the expression of firefly luciferase gene as the internal control. Figure 2-5 shows that renilla luciferase gene expression was decreased by all polymer vehicles for siRNA. PEI was able to reduce renilla gene expression to 33.6% and 18.8% at N/P 3 and 10, respectively. At an N/P ratio of 3, PEG-PEI showed the highest knockdown efficiency of 11.3%. This was significantly lower than 48.2% from the commercial transfection reagent siLenFect. Increasing N/P ratios of PEG-PEI to 10 reduced the knockdown efficiency to 41.4%. PEG-PEI-mannose showed 34.2% and 42.0% knockdown efficiencies at N/P ratios of 3 and 10, respectively. In contrast, PEI-PEG-mannose showed higher knockdown efficiencies of 19.9% and 22.9% at N/P ratios of 3 and 10, respectively.

Cytotoxicity of tri-component polymers

The toxicity of polymers in Raw264.7 cells was evaluated using the MTS assay. As shown in Figure 2-6, PEI showed the highest toxicity at 0.0078 mg/ml, reducing cell viability to 37.5%. PEI-mannose displayed the lowest toxicity with 85.4% cell viability. PEI-PEG showed 79.1% cell viability, comparable to PEI-mannose. PEG-PEI-mannose showed a slightly higher toxicity of 68.9, and PEI-PEG-mannose was 53.9%, which was significantly lower than PEI but higher than PEI-mannose. .

Discussion

Two distinctively different structures of tri-component polymers were designed, prepared, characterized and tested for the use as siRNA delivery vehicles. The idea was to investigate the influence of different assembled structures on the transfection and knockdown efficiency generated by siRNA delivery. PEG, as reported previously[123], was selected for its ability to improve the circulation half-life of polyplexes formed with polymers and siRNAs. The model ligand mannose was used to enhance the uptake of particles by receptor-mediated endocytosis and increased cell binding.

The major difference between the two tri-component polymers is the linking method amongst the respective components. In PEI-PEG-mannose, PEG was simply used as a spacer between PEI and mannose. In mannose-PEI-PEG, both PEG and mannose were directly attached to PEI. The spectra of ^{1}HNMR verified the existence of PEI, PEG and mannose in both tri-component polymers and their peak shifts were consistent with those reported in the literature. A relatively weak signal at 7 ppm was observed for mannose because of its low abundance compared to other components such as PEI and PEG. The resorcinol assay was therefore utilized to confirm and quantify the mannose moieties-.

The density of PEG molecules on the particles surface greatly influences the stealth properties. In the case of PEI-PEG, the molar ratio between PEI and PEG was 3.704 (ratio of monomers), suggesting 3.45 PEG (2 kDa) molecules were attached to 1 PEI (25 kDa) in average. In the case of PEI-PEG-mannose, the ratio of 1.23 was equal to 10.16 PEG molecules on a single PEI. PEG-PEI-mannose sample gave an estimate of 13.3 PEG on a PEI based on its PEI/PEG ratio 0.962. It was reported that about 6 PEG (5

kDa) or 1 PEG (20 kDa) were required to give a satisfactory stealth coating coverage on the surface of PEI/siRNA polyplexes[62,127]. Therefore, other samples showing 3.45-13.3 PEG (2 kDa) are expected to afford a similar PEGylation degree in terms of creating the right level of steric hindrance and stabilization. The content of mannose in PEI-mannose was 0.14 μmol/mg, suggesting 3.4 mannose molecules were attached to 1 PEI (25 kDa) on average. PEI-PEG-mannose had 0.12 μmol/mg, which was 3.0 mannose on a single PEI. PEG-PEI-mannose gave a value of 0.19 μmol/ml, equivalent to 4.7 mannose units on a single PEI. These concentrations of mannose in polymeric structures are expected to lead to significantly higher levels of receptor-ligand binding interactions.

As confirmed using zetasizer measurements, PEI/siRNA polyplexes and PEI-PEG/siRNA polyplexes had 214.57 and 201.80 nm average diameters respectively. Man-PEI-PEG formed polyplexes with siRNA with an average size of 169.10 nm. PEI-PEG-mannose/siRNA polyplexes had an average size of 357.33 nm. In general, particles less than 150-200 nm in size were preferred for efficient endocytosis. Larger particles observed by SEM were probably clusters or aggregates of small particles. PEGylation of PEI resulted in a modest increase in the average particle size. However, the increased size still fell in the range necessary for efficient endocytosis. The mechanism of the size increase was related to attenuated charge interaction between cationic and anionic molecules after peylation. . The use of PEI (25 kDa) was supposed to provide enough condensing capability to siRNA after PEGylation. In gel retardation assays, PEGylated materials were also shown to adequately condense siRNA when compared to PEI alone. In general, N/P ratios of 3 or above were recommended for complete complexation of siRNA using various polymers.

Raw264.7 cells were used for evaluation of gene knockdown efficiency. This cell line is a murine macrophage expressing mannose receptors and difficult to transfect. Confocal microscopy imaging demonstrated the co-localization of polyplexes and endosomes/lysosomes. siRNA is seen as red color due to Cy3 labeling and endosomes/lysosomes were stained with LysoTracker Green. Separation of red and green colors in photos was due to the translocation of siRNA from the endosomes/lysosomes into cytoplasm. Polyplexes were uptaken by cells and localized in the cytoplasm 30 min after transfection. In 2 hrs, polymer labeled with Oregon Green 488 and siRNA labeled with Cy3 were in discrete locations in the cytoplasm, suggesting polyplexes were released from endosomes/lysosomes and had dissociated in cytoplasm. The proton sponge effect generated in the presence of PEI is supposed to allow for cargo release from endosomes and lysosomes. The buffering capacity of PEI in combination with the influx of counter-ions causes swelling and rupture of vesicles. Fluorescent labeling provided an excellent tool to investigate the distribution of polymer and siRNA in cells. Perinuclear localization of siRNA is required for successful gene silencing by interaction with RISC to induce RNAi. The tri-component polymers were able to protect siRNA during transfection and transport siRNA into the cytoplasm. The inclusion of mannose did not improve uptake. One possible reason could be the PEG chain in the structure which was reducing the affinity between polyplexes and cells. In addition, an optimal balance between PEGylation and mannosylation could further improve uptake efficiency.

However, a major strength of this work is that the inclusion of mannose and PEG did not generate a lower knockdown efficiency compared to unmodified PEI. Numerous studies have talked about the advantages of PEGylation and ligand introduction for *in*

vivo applications of polymeric delivery vehicles. Another important benefit gained from PEGylation was toxicity reduction. Compared to mannosylation, PEGylation showed a much more significant toxicity lowering effect. PEGylation is also expected to reduce toxicity caused by aggregation of polyplexes and the resultant capillary embolism that is observed in the systematic administration of unmodified PEI. PEI-mannose did not increase transfection efficiency or greater gene knockdown compared to unmodified PEI. These results were corroborated by intracellular trafficking study results.

The impact of PEG and mannose ligands on binding affinity and gene knockdown efficiency in macrophages has not been well characterized. In our studies, PEI-PEG-mannose showed higher knockdown efficiency as well as higher toxicity on Raw 264.7 cells. The uptake of PEI-PEG-mannose/siRNA polyplexes was more stable than polyplexes prepared using PEG-PEI-mannose. The difference in gene knockdown efficiency is attributed to the structure modification on polymers. In PEI-PEG-mannose, mannose was placed on the tip of PEG chain in and more accessible to receptor relative to PEG-PEI-mannose. In PEG-PEI-mannose, the ligand-receptor interaction could be hindered by PEG molecules. Generally, the introduction of PEG into the structure is expected to reduce the affinity between particles and cells to some degree. The results from the intracellular trafficking study support the hypothesis that PEGylation delayed uptake/endocytosis of the polyplexes. PEI-PEG had higher knockdown efficiency over PEI-PEG-mannose or PEG-PEI-mannose and this was likely linked to the reduced toxicity observed from this polymer relative to other groups at N/P 3.

The knockdown efficiency of the tri-component polymers developed in this study was significantly lower than RNAiMax at targeted mRNA knockdown. Moreover,

TransIT-TKO can routinely generate 80-90% knockdown, which is also significantly more efficient than the modified PEIs. Quantitative gene expression data such as qPCR results were normalized to the expression levels of housekeeping genes used as a control. It relied on the assumption that the expression level of housekeeping genes was constant in cells or tissues. The HPRT housekeeping gene was used in our study as a target for endogenous knockdown.

When compared to another commercial transfection reagent siLentFect, our PEI-PEG-mannose polymers showed significantly higher luciferase knockdown efficiency (data not shown). In addition, both mannose and PEG have been reported to reduce toxicity and increase circulation half-life in previous studies.

Figure 2-1: ^{1}HNMR spectra

A

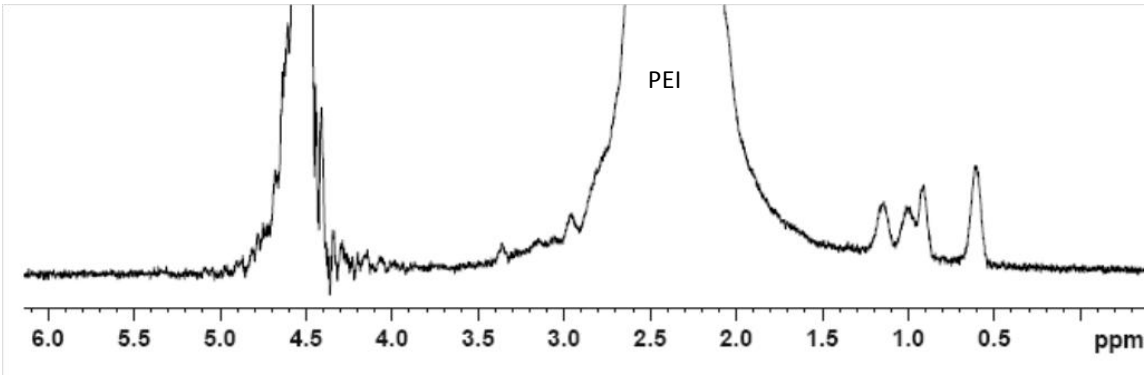

B

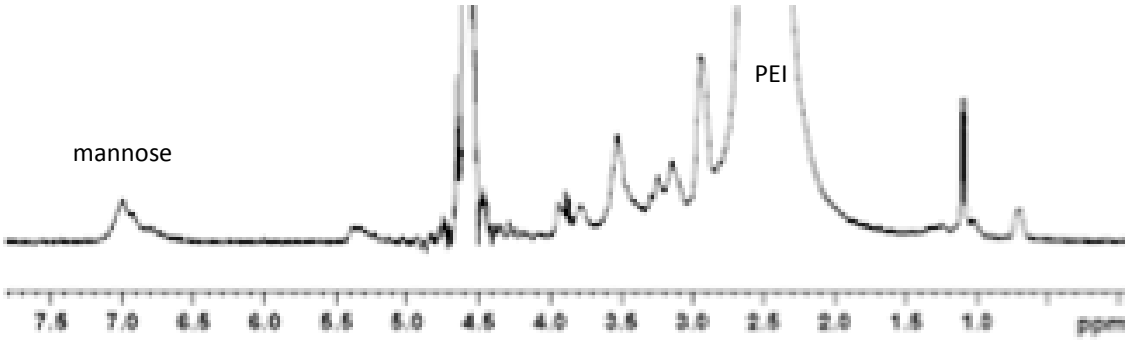

C

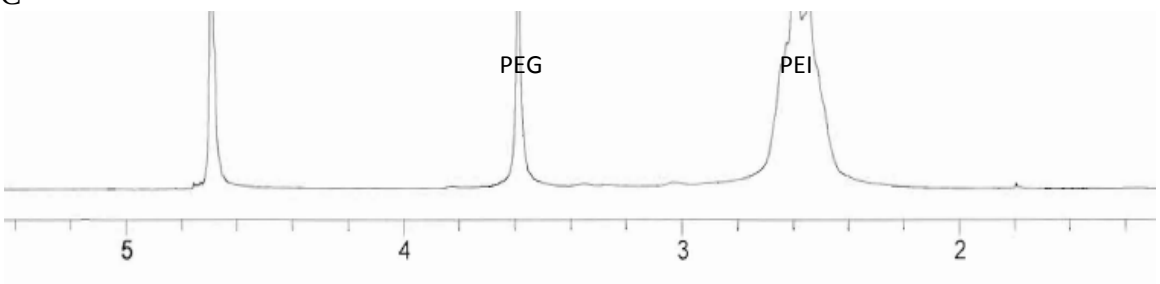

Figure 2-1 continued

D

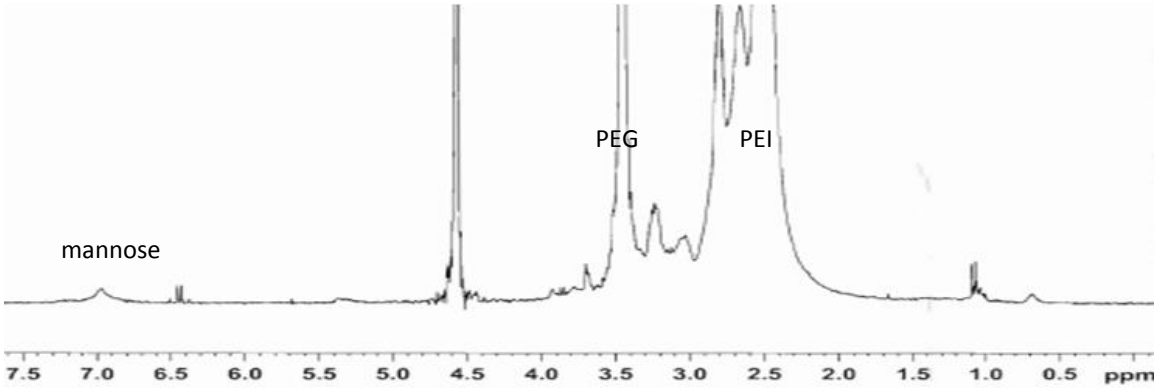

E

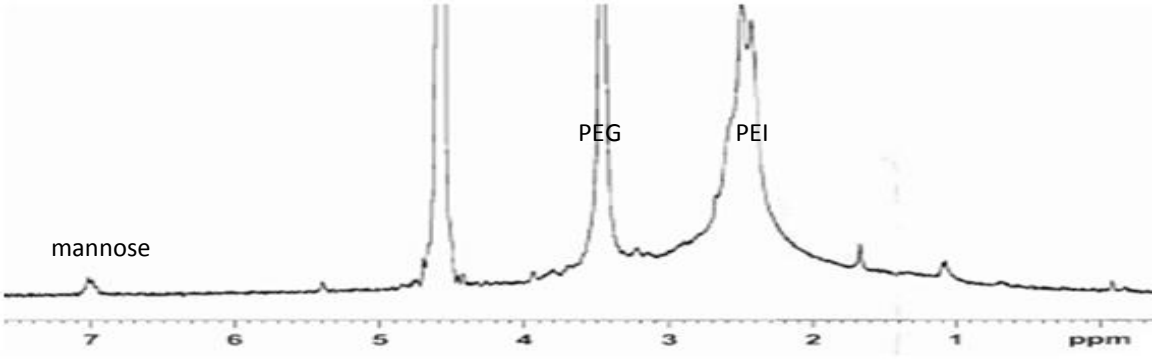

Note: *A*. unmodified PEI δ2.6 (C-H). *B*. Mannosylated PEI δ2.6 (C-H) and mannose at δ7.0 (MPITC phenyl-H). *C*. Pegylated PEI δ2.6 (PEI C-H) and PEG at δ3.5 (PEG C-H). *D*. Mannose-PEI-PEG δ3.5 (PEG C-H), δ2.6 (PEI C-H) and δ7.0 (MPITC phenyl-H). *E*. PEI-PEG-mannose also showed each component at the same peaks as mannose-PEI-PEG

Table 2-1: summary of PEI/PEG molar ratios and mannose content in conjugate polymer

Conjugate polymer	Polymer/PEG molar ratio	Mannose content (μmol/mg)
PEI-mannose	N/A	0.13671
PEI-PEG	3.704	N/A
Mannose-PEI-PEG (#1)	0.962	0.18679
Mannose-PEI-PEG (#2)	3.491	0.81315
PEI-PEG-mannose	1.23	0.12122

Note: the molar ratio was calculated based on the integration of ^{1}H NMR peaks. The content of mannose in μmol mannose per mg polymer was determined using resorcinol assay.

Figure 2-2: Scanning Electron Microscopy

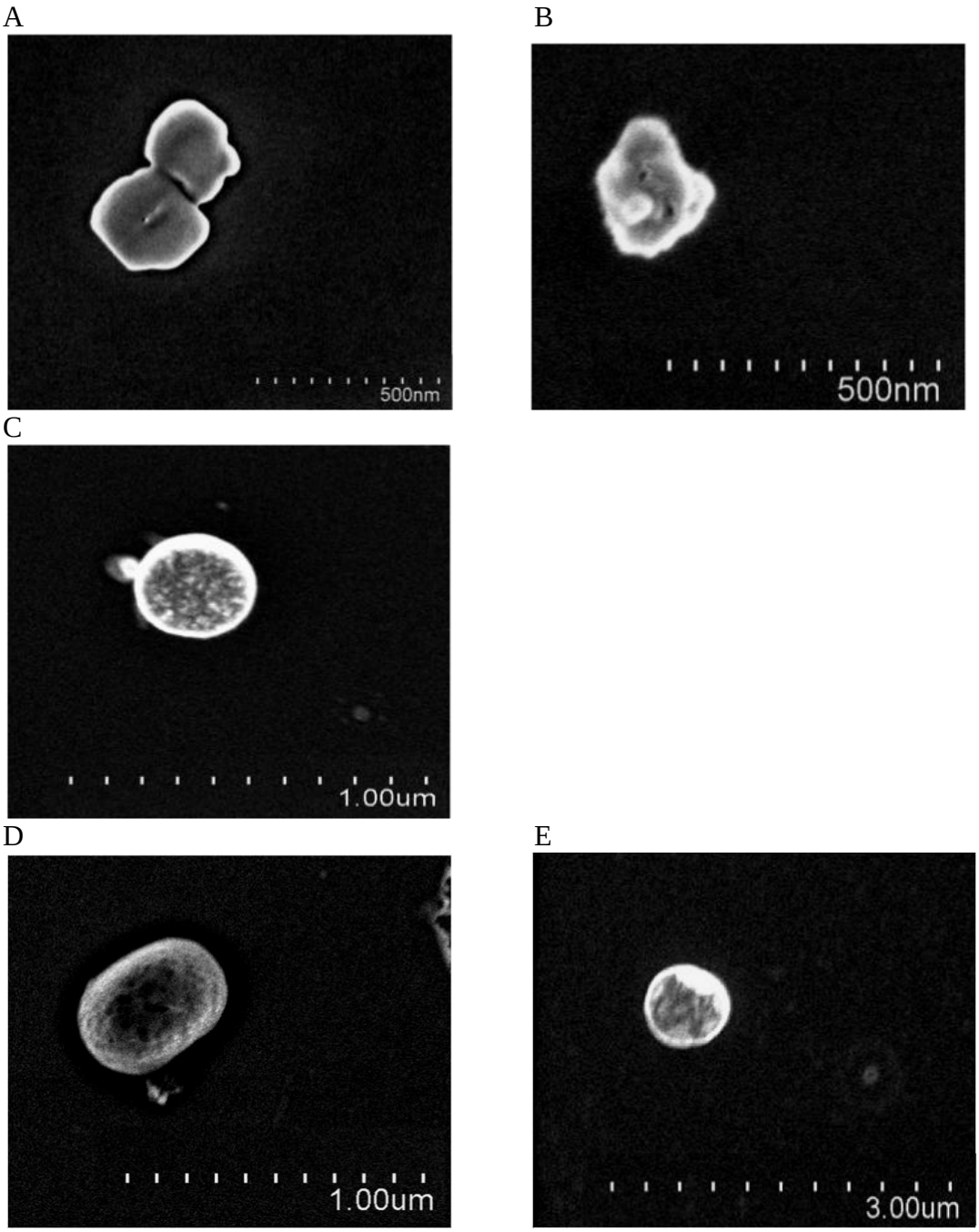

Note: *A*, PEI/siRNA polyplexes, *B*, PEI-mannose/siRNA polyplexes, *C*, PEI-PEG/siRNA polyplexes, *D*, Mannose-PEI-PEG/siRNA polyplexes, *E*, PEI-PEG-mannose/siRNA polyplexes. All the polyplexes were prepared with 1μM siRNA at N/P ratio 5

Figure 2-3: Gel retardation assay

A

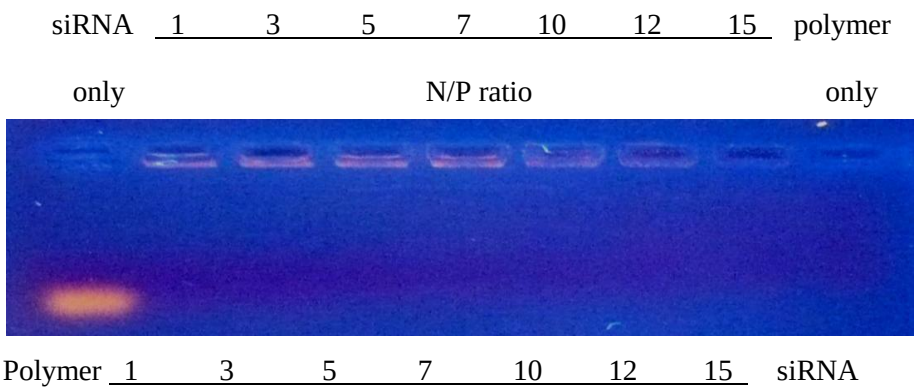

B

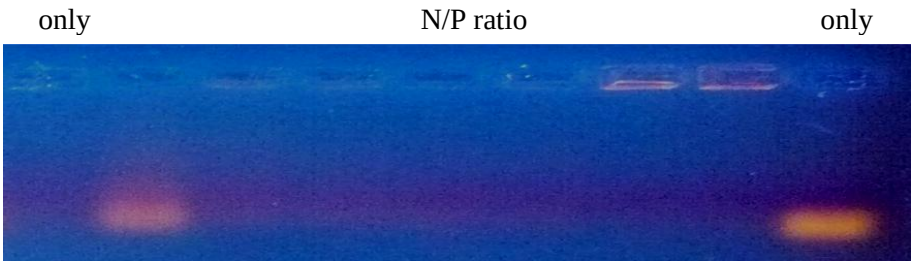

C

D

Figure 2-3 continued

E

Note: *A*, PEI/siRNA polyplexes, *B*, PEI-mannose/siRNA polyplexes, *C*, PEI-PEG/siRNA polyplexes, *D*, Mannose-PEI-PEG/siRNA polyplexes, *E*, PEI-PEG-mannose/siRNA polyplexes. All the polyplexes were prepared with 1μM siRNA from N/P ratio 1 to 15

Figure 2-4: Intracellular trafficking

A

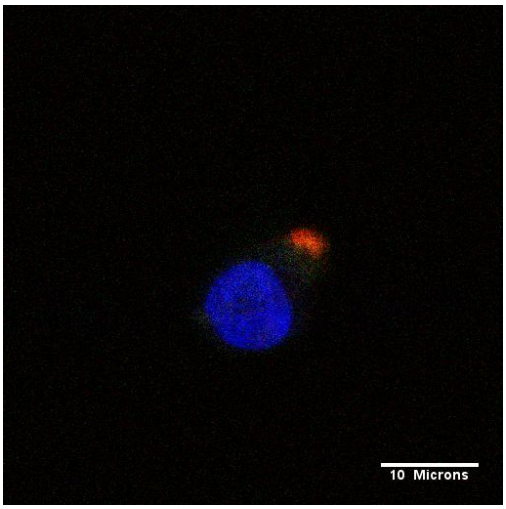

B

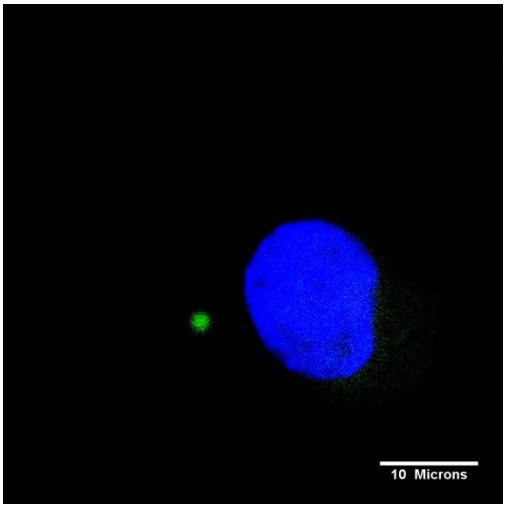

C

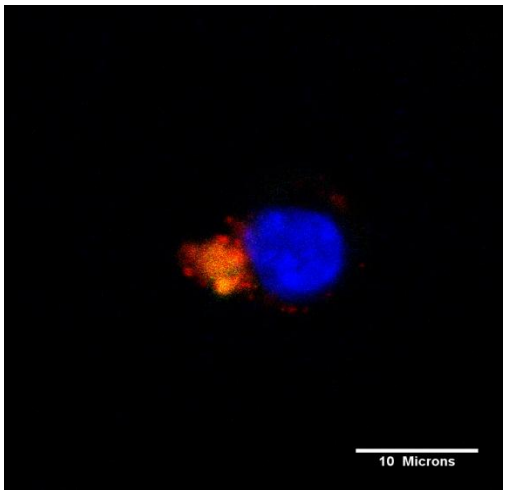

D

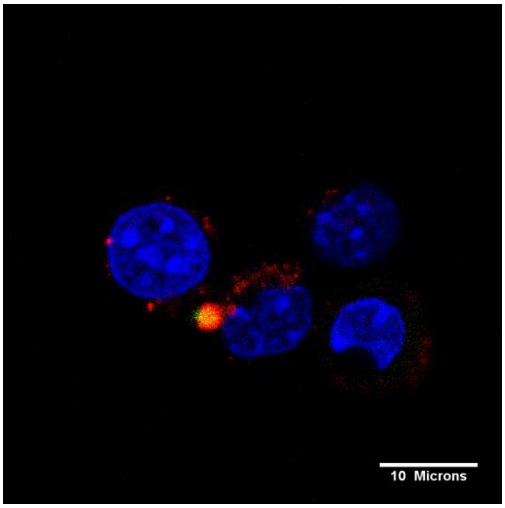

E

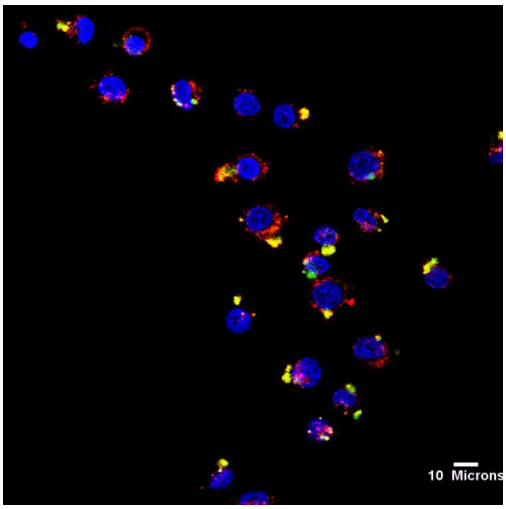

Figure 2-4 continued

Note: Raw264.7 cells were stained with Lysotracker Green (green), incubated with polyplexes formed using Cy-3 labeled siRNA (red), and then mounted with DAPI containing mounting solution after fixation. Co-localization of polyplexes and lysosomes are shown as a yellow signal. *A*, PEI/siRNA polyplexes, *B*, PEI-mannose/siRNA polyplexes, *C*, PEI-PEG/siRNA polyplexes, *D*, Mannose-PEI-PEG/siRNA polyplexes, *E*, PEI-PEG-mannose/siRNA polyplexes.

Figure 2-5: Knockdown of luciferase expression and HPRT mRNA expression

A

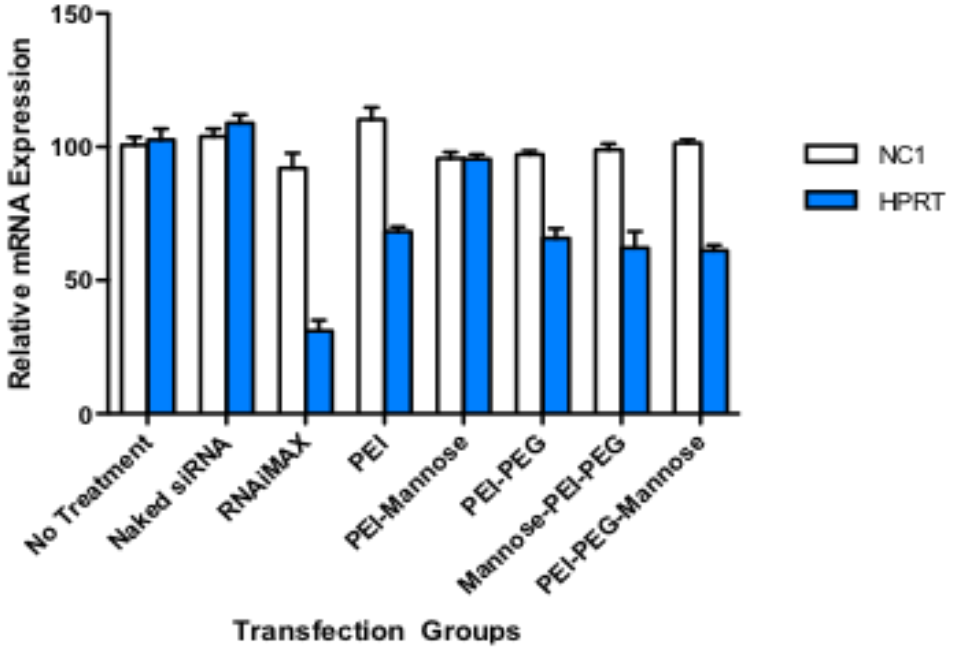

B

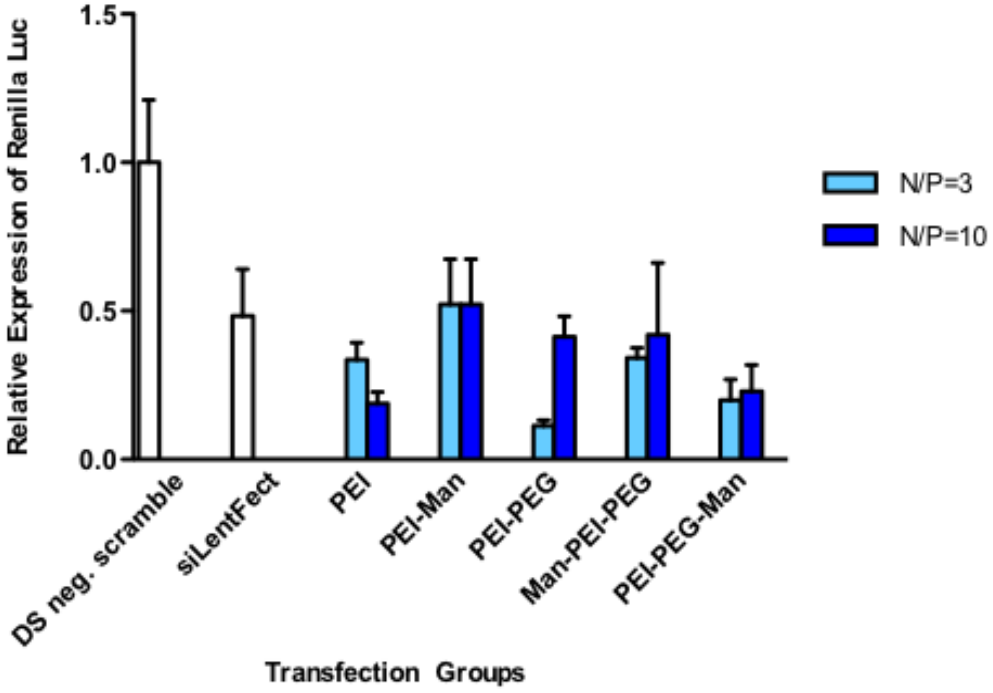

Figure 2-5 continued

Note: *A*, Relative expression of HPRT mRNA levels normalized to that of NC1 mRNA. From the left, no treatment, Naked siRNA, RNAiMax/siHPRT, PEI/siHPRT, PEI-mannose/siHPRT, PEI-PEG/siHPRT, mannose-PEI-PEG/siHPRT, PEI-PEG-mannose/siHPRT. *B*, Relative gene expression of *Renilla* luciferase is presented with firefly luciferase used an internal control. From the left, PEI/DS neg. scrambled siRNA served as negative control, siLentFect/sihRluc served as positive control, PEI/sihRluc, PEI-mannose/sihRluc, PEI-PEG/sihRluc, mannose-PEI-PEG/sihRluc, and PEI-PEG-mannose/sihRluc with N/P ratios at 3 and 10

Figure 2-6: Cytotoxicity

A

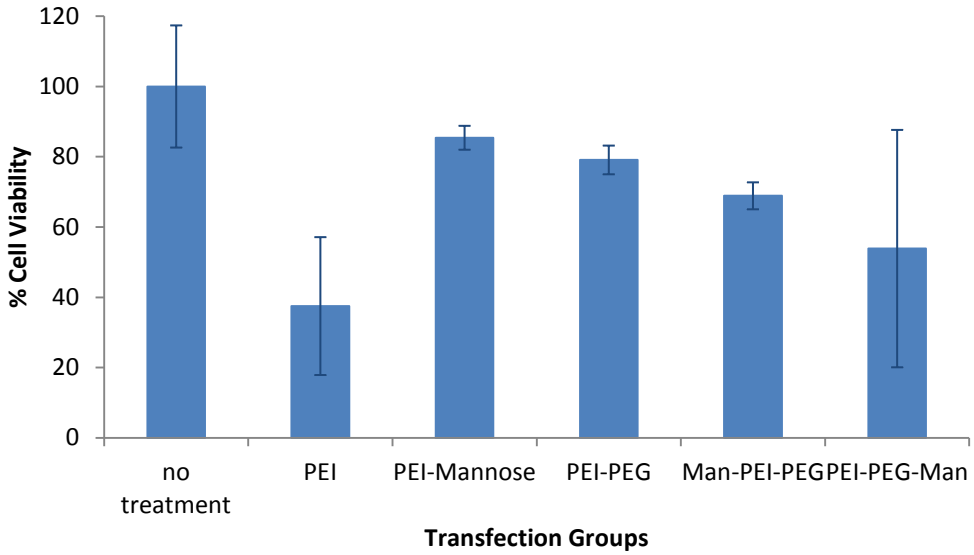

B

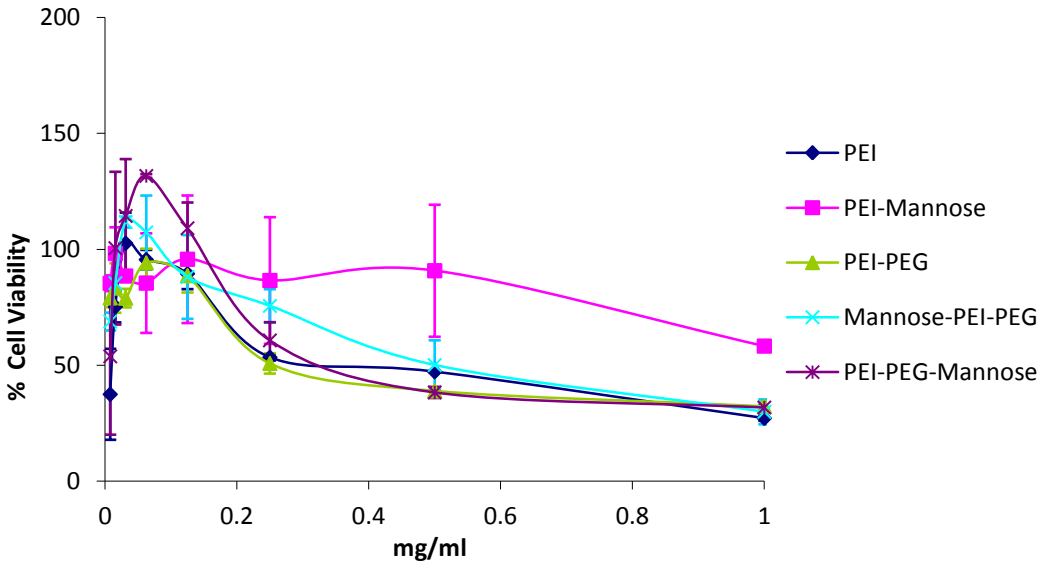

Note: *A.* Cytotoxicity of various polyplexes tested at the working concentration at 0.0078 mg/ml. From the left; no treatment, PEI, PEI-mannose, PEI-PEG, mannose-PEI-PEG and PEI-PEG-mannose groups. The relative cell viability was calculated by normalizing to the no-treatment group. *B.* Cytotoxicity of various polyplexes tested at various concentrations.

CHAPTER 3: DEVELOPMENT OF DEXTRAN-PEI CONJUGATE POLYMER FOR GENE DELIVERY

Introduction

Previously research on the development of PEI based materials for siRNA delivery has shown that PEI and PEI based materials are cytotoxic to cells. Incorporating degradability into PEI can be used to improve its toxicity profile. Small PEI units, when assembled into large but degradable structures using hydrolysable bonds, generated significantly reduced toxicity when compared to PEI 25k.

Biodegradability is a feature of natural polysaccharides such as dextran. The major linkage in dextran is either α-1,3 or α-1,6 glycosidic bond between the glucose monomers[128]. Dextran can be slowly depolymerized by enzymes present in various organs such as the liver, spleen and kidney[128,129]. Dextran with a MW of more than 50k is removed from the blood stream at a very slow rate, whereas 14-18k dextran has a plasma half-life of about 15 min[130,131]. The excretion of dextran is highly dependent on its size. Rat models suggest renal clearance is a major route of clearance for dextran < 10-20k[132,133]. A maximum 46.4k dextran fragment has also been observed in urine from human studies[134]. *In vitro* and i*n vivo* experiments have shown that chemical modification can reduce the de-polymerization rate of dextran by enzymes[135,136]. Cationic dextran derivatives such as DEAE-dextran and dextran-spermine have been tested as gene carriers in previous studies[137-142]. Gene delivery studies with conjugates containing dextran and PEI (MW 600 and 800) have also been reported in the past[140,143]. However, previous PEI dextran conjugates show reduced toxicity as well as reduced transgene

efficiencies. One interesting case involved increasing the MW of PEI to 25k in the conjugate, where small dextran molecules were grafted to PEI 25k and tested for gene transfer purpose[144,145]. At lower graft ratios, PEI was able to maintain its transfection efficiency. However, higher grafting degrees reduced its transfection efficiency, possibly due to weakening of its binding capacity with DNA.

In previous research studies, it has also been demonstrated that PEIs of lower MW failed to complex plasmid DNA and form compact and stable polyplexes. PEI 25 kDa is the most commonly used candidate in gene transfection studies. However, the PEIs branched structure and huge size restricts the excretion of PEI 25k from the renal route. Accumulation of PEI in the body from frequent treatments is undesirable. In addition, the polycationic characteristics of PEI are responsible for the aggregation and capillary embolism sometimes observed following intravenous injections. PEGylation can be used to reduce the charge density of PEI. A PEI based material combining toxicity-lowering and aggregation-reducing function is a preferred option for gene delivery applications.

We proposed that dextran-PEI conjugates can improve the stability of polyplexes in the presence of serum and generate high transfection efficiencies with reduced toxicity. We evaluate the impact of MW of dextran and PEI on transfection. In many previous studies, the condensing capability of PEI 800 was far less than PEI of higher MW[59]. It was proposed in this study that PEI 2000 be used in the conjugations. Dextrans of MW>70-90k were also utilized.

Materials

Dextran with an average MW 15k and 100-200k was obtained from USB (Cleveland, OH, USA, Lot#80995). Sodium cyanoborohydride, PEI 800 and 2000 were purchased

from Sigma-Aldrich (St Louis, MO, USA). Sodium periodate and PBS (phosphate buffer solution) tablet were supplied by Fluka (St Louis, MO, USA). Glycerin and glacial acetic acid (A.C.S. grade) were obtained from Fisher (Pittsburgh, PA, USA). PD-10 columns were purchased from Amersham (Piscataway, NJ, USA). MicroBCA Assay Kit and snake skin dialysis tubing with MWCO 10,000 were purchased from Pierce (Rockford, IL, USA). Agarose was purchased from Bio-Rad (Hercules, CA, USA). DMEM (Dulbecco's Modified Eagle's medium), trypsin and penicillin-streptomycin were obtained from Gibco (Carlsbad, CA, USA). FBS (Fetal Bovine Serum) was supplied by Atlanta Biologicals (Lawrenceville, GA, USA). MTS (CellTiter 96® AQ_{ueous} Non-Radioactive Cell Proliferation Assay Kit) was purchased from Promega (Madison, WI, USA). All other reagents were used as received at analytical grade. VR1255 plasmid was amplified and purified using a QIAGEN Giga plasmid purification kit (Valencia, CA, USA) according to manufacturer's protocol.

Methods

Synthesis of dextran-PEI

A modified method based on a previous study was followed to prepare the dextran-PEI conjugate polymer. Dextran (178 mg, 1 mM) was dissolved in 2 ml HAc/NaAc buffer (0.1 N, pH 5.0) and equilibrated in ice/water bath. Sodium periodate (10/21 mg, 0.046/0.098 mM) was dissolved in 400 µl HAc/NaAc buffer and added to the dextran solution for 30-mins oxidation. The reaction was stopped by the addition of (100 µl, 1.35 mM) glycerin. An Amersham PD-10 column (Mr 5000) (GE Healthcare, Buckinghamshire, UK, Lot#385703) was used to separate oxidized dextran. PEI 165 or 330 mg was dissolved in 5 ml HAc/NaAc buffer, and the oxidized dextran was added to

the PEI solution slowly. After overnight conjugation, $NaCNBH_3$ (58 mg, 0.92 mM) was dissolved in 1 ml HAc/NaAc buffer and added to the reaction solution for a second overnight reduction. Dextran-PEI was recovered after dialysis using Pierce tubing (MWCO 10,000) and lyophilization respectively.

Characterization of dextran-PEI

Dextran-PEI samples were dissolved in D_2O at 5 mg/ml, and ^{1}HNMR spectra were recorded with a Fourier transform nuclear magnetic resonance spectrometer (Bruker AVANCE 300MHZ)

Preparation of dextran-PEI/pDNA complexes

Plasmid (VR1255) encoding firefly luciferase was used to quantify the expression level of foreign genes in the host cells. All polymer/pDNA complexes were freshly prepared before use. Equal volumes of polymer solution and plasmid solution were mixed together with gentle vortexing, and incubated for 30 min at room temperature.

Agarose gel retardation assay on dextran-PEI/pDNA interaction

Agarose gel (0.8%) dyed with ethidium bromide (0.5 μg/ml) was used to investigate the particle condensation between dextran-PEI and plasmid DNA. Particle samples (1 μg pDNA/100 μl complexes) and corresponding amounts of polymers were prepared at N/P 5, 10 and 15. Particles (10 μl) from each sample with appropriate amounts of 10x gel-loading buffer were loaded and electrophoresed on gel in TAE buffer at 80 mV for 45 min. The DNA in the gel was visualized using a UV transilluminator (Spectroline TE-312S, Westbury, NY) and photographed.

Size and zeta potential measurement of the complexes

The size and zeta potential of polymer/pDNA complexes were measured using a Zetasizer (Malvern Nano ZS, SN#MAL500260). Particles samples (4 µg plasmid/800 µl complexes) at various N/P ratios were prepared with appropriate amounts of dextran-PEI and PEI controls.

Turbidity measurements to represent stability of complexes in serum

Complexes (50 µl) containing 5 µg pDNA and an appropriate amount of polymer were transferred to 96-well plates. 50 µl DMEM supplemented with 10% Fetal Bovine Serum (FBS) or de-ionized water was added to make up the volume to 100 µl. Changes in turbidity are represented by OD values measured with a UV/visible spectrophotometer (SpectraMAX Plus384, Molecular Device, Sunnyvale, CA) at 600 nm.

Cytotoxicity assay determined using the MTS assay

The MTS assay was used in HEK293 cells to evaluate the cytotoxicity of dextran-PEI polymers. HEK293 cells were grown in DMEM supplemented with 10% FBS, glutamate and Penicillin-Streptomycin (penstrep) at 37 ℃, 5% CO2 and 95% relative humidity. The MTS assay was performed according to a protocol from Promega. HEK293 cells (10^4 cells/well) in 50 µl DMEM culture medium were seeded in 96-well plates 24h prior to using the MTS assay. Polymer stock solutions were also prepared in DMEM at 5-10 mg/ml and sterile filtered. Serial dilutions of the polymers were prepared using DMEM. Sample solutions (50 µl) were transferred to each well followed by 4h incubation. MTS solution (20 µl) was added to each well for 2h incubation. The absorbance readings representing viability were recorded at 490 nm using a

spectrophotometer (SpectraMAX Plus384, Molecular Device, Sunnyvale, CA). The relative cell viability was calculated using untreated cells as control.

In vitro transfection (luciferase assay)

Luciferase gene transfection in serum-free culture media (4 h incubation)

The transfection efficiencies of dextran-PEI were quantified in HEK293 cells by the expression level of firefly luciferase. HEK293 cells were seeded in a 24-well plate at 10^5/well and incubated at 37 ℃ under 5% CO_2 for 24h prior to transfection in 1 ml DMEM medium supplemented with 10% FBS. Dextran-PEI complexes were prepared as described before. A volume of 500 µl DMEM (serum-free) was used to replace culture media immediately before transfection. Freshly-made 100 µl complex-containing suspensions at various N/P ratios containing 1 µg pDNA were added to each well. The transfection media was removed and replaced by 1000 µl DMEM with 10% FBS after 4h. Cells were further incubated for 44h. The luciferase expression level of harvested cells was determined with the Promega luciferase assay kit using a luminometer (Berthold Lumat LB 9507). Cells transfected with naked pDNA, PEI 800, PEI 2000 and PEI 25k were used as controls.

Luciferase gene transfection in serum-containing culture media (4 h incubation)

The method used for transfection experiments was the same as serum-free (4h incubation), with the exception that the transfection media was replaced with 500 µl DMEM with 10% FBS.

Luciferase gene transfection in serum-containing culture media (48 h incubation)

The method used for transfection experiments was similar to serum-present (4h incubation), except that transfection media was 1000 µl DMEM with 10% FBS instead, and transfection media was not removed in 4h but left as incubation media for 48h.

Intracellular trafficking of complexes prepared with Alexa-labeled dextran-PEI

Alexa 568 succinimidyl ester was used to label PEI and dextran-PEI. The labeling protocol followed Invitrogen instructions. Amersham PD-10 columns were used to separate untreated dye from PEI or dextran-PEI. Alexa 568 labeled PEI or DP3 was finally recovered by lyophilization. HEK293 cells were plated in 0.01% w/v poly-L-lysine coated 4 well chamber slides (Lab-Tak) at 5 x 10^4 cells/well and incubated overnight. The cells were incubated with 75 nM LysoTracker Green DND-26 (Invitrogen) containing DMEM for 1h prior to transfection to stain lysosomes and endosomes. Then cells were transfected with complexes made with Alexa 568 labeled DP3 and PEI 2000/25k carrying 0.5 µg pDNA (N/P=10) in fresh DMEM. At 2h post-transfection, the cells were washed with PBS and fixed with 4% paraformaldehyde, mounted with Vectashield Mounting Medium with DAPI for nucleus staining (Vector Laboratories, UK). The slides were covered with coverslips followed by 4 ℃ storage in the dark before visualization under a multiphoton/confocal microscope (Bio-Rad Radience 2100MP) with 60x oil immersion lens.

Statistical analysis

All results were presented as mean ± standard deviation. One way ANOVA analysis with Tukey's post-test was used to determine the difference between groups. Level of

significance was accepted at $p<0.05$. Statistical analyses were performed using Prism software (Graphpad Software Inc, San Diego, CA)

Results

Synthesis and characterization of dextran-PEI

Oxidation followed with conjugation is a convenient method to prepare dextran-oligoamine fusion structures. The imine bond formed between oxidized dextran and PEI can be further reduced to amine. After this, the linkage becomes irreversible in aqueous solutions. Figure 3-1 shows characteristic peaks of dextrose (dextran's monomer) and PEI in the ^{1}HNMR spectra of the conjugate polymer. The nitrogen normalized MW (N-MW) of dextran-PEI was calculated based upon the peak area at 4.9 ppm for dextrose and 2.6 ppm for PEI, by the following equation:

$$N - Mw = 43 + \frac{A(4.9ppm) \times 178}{A(2.6ppm)/4}$$

Table 3-1 summarized the N-MW and corresponding PEI content in the various dextran-PEI samples. In the ^{1}HNMR spectra, two conjugates of dextran 15 kDa and PEI 800 failed to show significant peaks at 2.6 ppm (figure not shown), indicating the lack of conjugation between dextran and PEI. The combination of dextran 15 kDa and PEI 2000 showed 16.195% and 27.497% PEI contents in the final products, corresponding to the consumption of 10 and 21 mg sodium periodate in the reaction, respectively. When dextran 100-200 kDa was used in the conjugation, both PEI 800 and 2000 can react with it effectively. These conjugates were named from DP1 to DP4. DP1 and DP2 were based on PEI 800, showing PEI contents as 6.5% and 13.0%. DP3 and DP4 were made with PEI 2000, and showing a higher PEI amounts as 20.0% and 36.7%.

Cytotoxicity assay by MTS

The MTS assay is a modified MTT assay which produces soluble formazan with λ_{max} at 490 nm in living cells only. HEK293 cells are exposed to polymer solutions at various concentrations for 4h, followed by 2h incubation with MTS solution. PEI 800, 2000 and 25k are used as controls. As seen in Figure 3-2, the general order of cytotoxicity is PEI 800 < PEI 2000 < PEI 25k in the concentration ranges tested. All dextran-PEI samples show a significantly reduced cytotoxicity when compared to PEI 25k. DP1 and DP2 show lower toxicity, even when compared to PEI 800. DP3 displays similar cytotoxicity profiles to PEI 2000. DP4 is slightly more toxic than PEI 2000, but significantly less toxic than PEI 25k. The working concentration of PEI in gene delivery is commonly between 0.01 and 0.1 mg/ml, depending on the dose of pDNA and N/P ratios. During this concentration range, our dextran-PEIs showed significantly less damage to HEK293 cells.

Agarose gel retardation assay, size and zeta potential measurement on pDNA-dextran-PEI complexes

Effective condensation of pDNA by dextran-PEI into particles is critical for its successful application in gene therapy. Condensation protects pDNA from enzymatic degradation and facilitates uptake of particles by cells. Using agarose gel assays, dextran-PEI samples and PEI controls (800, 2000 and 25k) were evaluated for their ability to form complexes at various N/P ratios. Figure 3-3 shows that PEI 800-based DP1 and DP2 exhibits poor complexation with pDNA at N/P 5, which improves as the N/P ratio increases above 10. DP3 and DP4, which are made from PEI 2000, fully retard migration of pDNA at all N/P ratios, suggesting more compact complexes are formed when compared to PEI-800 based conjugates. Complexes based on PEI 25k and 2000 display

limited migration of pDNA. In contrast, PEI 800 results in poor pDNA condensation. Comparing DP3/4 to PEI 25k, no significant differences in terms of complexation are found.

An appropriate size and net positive charge on the surface of the particles is also crucial for endocytosis of complexes. Consistent with the gel retardation assay results, all dextran-PEI conjugates are able to form complexes with pDNA with net positive surface charges, as shown in Figure 3-3 & 3-4. PEI 800 is not as potent as other PEIs in the formation of complexes. At N/P 5, PEI 800 forms the largest particles in comparison to all other groups. PEI 800-based dextran-PEIs (DP1/2) also give relatively large particles more than 200 nm in size, but these particles were significantly smaller than PEI 800. PEI 2000 generates a reduced particle size which is less than 210 nm, comparing to particles prepared with PEI 800. DP3 and DP4, made with PEI 2000, also generate smaller particles which are around 200 nm in comparison to DP1/2. Decreased particle sizes are observed as the N/P ratios increases. At N/P 15, particles formed with DP4 are as small as 83 nm and similar to the 89 nm particles created by PEI 25k. The surface charge of the particles is reversely correlated to increasing particle size. As seen in Figure 3-5, increasing N/P ratios result in higher zeta potentials. Complexes with PEI 25k show the highest zeta potential of around 30 mV at N/P 10 and 15. Dextran-PEI/pDNA exhibits lower values of 15-24 mV when compared to PEI 25k. Most of the dextran-PEIs surface charges are approximately 15-20 mV, which are at the same level of PEI 800 and 2000.

Turbidity measurements to represent stability of complexes in serum

Turbidity is a commonly used method to detect aggregates or particles in fluid. The turbidity index of a particulate sample will be reflected by the reduction of the incident

beam intensity. This reduction is represented by optical density (OD) or absorbance value change on a UV-Vis spectrometer (SpectraMAX Plus384). The increase in turbidity is due to the increased average particle size when aggregation occurs. In Figure 3-6, particles formed with PEI 25k shows significantly higher turbidity than DP4 at N/P 5 (one-way ANOVA, $p<0.001$). Furthermore, as the N/P ratio increases, the turbidity of PEI 25k complexes also rises. In contrast, DP4's turbidity decreases when the N/P ratio increases. N/P values reflect the amount of cationic polymers in the complexes if pDNA amount is constant. The greater turbidity difference at N/P 15 than N/P 5 between PEI and DP4 groups suggests that the presence of dextran in polymer/pDNA complexes incurs less aggregation in the presence of serum, whereas PEI alone is more susceptible.

In vitro transfection (luciferase assay)

As mentioned earlier, one of the major obstacles to PEI based gene delivery is aggregation in the presence of serum and subsequent lung embolism. The transfection efficiencies of dextran-PEI and PEI materials are investigated under three conditions: Serum-free (4h incubation), serum-containing (4h incubation), and serum-containing (48h incubation).

Luciferase gene transfection in serum-free culture media (4 h incubation)

As shown in Figure 3-7, PEI 800 generates the lowest transfection efficiency, whereas PEI 25k generates the highest. Naked DNA exhibits similar transfection efficiency levels to those achieved using PEI 800 (one-way ANOVA, $p=0.4567$). Increasing the N/P ratio improves the luciferase expression level. When examining dextran-PEIs, all DPs show lower transfection efficiencies than PEI 25k. At N/P 15, DP4 shows lower transfection efficiency than PEI 25k, but this difference is not significant

(one-way ANOVA, p=0.6060). All DPs display similar transfection profiles regardless of the type of PEI used in the DP construct. These results are consistent with a number of previous studies[143,146].

Luciferase gene transfection in serum-containing culture media (4 h incubation)

As suggested by results from the turbidity experiments, dextran-PEI is able to reduce particle aggregation caused by serum in culture media. Normal DMEM (with 10% FBS) is used to replace the DMEM w/o serum in the previous study and the transfection study is repeated. A similar pattern is found for all PEI samples (Figure 3-8). PEI 800 is not more efficient than naked pDNA (one-way ANOVA, p=0.4144) in terms of transfection efficiency at N/P 5. PEI 25k shows the highest transfection efficiency at N/P 15. Higher N/P ratios lead to higher efficiencies. In contrast to experiments carried out in serum free-media, dextran-PEI conjugates, show improved efficiencies of transfection relative to PEI when the experiment is carried out in serum containing media. The overall expression level of luciferase generated by dextran-PEIs follows the order DP1<DP2<DP3<DP4, and is correlated with decreasing N-MW values. DP4 exhibits high transfection efficiency with no significant difference to PEI 25k (one-way ANOVA, p=0.1273/0.9972, N/P 10/15).

Luciferase gene transfection in serum-containing culture media (48 h incubation)

As shown by the cytotoxicity data, dextran-PEI is significantly less toxic than PEI 25k. When the incubation (transfection) time length is extended to 48h, PEI 800 generates the lowest transfection efficiency among all the controls (Figure 3-9) and is at the same level as naked DNA (one-way ANOVA, p=0.3330). Since PEI 2000 is significantly less toxic than PEI 25k, we hypothesize that the lower toxicity offsets lower

transfection efficiencies to generate similar total luciferase expression levels. The expression of luciferase from PEI 2000 is close to that of PEI 25k, but the latter causes more death of cells at the 48h time-point. DP1 and DP2 still result in poor transfection efficiencies, probably due to the relatively large particles formed. However, DP3 and DP4 exhibit significantly higher transfection efficiencies to PEI 25k at N/P 10/15 (one-way ANOVA, $p<0.0001$; $p=0.0315$). When compared to the results from complexes incubated for 4h incubation in serum-containing media, we presume that 4h was not long enough to show the influence of the toxicity on transfection efficiencies between DP3/4 and PEI 25k. When the incubation length was increased to 48h, dextran-PEI clearly demonstrated lower toxicity, in conjunction with an improved efficiency on transfection. Similar results were observed on transfection study with COS7 cells (data not shown).

Intracellular trafficking of complexes prepared with Alexa-labeled dextran-PEI

The intracellular fate of DP-pDNA complexes was visualized by confocal microscopy. Lysosomes and endosomes were stained with LysoTracker Green. The nucleus was stained with DAPI. Alexa 568 was used to label DP3 or PEI. As shown by photos in Figure 3-10, 3-11 and 3-12, complexes were well internalized at 2h post-transfection. The co-localization of PEI 25k and DP3 with lysosomes were represented as yellow color in the picture. DP3/pDNA complexes showed some level of dissociation with lysosomes. The color dissociation may suggest a faster escape of DNA cargo from lysosomes into cytoplasm, which could be a reason for the high efficiency of dextran-PEI in the transfection study.

Discussion

Periodate is a commonly used reagent in oxidizing polysaccharide and allowing further conjugation with amine-containing molecules such as proteins and peptides. The method has been widely used in making functionalized macromolecules. In this research study, dextran was oxidized and linked with PEI via glucose monomers. The bonds between C2, C3 and C4 in glucopyranose are cleaved by periodate and aldehyde groups are created. These aldehyde groups are highly reactive to amines and form imine bonds between carbon and nitrogen atoms. Irreversible linkage is generated if a reducing agent such as sodium cyannoborohydride is added to convert imines to C-N bonds.

As shown in ^{1}HNMR spectrum, the peak at 4.9-5.0 ppm represents the proton signal of C1 (glucopyranose monomer). The remaining peaks from 3.4 to 4.1 ppm are corresponding to other protons of C2 to C6. The peak at 2.6 ppm, after comparison to the spectra of PEI (not shown), is the signal of CH_2 monomers in PEI. Therefore, the spectrum of DP4 (Figure 3-1) confirmed the existence of both dextran and PEI in the conjugate structure. By comparing the integration of the peak area of C1-H (glucopyranose) and CH_2-H (PEI), it is feasible to calculate the molar ratio between dextran monomers and PEI monomers and thus calculate the amount of PEI conjugated to dextran. A lower N-MW value represents a higher amount of PEI in the dextran-PEI samples. Using the data in table 3-1, the extent of PEI conjugation was correlated to the amount of sodium periodate added. Higher doses of sodium periodate resulted in a higher conjugation degree and lower N-MW. The MW of dextran used in the reaction also affected the results. Dextran 15k was not as efficient as dextran 100-200k for conjugation in the reaction, especially with PEI 800. While examining the reaction efficiency

differences between PEI 800 and 2000, it was noticed that PEI 800 had lower substitution degrees in the conjugates, which can be explained by the difference in degree of polymerization of PEI. Among all the conjugates prepared, Dextran(100-200k)-PEI(2000) (DP4) showed the highest conjugation degree.

Our hypothesis proposes that dextran would incorporate degradability into the conjugate polymer. The introduction of degradability into the PEI structure has been previously demonstrated to reduce PEI toxicity. In addition, previous studies have also shown that grafting dextran to PEI can also reduce the toxicity of PEI significantly. Therefore, the reduction in toxicity for dextran-PEI is reasonably attributed to the inclusion of the dextran. Increasing conjugation degrees is correlated to the increasing cytotoxicity, which may be explained by higher charge densities and more intensive charge interactions between the polymer and the cell membrane. It was believed that this charge interaction was related to the development of toxicity at a cellular level.

The sizes of polyplexes formed with dextran-PEIs ranged from 80 to 200 nm. As mentioned in the previous PEI-PEG-mannose study, particles less than 150-200 nm in size showed higher endocytosis efficiency than particles of bigger size. The inclusion of dextran in polyplexes produced a size increase compared to PEIs. Similar to the explaination of toxicity, attenuation on charge density could be the reason for the size increase. Compared to PEI, the N-Mw values of dextran-PEI are greater, indicating a larger average molecular size corresponding to each amino group. Our results showed that PEI 800 was incapable of condensing pDNA into particles. However, after conjugation to dextran, PEI 800 showed improved condensing capability. In combination

with other studies assembling small PEIs into large constructs, it was believed that a certain minimum MW was indispensible in condensation and complexation with pDNA.

Another hypothesis is that the conjugate of dextran and PEI would reduce aggregation of particles in the presence of serum. It is important to note here that aggregation could result in embolism in the lung which is a major obstacle to the *in vivo* application of PEI. Turbidity was originally a method for monitoring the purity of water, where a high turbidity value suggests "muddy" appearance. In this study, turbidity value was used as indirect measurement of aggregation and/or average size. In the case of pure solution, because there are no insoluble particles in the liquid, it should exhibit a similar turbidity index to pure water. Therefore, PEI and DP4 colloidal particles showed comparable OD values to DI water. DMEM (supplemented with 10% FBS) exhibited an increased OD, suggesting insoluble particles in the media. Particles subjected to DMEM showed even higher OD values than media itself, suggesting an increase in average size of particles. An assessment of the trend of turbidity values at different N/P ratios showed that a higher concentration of DP4 was able to stabilize particles in the presence of serum. In a previous study, the dextran-graft on PEI 25k was thought to attenuate the interaction between serum components and particles, and thus reduce the particles size change.

Several dextran PEI conjugate polymers have been developed but have led to few successes. In an earlier screening of polysaccharide-oligoamine conjugates as a gene carrier, Dextran (20-500 kDa)-PEI 600 was ruled out because of poor transfection efficiencies[140]. In another two studies, grafting of dextran (1500 and 10,000) to PEI (25k) reduces its buffering capacity, cytotoxicity and transfection efficiency, and it was concluded that dextran grafting prevented particles from passing the cell membrane[144,145].

Two newer studies bypassed oxidation and utilized spacer linking between dextran (15-25k and 60-90k) and PEI (800)[143,146]. In these studies, Dextran PEI conjugate polymers also showed lower toxicity and transfection efficiencies when compared to PEI 25k at the same N/P ratios. While examining the compositions of conjugates, it must be noted that the MW of PEI used was relatively low (600, 800). In our study, the structure of the conjugate polymer is different to previous conjugates because dextran is used as a core rather than a grafting material, and higher MW materials were used to achieve better complexation with pDNA[59]. HEK293 cells were selected to evaluate transfection efficiency. This cell line derives from human kidney epithelial cells and is a commonly used cell line for evaluating non-viral gene transfer vectors. Our transfection results showed that in serum-free conditions, dextran-PEI polymers were not more competent than PEI 25k, which is consistent with previous findings on dextran PEI conjugates[143,146]. After changing to serum-containing conditions, improvements on transfection efficiency were observed with the use of our conjugate polymers. The cytotoxicity profiles suggested that conjugate polymers generated significantly less damage to HEK293 cells in working concentrations. It was presumed that the reduced cytotoxicity help increase the overall transfection efficiency. Meanwhile, improved stability of particles by dextran-PEI in the presence of serum could allow for higher endocytosis efficiencies compared to PEI 25k. Confocal microscopic imaging showed the co-localization of particles and endosomes/lysosomes 2 hrs after transfection. The dissociation of red and green colors could be explained by the rapid escape of particles by dextran-PEI conjugates into the cytoplasm. Because the conjugate was built with dextran and PEI, it would be reasonable to infer that the buffering capacity of PEI remained in dextran-PEI conjugates and

produced a similar proton sponge effect to PEI alone. At the same N/P ratio, the total amine amount in PEI 25k is equal to DP3 so that dextran could possibly increase the viscosity of liquids in endosomes, increase the osmotic pressure difference and thus facilitate the rupture of endosomes.

Table 3-1: **Characterization of dextran-PEIs**

sample	Dextran MW (kDa)	PEI MW (Da)	PEI wt %	N-MW	Ref code
D15P800-l	15	800	N/A	N/A	
D15P800-h	15	800	N/A	N/A	
D15P2000-l	15	2000	16.195	266	
D15P2000-h	15	2000	27.497	156	
D150P800-l	100-200	800	6.5469	648	DP1
D150P800-h	100-200	800	13.026	328	DP2
D150P2000-l	100-200	2000	20.079	214	DP3
D150P2000-h	100-200	2000	36.699	117	DP4

Note: -l: low oxidation/substitution degree, 11 mg sodium periodate added; -h: high oxidation/substitution degree, 21 mg sodium periodate added; N/A: not available

Figure 3-1: **^{1}HNMR spectra of DP4**

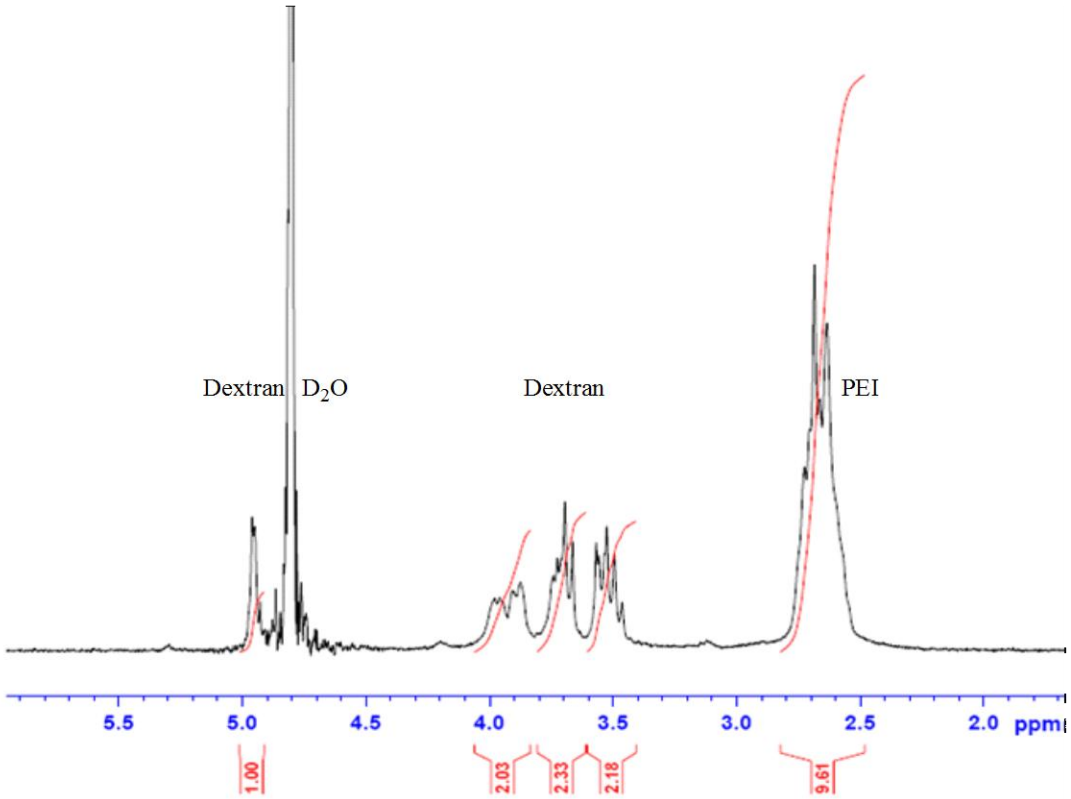

Note: δ5.0-4.9 (C1-H, Dextran(Dextrose)), δ4.8 (H, H_2O), δ4.1-3.4 (C2-C6-H, Dextran(Dextrose)), δ2.8-2.5 (PEI-H), Bruker AVANCE 300MHz, DP4's spectra shown only

Figure 3-2: Cytotoxicity profiles of Dextran-PEI

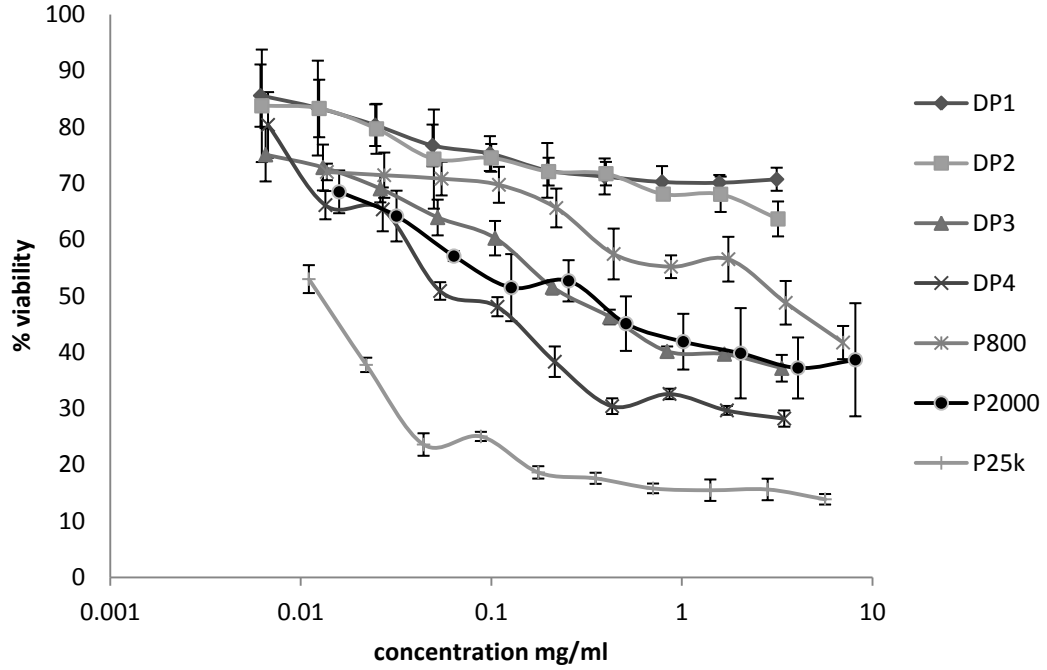

Note: 4h incubation with polymer solution and 2h incubation with MTS solution. HEK293 cell treated with dextran-PEIs and controls in the concentration range: DP1: 0.00615-3.15 mg/ml; DP2: 0.00625-3.20 mg/ml; DP3: 0.00654-3.35 mg/ml; DP4: 0.00674-3.45 mg/ml; P800: 0.01372-7.03 mg/ml; P2000: 0.01592-8.15 mg/ml; P25k: 0.01104-5.65 mg/ml Cells were treated with polymers for 4h. Mean ±SD, n=4

Figure 3-3: Gel retardation assay

A

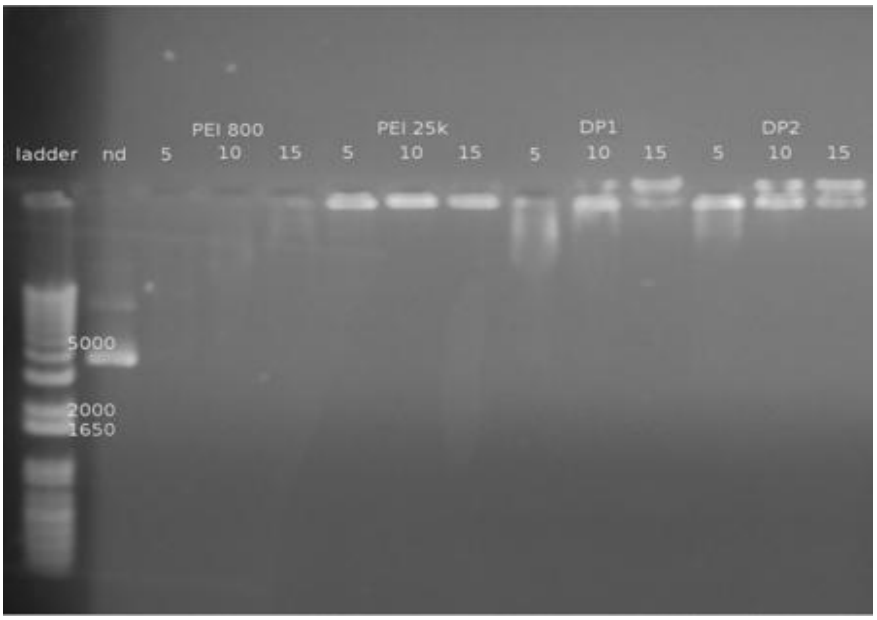

B

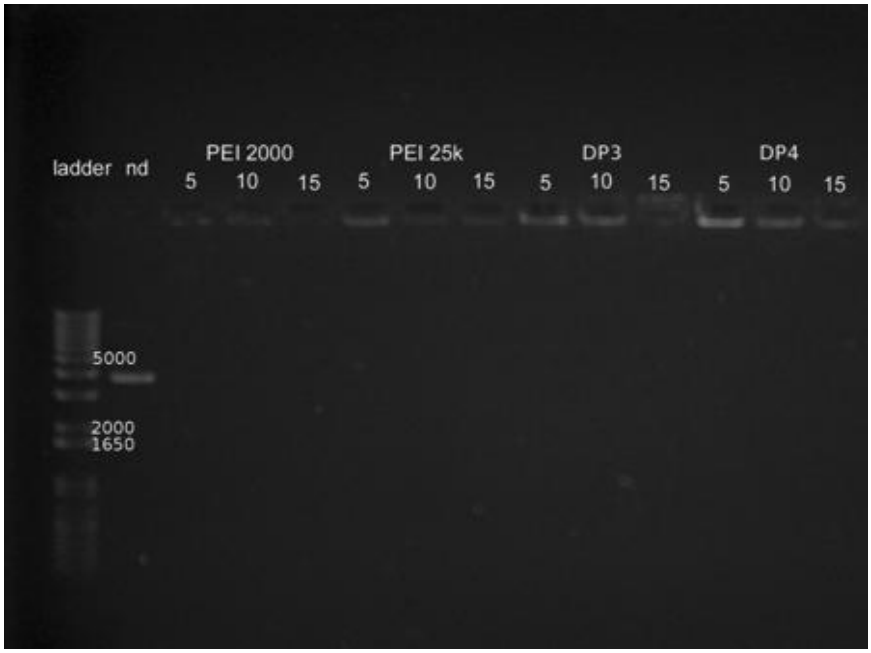

Note: agarose gel electrophoresis of DPs-DNA complexes at N/P ratio 5, 10 and 15. (nd: naked pDNA)

Figure 3-4: Particle size

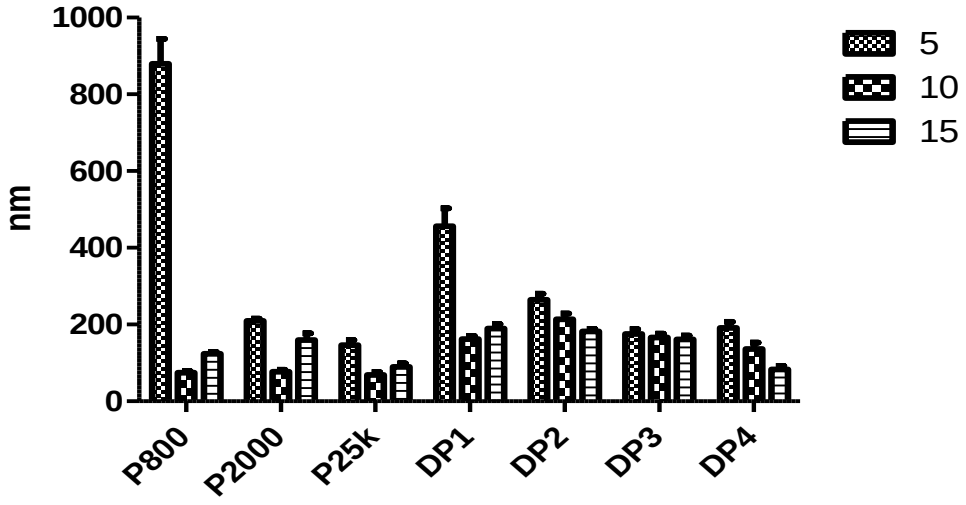

Note: sizes of complexes formed by dextran-PEIs and controls at various N/P ratios. Mean+SD, n=3

Figure 3-5: Zeta potential

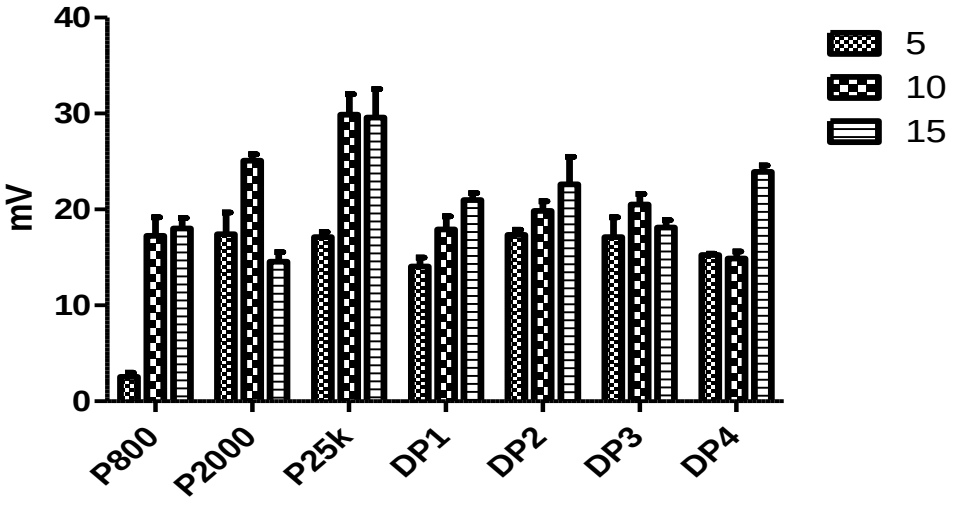

Note: zeta potential of complexes formed by dextran-PEIs and controls at various N/P ratios. Mean+SD, n=3

Figure 3-6: Turbidity

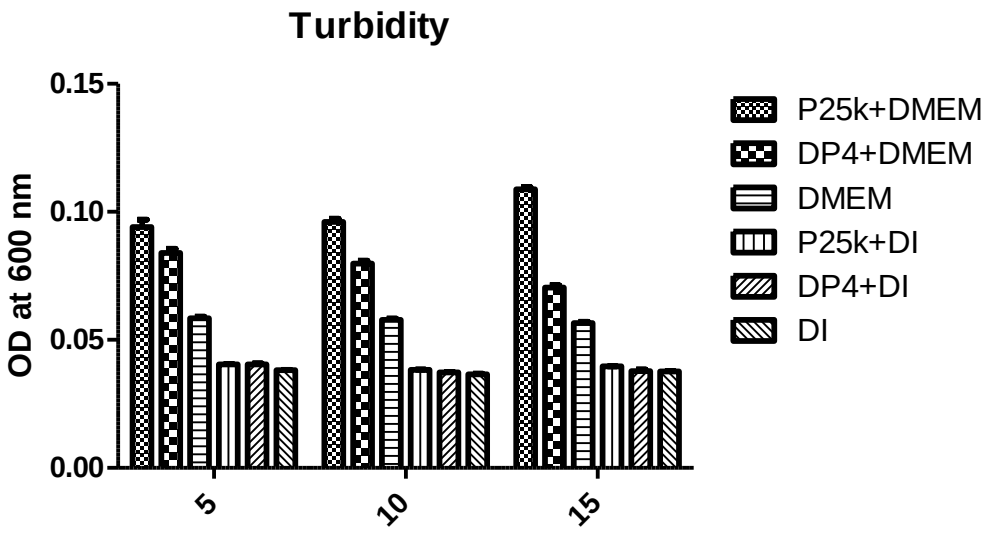

Note: turbidity of dextran-PEI/pDNA complexes in DMEM (with 10% FBS). Mean+SD, n=6

Figure 3-7. Gene transfection efficiency (4h w/o serum)

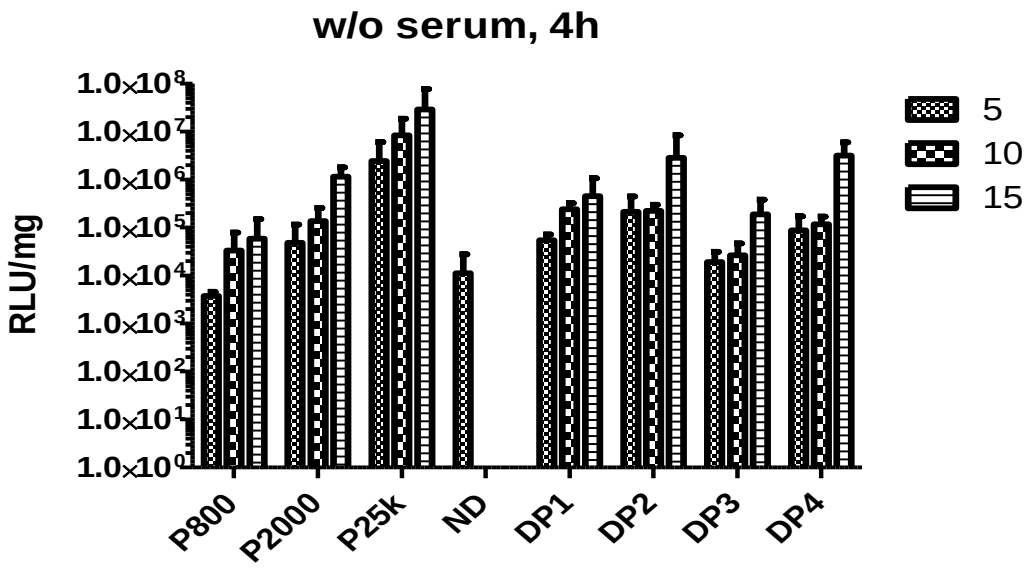

Note: efficiency of Dextran-PEIs and controls at various N/P ratios in HEK293 cells. 4h transfection (w/o serum) and 44h incubation. Mean+SD, n=4

Figure 3-8: **Gene transfection efficiency (4h w/ serum)**

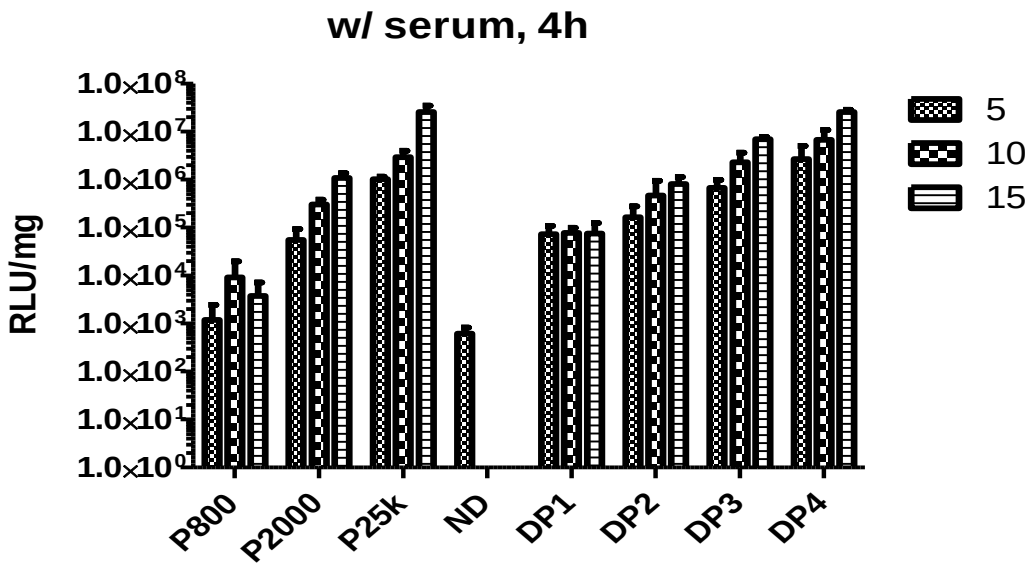

Note: efficiency of dextran-PEIs and controls at various N/P ratios in HEK293 cells. 4h transfection (w/ serum) and 44h incubation. Mean+SD, n=4

Figure 3-9: **Gene transfection efficiency (48h w/ serum)**

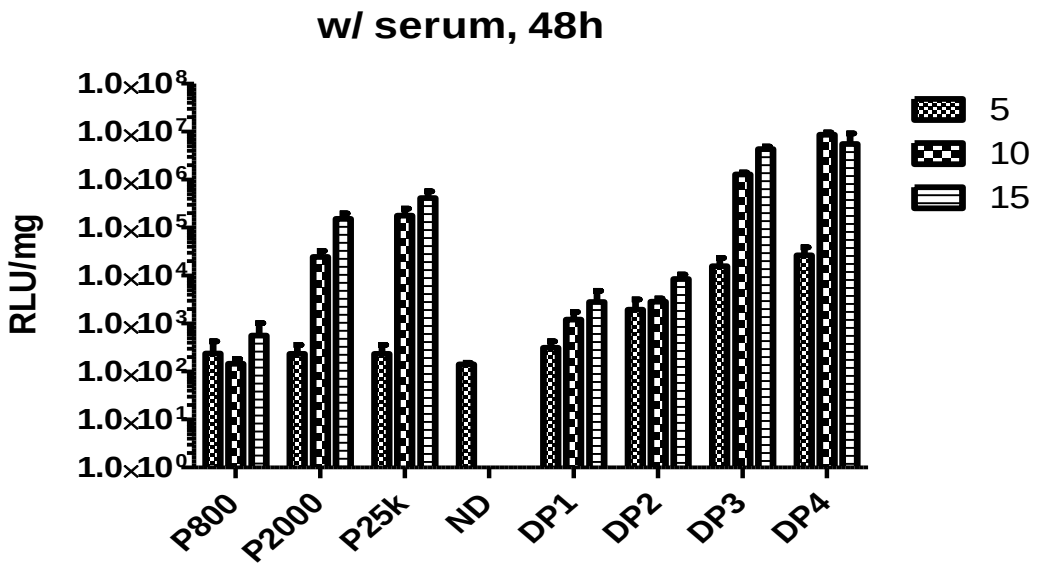

Note: efficiency of dextran-PEIs and controls at various N/P ratios in HEK293 cells. 48h transfection (w/ serum). Mean+SD, n=4

Figure 3-10. Confocal microscope image of PEI2000-DNA complexes localization at N/P 10, 2h post-transfection (w/ serum)

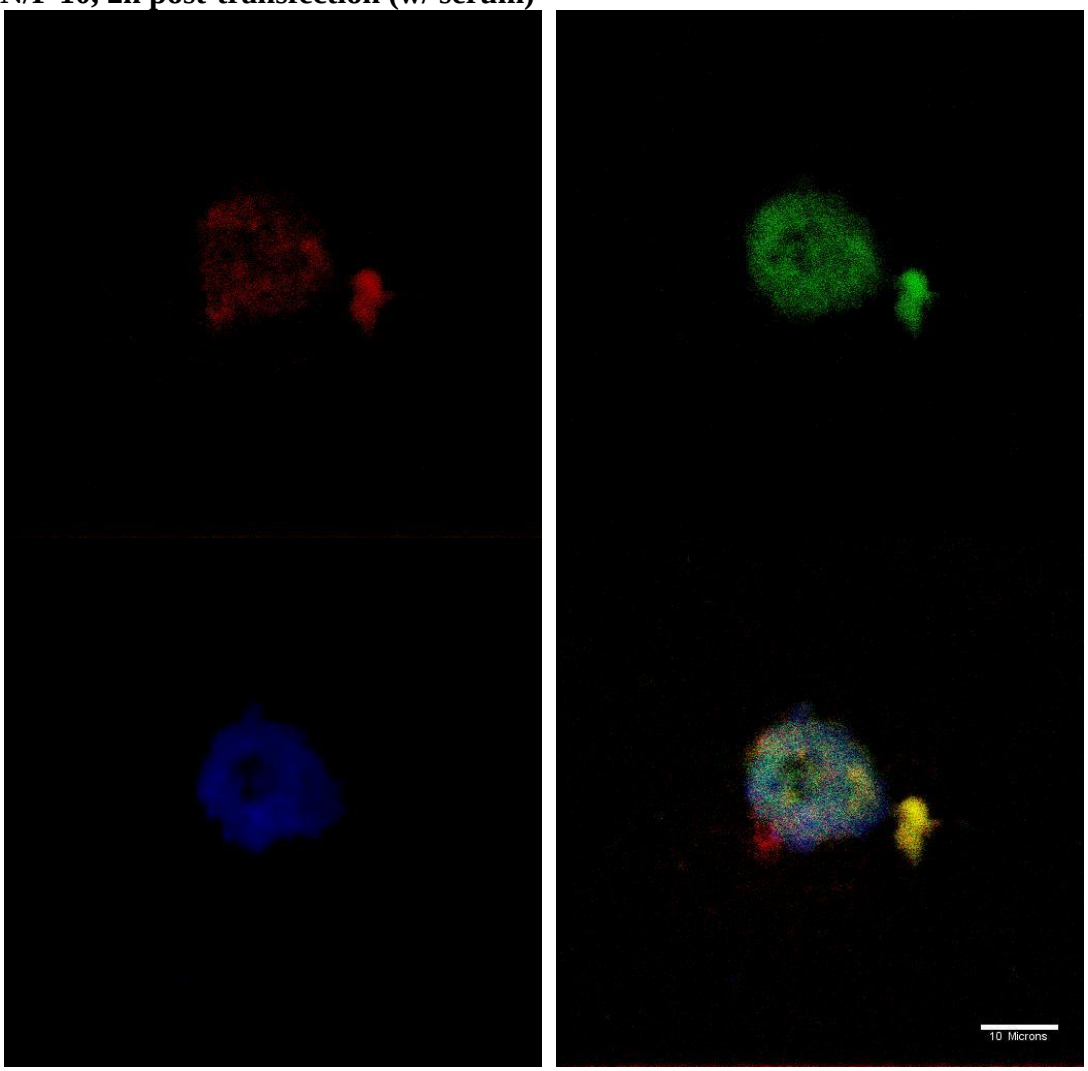

Note: nucleus stained with DAPI (blue); Lysosome stained with LysoTracker (green); Polymer stained with Alexa 568 (red)

Figure 3-11: Confocal microscope image of PEI25k-DNA complexes localization at N/P 10, 2h post-transfection (w/ serum)

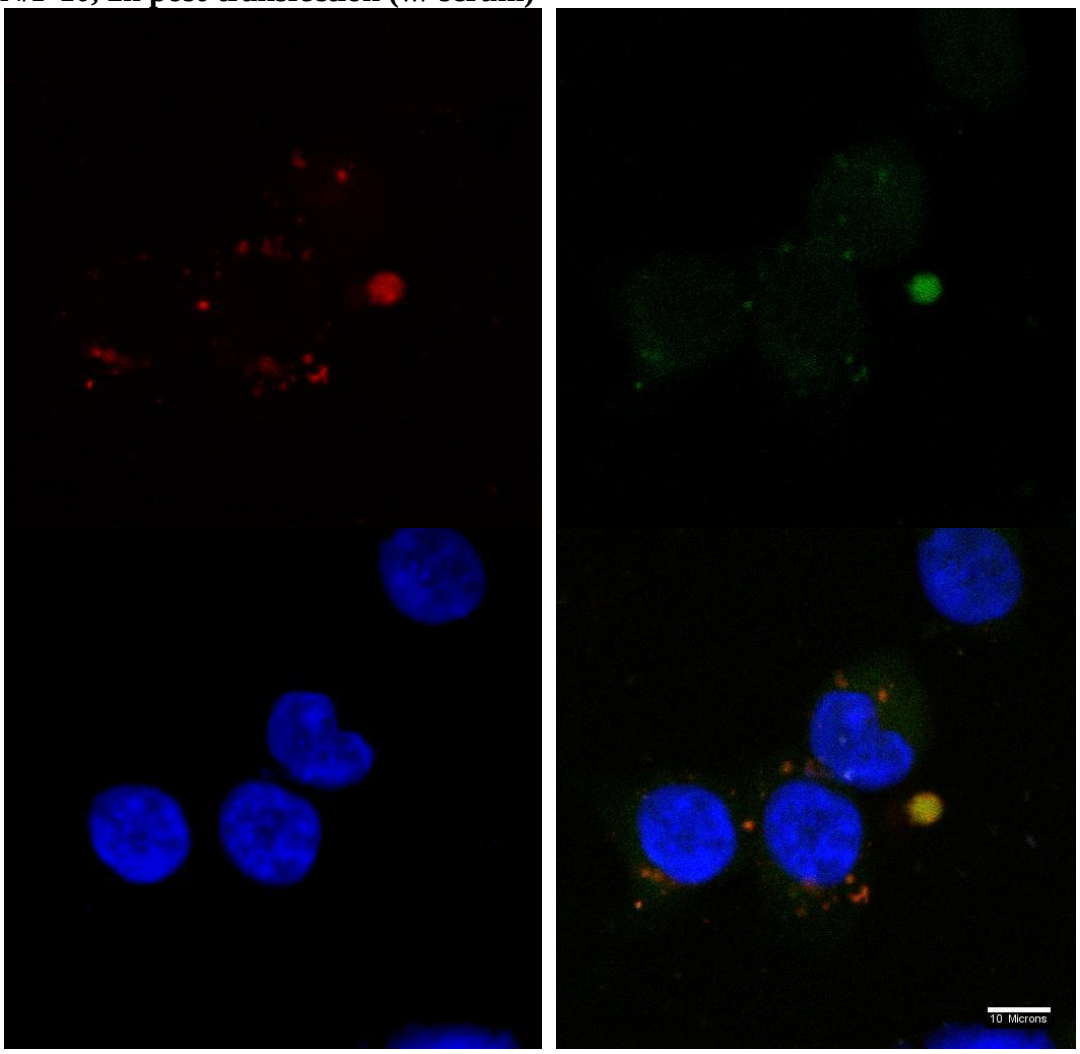

Note: nucleus stained with DAPI (blue); Lysosome stained with LysoTracker (green); Polymer stained with Alexa 568 (red)

Figure 3-12: Confocal microscope image of DP3-DNA complexes localization at N/P 10, 2h post-transfection (w/ serum)

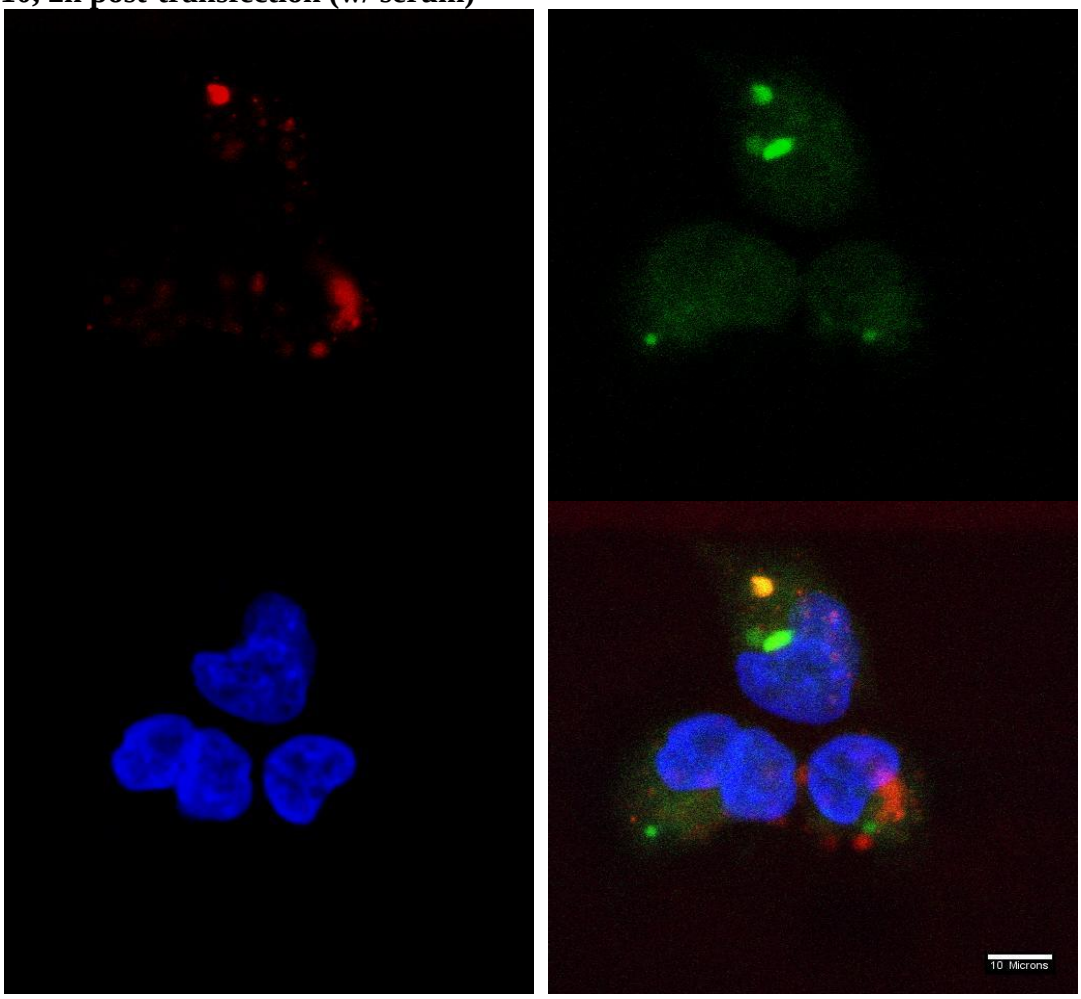

Note: nucleus stained with DAPI (blue); Lysosome stained with LysoTracker (green); Polymer stained with Alexa 568 (red)

CHAPTER 4: DEVELOPMENT OF OVA/CpG CO-LOADED PLGA MICROPARTICULATE VACCINE

Introduction

PLGA is a biodegradable and biocompatible polymer which has shown great potential in drug delivery. Due to its hydrophobicity, PLGA can be fabricated into microparticles loaded with peptides, proteins and nucleic acids. The PLGA microparticles can protect loaded macromolecules from degradation and improve their stability. Vaccines in the form of PLGA microparticles show enhanced immune responses because PLGA microparticles can be fabricated with similar sizes as natural pathogens. PLGA microparticles can also provide sustained release of antigen so that vaccinations can be simplified as a single bolus dose.

Various fabrication techniques in producing PLGA microparticles have been developed in the past decades. One of the most successful methods is the water-in-oil-in-water w/o/w double emulsion technique. By controlling various parameters during fabrication, PLGA microparticles can be tailored to the desired size, shape and loading. PLGA is commercially available in different MW (inherent viscosity) and compositions of lactic acid and glycolic acid, which allows for the preparation of particles with a wide range of release profiles. Some PLGAs are also supplied with free carboxylic terminals, thereby enabling further chemical modification for customized needs. Our lab has developed PEI/PAMAM coated PLGA microparticles for delivery of genetic material[147,148]. Using NHS/EDC reagents, PEI/PAMAM was covalently coated on the surface of PLGA microparticles (PLGA carries carboxylic acid terminals). After coating,

PLGA microparticles showed a surface charge reversion from -40 mV to 40 mV[147,148]. The net positive charge on the particle surface allows for electrostatic interaction between pDNA and microparticles allowing for potential applications for gene delivery. The PEI/PAMAM coated microparticles also exhibited a moderate buffering capacity in titration tests, which might be able to introduce the proton sponge effect and improve transfection efficiency. Given that both pDNA and CpG ODN have similar net negative backbones, the coated microparticles could be used to deliver CpG ODN in the development of vaccine formulations.

Our lab has also demonstrated that OVA-CpG conjugate molecules are able to induce stronger immune responses than OVA alone[115]. This finding was consistent with the result that OVA and CpG co-loaded microparticles generated higher IgG2a/IgG1 than OVA loaded microparticles alone[114]. Another interesting finding was that mixture of OVA loaded particles and CpG loaded particles generated lower immune response than co-loaded particles. Therefore, it was proposed that particulate formulation loaded with OVA-CpG conjugate would able to induce strong antigen-specific immune response in mice. In addition, we demonstrated that the antigen-specific immune response could be improved by careful control over the sequential delivery of CpG to TLR9[149]. The TLR9 receptor is mainly distributed in the endoplasmatic reticulum of B cells and plasmacytoid dendritic cells in human[109,150,151]. In mice, TLR9 is found in B cells, monocytes and all DC sublets[151]. Translocation of CpG to endosomes/lysosomes allows for co-localization and recognition of DNA by TLR9[150]. After the endocytosis or phagocytosis of pathogen, the stimulation of TLR9 occurs when DNA is in the endosomal or lysosomal vesicles and

binds to TLR9. Therefore, the release profile of OVA and CpG loaded microparticles could influence the final outcomes of immune boost.

In our studies, OVA and CpG ODN were loaded to PLGA microparticles by several different methods. We propose that different loading methods may allow for different release profiles of antigen and adjuvant, the manipulation on sequential release of OVA and CpG, and optimization on the immune response generated by biodegradable microparticles.

Materials

PLGA (75:25) with carboxylic ends (inherent viscosity 0.15 dl/g in chloroform) was purchased from Absorbable Polymers (Pelham, AL).Poly vinyl alcohol (PVA, 87-89% hydrolyzed, MW 30-70 kDa, Lot 039K0147) and PAMAM G3 was purchased from Sigma-Aldrich (St. Louis, MO). CpG was bought from Trilink Biotechnologies (La Jolla, CA). Chicken ovalbumin (OVA) grade VI was purchased from Sigma-Aldrich (St Loius, MO). MicroBCA assay kit was purchased from Promega (Madison, WI). Precast polyacrylamide (PAGE) gel was purchased from Bio-Rad (Hercules, CA). OligoGreen assay kit was bought from Invitrogen (Carlsbad, CA). Dichloromethane (DCM), DMSO and other chemicals were purchased from Fisher Scientific (Pittsburgh, PA).

Methods

Synthesis of OVA-CpG conjugate molecule

PBS-EDTA buffer solution was prepared by dissolving appropriate amounts of EDTA in PBS at 5 mM, and the pH of buffer was adjusted to 7.05. Chicken ovalbumin 116.3 mg was dissolved in 2 PBS-EDTA 3 ml. Sulfo-MBS 26.1 mg was dissolved in DMSO as stock solution and added to OVA solution. The reaction was stopped after 2.5

hrs and mixture was loaded into a P6 column. A total volume of 6 ml elution was collected.

CpG-ODN (15 μmol) was dissolved in 3 ml PBS. Dithiothreitol (DTT) 24.5 mg was added to the CpG solution. The reaction was stopped after 2 hrs and the mixture was loaded into another P6 column (Bio-Rad). Similarly, a total volume of 6 ml elution was collected.

The elutions of OVA and CpG were mixed. In 3 hrs, cystine 60.1 mg was dissolved in 1 ml PBS-EDTA and added to the mixture to stop reaction. Dialysis tubing with MWCO 10,000 was used to purify OVA-CpG conjugate in sterile water. The OVA-CpG was recovered by lyophilization after 3 days dialysis.

Characterization of OVA-CpG conjugate molecule

MicroBCA assay

OVA solution at 2 mg/ml was used as a protein standard and prepared into serial dilutions at x0.5 factor. OVA-CpG was dissolved at 1.1 mg/ml. A volume of 100 μl MicroBCA solution and equal volume of test samples (or dilutions) were mixed and heated for 1 hr before being subjected to a UV-Visible spectrometer set at 562 nm. All dilutions were made with PBS. The amount of OVA in the OVA-CpG conjugate was calculated based on the standard curve.

SDS-PAGE electrophoresis

A pre-cast 4-20% polyacrylamide gel was used to analyze OVA-CpG conjugate molecule. OVA, CpG and OVA-CpG were loaded to gel and run at 100V for 65 min before visualized by Coomassie Brilliant Blue (CBB) staining. Photo of the gel was taken using a Fujifilm F20 digital camera.

The gel was also run in a buffer without SDS under the same conditions as above. Further staining with EtBr was applied to visualize CpG in the conjugate molecule under UV light. Photo of the gel was taken using a Fujifilm F20 digital camera.

Fabrication of PLGA microparticles loaded with OVA, CpG, OVA+CpG, OVA-CpG, (OVA)-CpG and (CpG)-OVA (brackets represent encapsulated particles)

OVA (OVA-loaded PLGA microparticles)

PLGA (100 mg) was dissolved in 1 ml DCM. OVA (5 mg) was dissolved in 100 µl 1.0% w/v PVA solution. OVA solution (100 µl) was transferred into 1 ml PLGA DCM solution and sonicated for 30 sec to produce the first emulsion. The first emulsion was further dropped into a beaker containing 50 ml 1.0% w/v PVA solution under homogenization at 13.5k rpm for 30 sec. The resultant emulsion was kept stirring in the hood for 5-6 hrs to get rid of DCM. OVA loaded PLGA microparticles were collected using centrifugation at 5k rpm for 5 min. PLGA microparticles were washed three times before final lyophilization.

CpG (CpG-loaded PLGA microparticles)

PLGA 100 mg was dissolved in 1 ml DCM. CpG stock solution (approximately 26 mg/ml) containing 2.5 mg CpG 1826 was diluted using 1.0% w/v PVA solution to make 100 µl solution. CpG solution 100 µl was transferred into 1 ml PLGA DCM solution and sonicated for 30 sec to produce the first emulsion. The first emulsion was further dropped into a beaker containing 50 ml 1.0% w/v PVA solution under homogenization at 13.5k rpm for 30 sec. The resultant emulsion was kept stirring in the hood for 5-6 hrs to get rid of DCM. CpG loaded PLGA microparticles were collected

using centrifugation at 5k rpm for 5 min. PLGA microparticles were washed three times before final lyophilization.

OVA+CpG (OVA and CpG co-loaded PLGA microparticles)

PLGA (100 mg) was dissolved in 1 ml DCM. OVA 5 mg was dissolved in 100 µl CpG solution containing 2.5 mg CpG 1826 (stock solution diluted using 1.0% w/v PVA solution to make 100 µl). OVA+CpG solution (100 µl) was transferred into 1 ml PLGA DCM solution and sonicated for 30 sec to produce the first emulsion. The first emulsion was further dropped into a beaker containing 50 ml 1.0% w/v PVA solution under homogenization at 13.5k rpm for 30 sec. The resultant emulsion was kept stirring in the hood for 5-6 hrs to get rid of DCM. OVA+CpG co-loaded PLGA microparticles were collected using centrifugation at 5k rpm for 5 min. PLGA microparticles were washed three times before final lyophilization.

OVA-CpG (OVA-CpG conjugate loaded PLGA microparticles)

PLGA (100 mg) was dissolved in 1 ml DCM. OVA-CpG (5 mg) was dissolved in 100 µl 1.0% w/v PVA solution. OVA-CpG solution (100 µl) was transferred into 1 ml PLGA DCM solution and sonicated for 30 sec to produce the first emulsion. The first emulsion was further dropped into a beaker containing 50 ml 1.0% w/v PVA solution under homogenization at 13.5k rpm for 30 sec. The resultant emulsion was kept stirring in the hood for 5-6 hrs to get rid of the DCM. OVA-CpG loaded PLGA microparticles were collected using centrifugation at 5k rpm for 5 min. PLGA microparticles were washed three times before final lyophilization.

PLGA microparticles coating with PAMAM

PLGA microparticles (50 mg) were suspended in 3 ml MES buffer. Sulfo-NHS 18 mg and EDC 16 mg were dissolved in 500 µl MES buffer respectively. Both sulfo-NHS and EDC were added into the PLGA suspension under magnetic stirring. The suspension was spun at 5k rpm for 5 min in 1.25 hrs. The microparticles collected were re-suspended using 3 ml PBS buffer. PAMAM 40 mg was dissolved using 2 ml PBS under magnetic stirring. PLGA suspension in PBS was dropped into PAMAM solution slowly. The coating reaction was stopped in 5 hrs by centrifugation at 5k rpm for 5 min. Coated microparticles were washed using 0.1M NaCl twice and DI water three times before lyophilization.

(OVA)-CpG (OVA-loaded PLGA microparticles surface adsorbed with CpG)

The coated PLGA-OVA microparticles were suspended in 1 ml DI water. CpG 2.5 mg was added to suspension for 6 hrs incubation at 4 ℃. Micropaticles were spinned at 13.5k rpm for 1 min to remove supernatant and washed once using 500 µl DI water. Finally PLGA-(OVA)-CpG microparticles were regenerated after lyophilization.

(CpG)-OVA (CpG-loaded PLGA microparticles surface adsorbed with OVA)

Similarly, the coated PLGA-CpG microparticles were suspended in 1 ml DI water. OVA (5 mg) was added to the suspension for 6 hrs incubation at 4 ℃. Microparticles were spun at 13.5k rpm for 1 min to remove supernatant and washed once using 500 µl DI water. Finally PLGA-(CpG)-OVA microparticles were regenerated after lyophilization.

Determination of particles size determination, zeta potential and surface morphology

PLGA microparticles were suspended in DI water at 0.5 mg/ml. Approximately 150 µl suspension was transferred to a silicon wafer and dried under the hood overnight. The wafer was mounted on aluminum stubs using liquid colloidal silver adhesives followed with 6 hrs drying at room temperature. Specimens were observed using SEM (Hitachi S-4800). Size of PLGA microparticles was determined using a zetasizer (Malvern Nano ZS, SN#MAL500260) by observing the scattered light at 173 °angle.

Determination of OVA/CpG Loading

The amount of OVA loaded in the PLGA microparticles was determined using the MicroBCA assay. PLGA microparticles (5-10 mg) were treated with 0.3M NaOH solution overnight to break the microparticles and release their cargo. The hydrolysis was neutralized using 1M HCl 300 µl and supernatant was collected after spinning at 13.5k rpm for 30 sec. The supernatant 50-100 µl was subjected to MicroBCA assay using OVA solution of known concentration as standard. The amount of OVA loaded was calculated by multiplying the concentration of OVA in the test sample to adjusted volume.

The amount of CpG loaded into PLGA microparticles was determined using the OligoGreen kit. Similarly, PLGA microparticles (5-10 mg) were treated with 0.3M NaOH solution overnight to break microparticles and release cargo. The hydrolysis was neutralized using 1M HCl (300 µl) and supernatant was collected after spinning at 13.5k rpm for 30 sec. The supernatant (100 µl) was mixed with OligoGreen dilution (100 µl) using CpG solution of known concentration as standard. The amount of CpG loaded was calculated by multiplying the concentration of CpG in the test sample to the adjusted volume.

In vitro release profile at physiological pH and temperature (37 ℃)

PLGA microparticles (30-50 mg) were suspended in 2 ml PBS solution and placed on a shaking bath for 14 days period. 500 µl samples were centrifuged at 13.5k rpm for 30 sec at pre-determined time points and 200 µl supernatant was collected. Samples were analyzed using the MicroBCA and OligoGreen assays to determine the concentration of OVA and CpG. The amounts of OVA and CpG released were calculated based on the concentration and volume of samples.

Animal Care and Handling

Female C57Bl/6 mice of 8 to 10 weeks old were used for immunization. Before beginning any animal experiments, animal training and education courses were carried out through the University of Iowa's Animal Care and Use committee (http://research.uiowa.edu/animal/). Instruction including proper handling and restraint of mice, which minimizes stress on the animal and prevent aggression or defensive responses to handling. For all cases involving anesthesia, a ketamine/xylazine mixture was injected i.p. to deliver 87.5 mg/kg ketamine and 2.5 mg/kg xylazine in a 100 µl injection. This provides full anesthesia within a few minutes and last for approximately 20-30 minutes, with animals returning to full consciousness and mobility within 2 hours. At the end of the studies, or to harvest organs, mice were euthanized using CO_2 and death confirmed by cervical dislocation. Throughout the course of all experiments, mice were monitored daily by the University of Iowa Animal Care. Great care was taken to optimize formulations prior to injection to minimize the number of animals necessary for each experiment while retaining significance.

Immunization studies

Mice were administered vaccines subcutaneously (s.c.) on the flank on day 1(week 0) and day 14 (week 2). The PLGA microparticle formulations administered were the following: empty microparticles; PLGA-OVA; PLGA-CpG; PLGA-(OVA+CpG); PLGA-(OVA-CpG); PLGA-(OVA)-CpG; PLGA-(CpG)-OVA. The amount of OVA administered was normalized to 50 μg.

Antigen-specific antibody response and Th-1 response quantification by Enzyme-linked immunosorbent assay (ELISA)

Serum was collected by sub-mandibular bleeding from mice at pre-determined time points after immunization injection. Microtiter plates were coated using 5 μg/ml OVA antigen and incubated overnight at 4 ℃. Wells on plates were saturated using 5% milk and serum serial dilutions were added. Plates were washed before adding heavy chain-specific goat anti-mouse IgG, IgG1 or IgG2a and the colometric substrate P-nitrophenylphosphate. Serum from naïve mice to which a known concentration of monoclonal anti-OVA (4A9) antibody was added served as the standard and positive control. The negative control was pre-treatment (naïve) mouse serum. Plates were recorded using a microplate reader and curves established for each sample. The concentration of anti-OVA IgG2a was determined by comparing standard curves and test samples.

Tetramer staining for enumeration of antigen-specific CD8+ cells

MHC tetramers are complexes of 4 MHC molecules, which are associated with a specific peptide and bound to a fluorochrome. Class I tetramers bind to a distinct set of T cell receptors (TCRs) on a subset of CD8+ cells and thus helps in an accurate

enumeration of cytotoxic T cells (CD8+) that are essential for lysis of tumor cells. At the end of day 28 of the immunization cycle, the mice vaccinated are sacrificed and spleen harvested for tetramer staining to enumerate a CD8+ response.

DC proliferation study

Bone marrow derived DCs were obtained from a 12 week old naïve C57BL/6 mouse. They were cultured in RPMI (+10% FCS) Plus GM-CSF. Detailed method was described in the literature[152].

On day 8 of culture, floating DCs were harvested and seeded into 6 well trays at 7.5 x 10^5/well and allowed to incubate for 1 hour in 3 ml media (+GM-CSF). Then particles were added so that all wells (except untreated and control CpG wells) experienced 2 μg/ml of CpG. This resulted in each well receiving 1 mg of particles except for the PLGA (OVA)-CpG well which received approx 2.4 mg. Untreated control and positive control wells were included (The positive control included the addition of soluble CpG at 2 μg/ml)

Immunofluorescence on DCs

After 48 hours (37 ℃, 5% CO_2) adherent and floating DCs were harvested and stained for CD86, MHC class II and H2Kb independently using PE-labeled antibodies. A PE-labeled Rat Antibody with no specificity was used as a negative control. In brief DCs were allowed to incubate on ice with specific antibodies at a final concentration of 5 μg/ml for 45 minutes unbound antibody was washed away and cells were fixed and later acquired and analyzed using a FACScan flow cytometer and FlowJo software respectively.

Results

Synthesis and characterization of OVA-CpG conjugate molecule

The method for synthesizing the OVA-CpG conjugate molecule was a modified method based on a previous study conducted in our lab[115]. OVA and CpG were linked together by the reaction between maleimide and thiol groups. The concentration of OVA was normalized using BSA standard. By calculating the amount of OVA in OVA-CpG, it was estimated that on average every 3.5 CpG molecules were conjugated to a single OVA molecule. Considering the MW of OVA is about 44 kDa, the influence of CpG on the MW of OVA-CpG conjugate was not significant. Therefore, it was reasonable to predict that band migration of OVA and OVA-CpG conjugate on SDS-PAGE gels were comparable to each other. As shown in Figure 4-1 and 4-2, the CBB/EtBr staining and following visualization demonstrated that the existence of both OVA and CpG in the same molecule. These results leads to the conclusion that OVA and CpG were linked together successfully in this study.

Fabrication of PLGA microparticles loaded with OVA, CpG, OVA+CpG, OVA-CpG, (OVA)-CpG and (CpG)-OVA

The fabrication of PLGA microparticles was carried out using the water in oil in water (w/o/w) double emulsion technique. PVA was selected to serve as a surfactant in the preparation. All the microparticle formulations were analyzed using a Malvern zetasizer to determine size and zeta potential values. Table 4-1 shows a summary of particle size and zeta potential data. The size of microparticles prepared using the double emulsion method was around 4 μm. Microparticles had a net zeta potential of -20 mV or lower because the PLGA material used in the fabrication had carboxylic acid end groups.

The free carboxylic acid terminals generate a negative charge on the surface of microparticles. The sizes of (OVA)-CpG and (CpG)-OVA were greater than (OVA) and (CpG) (the parent microparticles) and this corresponded to a slight size increase after PAMAM coating.

OVA/CpG Loading, size and zeta potential determination

The amounts of OVA and CpG loaded into PLGA microparticles were analyzed using MicroBCA and OligoGreen assays respectively. Protocols were adopted from the manufacturer's instruction. The summary of results from these assays is listed in Table 4-1.

The size and zeta potential of polymer/pDNA complexes was measured using a Zetasizer (Malvern Nano ZS, SN#MAL500260). Microparticles were prepared into suspension at 0.5 mg/ml and loaded into sample cuvettes. The SEM micrographs in Figure 4-3 show spherical PLGA microparticles were fabricated. The PLGA microparticles had a uniform size distribution. No obvious surface defects were found in any of the microparticle formulations.

In vitro release profile

In vitro release profiles are shown in Figure 4-4. Overall the microparticles showed sustained release of OVA and CpG over 14 days period. (CpG)-OVA displayed faster release of OVA relative to all other groups because OVA was physically adsorbed on the microparticles surface. At day 7, 82% of OVA was released from (CpG)-OVA. (OVA)-CpG also showed a fast release of OVA after day 3, reaching 69% by day 7. (OVA-CpG) exhibited fast release on day 1, followed by a sustained release over the following 13 days. (OVA) and (OVA+CpG) microparticles showed less burst release

compared to other formulations, but at day 5 followed with steady release of OVA over the rest of the next 9 days. A similar pattern was seen for CpG release as well. All formulations containing CpG showed a rapid release of CpG on day 1 except for co-loaded (OVA+CpG). (OVA+CpG) did not undergo a rapid release until day 4. (OVA)-CpG and (CpG)-OVA exhibited the fastest release of CpG and OVA. (CpG) and (OVA-CpG) microparticles showed a sustained release of CpG after the initial burst. At day 14, all formulations released at least 46% OVA/CpG into the media.

Immunization studies

We evaluated the effect of microparticles on primary DCs. The DCs were generated from mice marrow and incubated with microparticles for 24 or 48 hrs and assessed for CD86, H2Kb and MHC II markers by flow cytometry. Figure 4-5 summarized expression of markers after incubation co-loaded PLGA microparticles. CD86 is marker for activation and maturation of DCs. Empty microparticles, did not induce DC activation and maturation. All formulations induced up regulation of CD86. Among them, OVA+CpG, OVA-CpG and (OVA)-CpG showed higher expressions of CD86 than OVA loaded microparticles. The level of CD86 after activation was significantly higher than the positive control of a soluble form of CpG ODN. (CpG)-OVA did not induce significant CD86 marker up-regulation probably due to the rapid release of OVA after administration and before endocytosis by DCs. (OVA)-CpG generated the highest expression of CD86. OVA+CpG, (OVA)-CpG and (CpG)-OVA up-regulated H2Kb markers more than any of the other microparticles, but less than the positive control of soluble CpG. These results suggest that a strong stimulus for clonal expansion and differentiation of T cells into cytotoxic CD8+ T cells could be generated

by microparticles co-loaded with OVA and CpG. Additional experiments that evaluated MHC II expression showed that particles did not generate significant differences to control groups. Co-delivery of CpG and OVA generated stronger antigen-specific immune responses than delivery of OVA alone.

Figure 4-6 confirm that (OVA)-CpG microparticles can induce strong DC activation. Microparticles induced a significantly higher percentage of CD86 markers on DCs than soluble CpG, suggesting a more robust activation and maturation. Both soluble form CpG and (OVA)-CpG microparticles induced CTL proliferation but the soluble CpG also generated strong stimulus for CD4+ T cells.

The IgG response shown in Figure 4-7 was quantitatively measured by ELISA using serum collected from mice two and four weeks after vaccination. OVA+CpG and (OVA)-CpG microparticles showed the strongest overall antigen-specific antibody responses. Significant increases were observed for anti-OVA IgG1 levels relative to all other microparticle formulations. The IgG2a levels were significantly higher in mice administered with (OVA)-CpG than any other group. Interestingly, OVA-CpG conjugate loaded microparticles did not show a high level of IgG1 and IgG2a. Mice boosted with empty microparticles did not generate OVA-specific IgG1 or IgG2a responses. Similar results were found in mice treated with CpG loaded microparticles in the absence of OVA. Mice injected with OVA loaded microparticles generated a weak response, compared to (OVA+CpG) and (OVA)-CpG.

These results are consistent with our hypothesis that co-delivery of TLR9 ligand CpG ODN and OVA antigen help increase Th-1 type immune responses. The IgG1 and IgG2a levels also showed a progressive increase over time, from 2 weeks to 4 weeks after

vaccination. These results suggest that microparticles are able to induce and maintain a high Th-1 type immune response over time.

Figure 4-8 shows that mice had a significant increase in antigen-specific CD8+ T-cells if vaccinated with OVA-CpG, (OVA)-CpG and (CpG)-OVA microparticles. OVA or CpG only loaded microparticles did not generate a high percentage of OVA specific cytotoxic CD8+ cells, suggesting a small population of killer cells against OVA. OVA+CpG generated a slightly higher percentage but not significant. OVA-CpG was the most potent formulation in generating OVA-specific CD8+ cells. Both (OVA)-CpG and (CpG)-OVA also generated robust antigen-specific immune responses albeit lower than OVA-CpG microparticles.

Discussion

Our goal was to deliver both antigen and adjuvant to the same APCs to generate a stronger antigen-specific immune response. Several aspects were considered in the development of this particulate based vaccination system. Particulate delivery can provide sustained release of antigen and adjuvant, eliminating the need for repeated administrations. It has also been demonstrated that particulate delivery of CpG can significantly improve its potency as an adjuvant in inoculation[111]. OVA and CpG co-loaded microparticles also generate enhanced Th-1 type immune response relative to delivery of either component alone[114].

First OVA and CpG were linked via a maleimide-thioether bridge. The CpG used in this study was in a dimer form connected via a disulfide bond.A reducing agent, DTT, was added to convert dimer into CpG ODN with reactive thiol terminals. At the same time OVA was reacted with sulfo-MBS to create a maleimide group, which provided an

insertion site for thiol under ambient conditions. The conjugate molecule was prepared by mixing CpG thiol and OVA maleimide together and the conjugate CpG-OVA molecule was then purified.

SDS-PAGE and native PAGE gels were used to analyze the conjugate molecule. Because EtBr was used to visualize OVA-CpG, SDS was excluded from the electrophoresis buffer. SDS is s surfactant and greatly increases the solubility of EtBr in buffer. Therefore, CpG would not bind to OVA-CpG in the SDS-PAGE gel after rinsing.

Using the double emulsion solvent evaporation technique, PLGA can be fabricated into microparticles that are on average 3-4 μm in size, leaving carboxylic groups on the particles surface for further modification. The surface charge of PLGA particles was -20 to -30 mV before coating with PAMAM G3. Coating treatment reversed the surface charge to +20 to +30 mV. The net positive charge allows for the adsorption of OVA or CpG which has a net negative charged. A near neutral surface charge was observed after adsorption, and size change of particles was not significant. Both PLGA particles and PAMAM coated particles showed smooth and spherical appearance under SEM microscope. The additional steps carried out after loading of particles such as PAMAM surface modification moderately reduced the overall loading levels of CpG or OVA respectively. The possible reason could be the burst release loaded agents in the particles whilst they were stored in buffers used for chemical modification. The OVA or CpG that diffused into buffers was lost during each round of treatment.

Release profiles showed that both OVA and CpG were successfully loaded to PLGA microparticles, and sustained release was observed over a 14 days period. The release of CpG was more rapid than OVA, possibly due to the smaller MW of CpG

relative to OVA. Another finding was the fast release of surface adsorbed materials during the first 7 days period. The electrostatic interaction was relatively weak so that the dissociation of OVA or CpG from the particles surface was easier than the diffusion from the PLGA matrix.

It was reported that two doses of vaccine can generate significantly higher antigen-specific immune responses than one inoculation but further vaccinations had no additional benefit. Therefore, in this study, mice were boosted twice on day 1 and day 14. Analysis of in vitro DC activation revealed that co-delivery of OVA and CpG by microparticles was able to induce maturation of DCs. Probably due to the loss of CpG in loading OVA to the particles surface, PLGA-(CpG)-OVA did not induce strong maturation of DC. The microparticulate formulations of OVA+CpG, OVA-CpG and (OVA)-CpG all generated strong DC activation. ELISA results showed that (OVA)-CpG microparticles generated the highest anti-OVA specific IgG1 and IgG2a levels relative to all other formulations. The OVA+CpG microparticles also showed high IgG2a levels, but the IgG1 levels were not significantly higher than others. The IgG2a/IgG1 ratio of OVA+CpG particles was the highest, suggesting a polarized Th-1 type antigenspecific response. However, the OVA-CpG conjugate loaded particles did not generate as strong IgG1/IgG2a levels as other co-loaded particles. One explanation for this might include the lower dose of CpG in the conjugate molecule, or conformational changes during conjugation. A significant improvement of IgG1 and IgG2a levels over time suggest that a boost dose of microparticles is critical for a maximal antigen-specific immune response, which is consistent with other studies. The tetramer staining results also showed (OVA)-CpG particles were more efficient in generating anti-OVA specific CD8+ T cells.

OVA+CpG co-loaded particles were not significantly more efficient than OVA loaded particles. (CpG)-OVA particles were efficient at generating antigen-specific immune responses, although this was not significantly higher than other formulations.

In summary, our results demonstrated that co-loaded microparticles of OVA and CpG can deliver both antigen and adjuvant to the same DCs, and induce strong Th-1 polarized antigen-specific immune responses. The sequential release of OVA and CpG from microparticles can also be used to optimize the magnitude and type of immune response generated. Amongst all the particles loaded with OVA and CpG, (OVA)-CpG was the most efficient in inducing DCs maturation, generating high IgG level, and generating OVA-specific CD8+ T lymphocytes.

Table 4-1: summary of size, zeta potential and OVA/CpG loading of microparticles

	size nm	zeta potential mV	OVA μg/mg	CpG μg/mg
OVA	3640.3 ±620.3	-26.7 ±1.1	33.8 ±3.7	
CpG	4573.6 ±570.5	-21.2 ±0.4		17.9 ±1.1
OVA+CpG	5870.3 ±522.1	-22.2 ±0.3	20.6 ±3.3	9.83 ±0.31
OVA-CpG	3899.3 ±590.9	-26.8 ±1.7	23.4 ±2.3	6.48 ±0.49
(OVA)-CpG	4478.0 ±148.9	1.86 ±0.25	18.1 ±0.9	2.71 ±0.26
(CpG)-OVA	4595.0 ±451.8	-2.4 ±0.6	1.46 ±0.13	6.39 ±0.2

Note: data shown as Mean ±SD, n=3; (OVA)-CpG and (CpG)-OVA group, n=2

Figure 4-1: SDS-PAGE gel electrophoresis stained with CBB

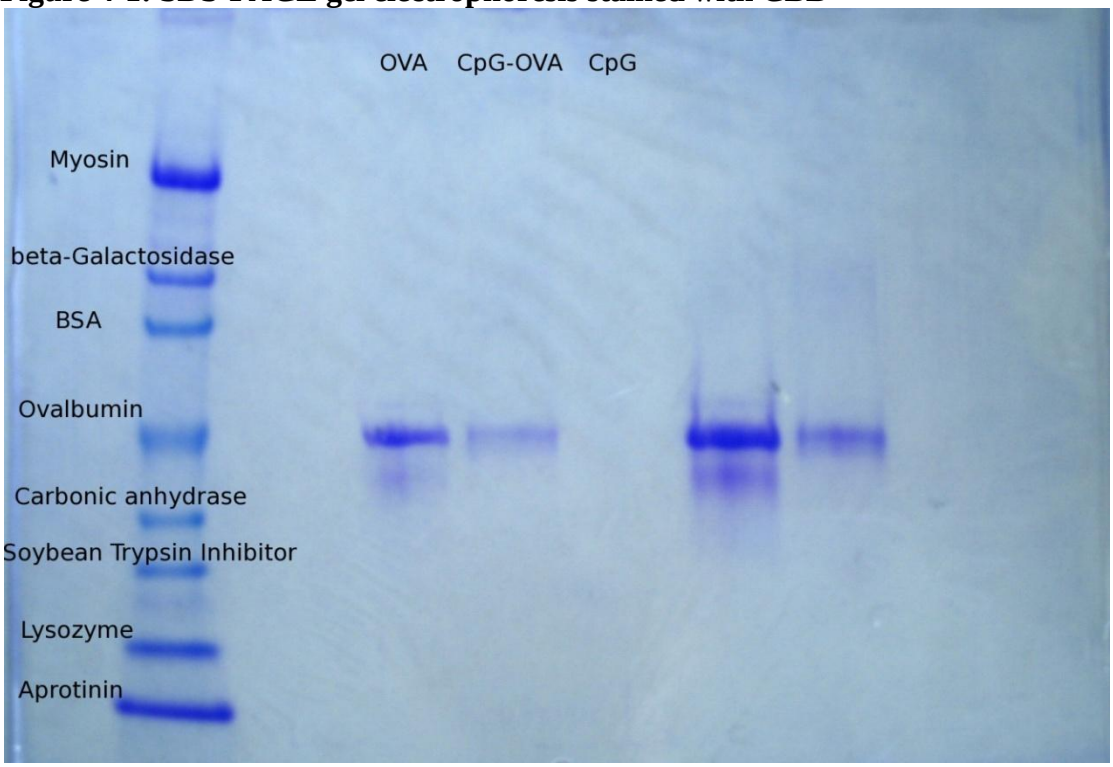

Note: from left to right: ladder, OVA, OVA-CpG conjugate and CpG

Figure 4-2: PAGE gel electrophoresis stained with EtBr

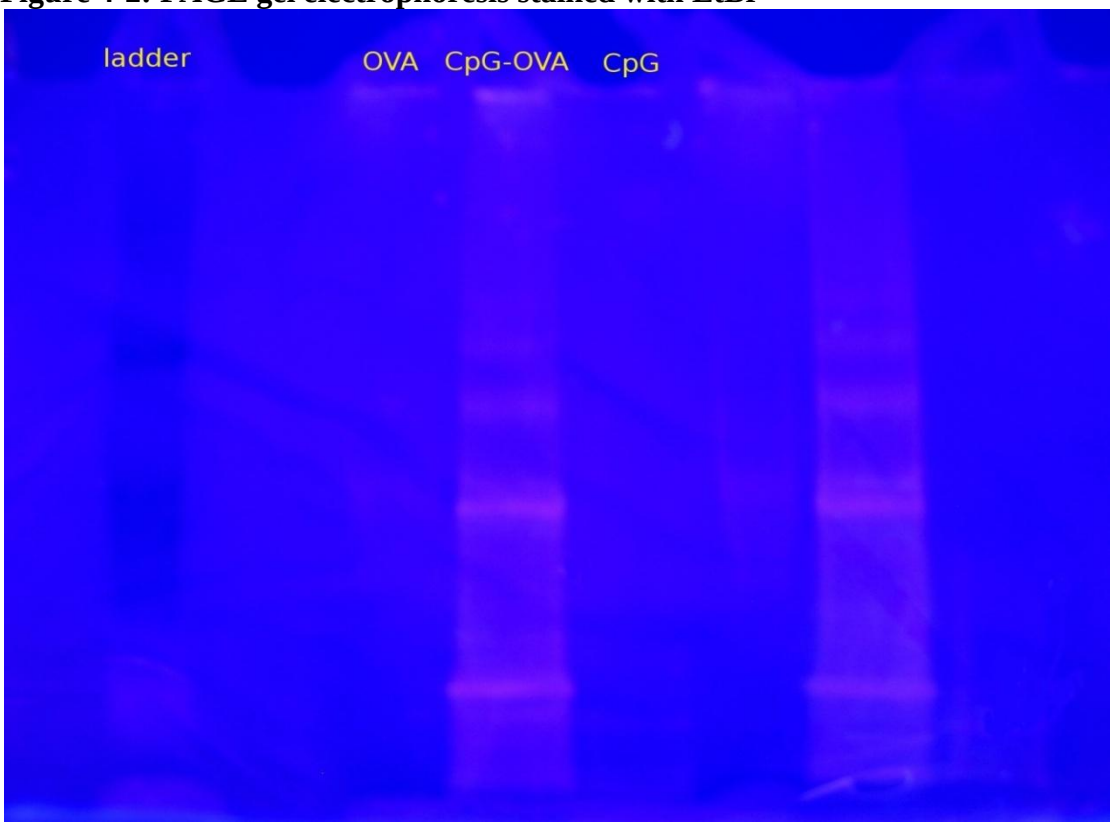

Note: from left to right: ladder, OVA, OVA-CpG conjugate and CpG.

Figure 4-3: Scanning Electron Microscopy

A

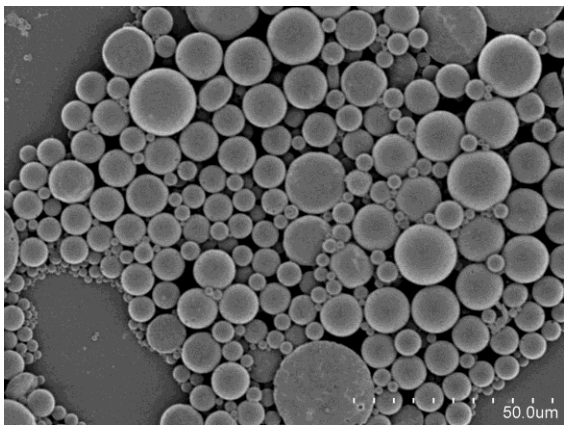

B

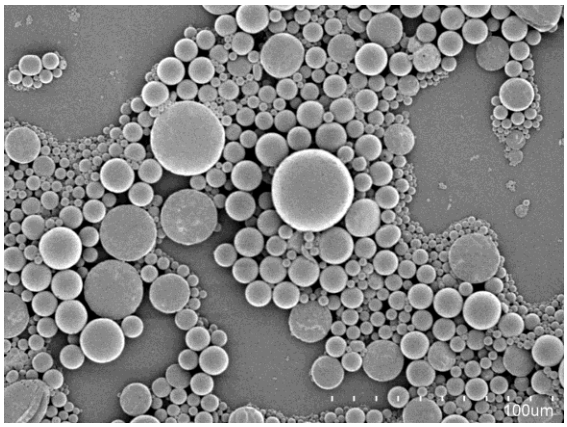

C

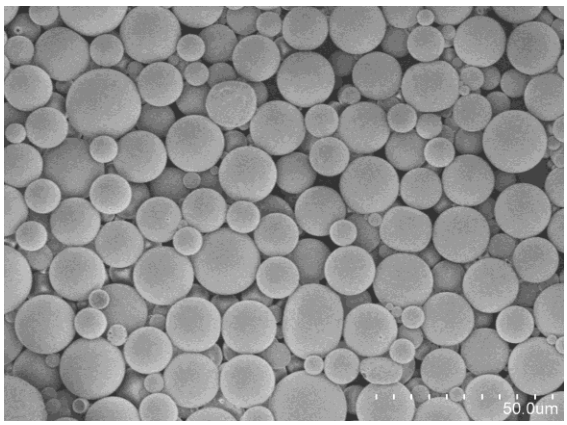

Figure 4-3 continued

D

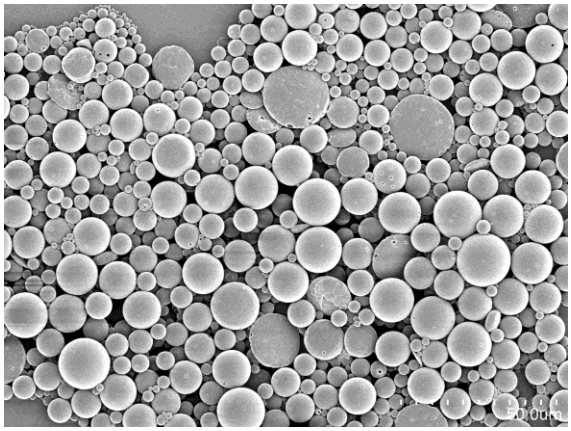

E

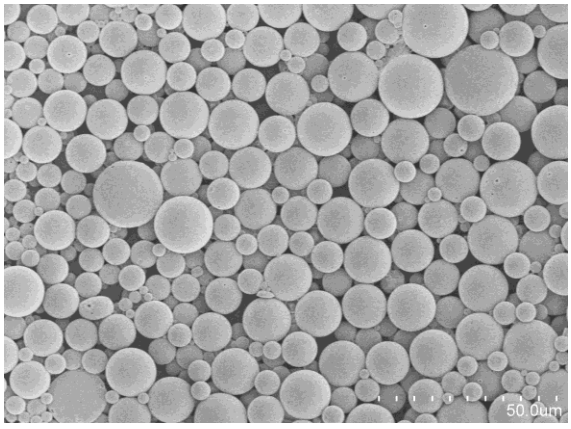

F

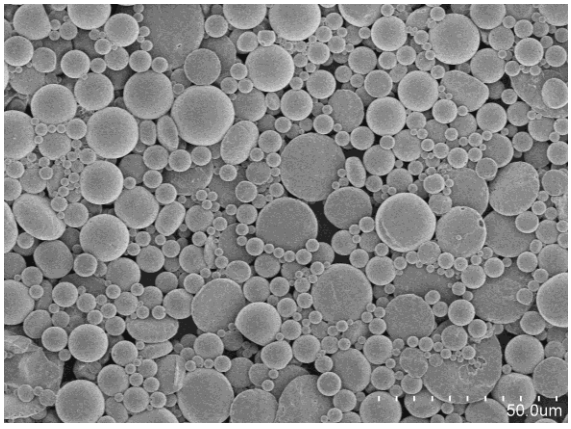

Note: A, PLGA-OVA; B, PLGA-CpG; C PLGA-OVA+CpG; D, PLGA OVA-CpG; E, PLGA-(OVA)-CpG; F, PLGA-(CpG)-OVA

Figure 4-4: *in vitro* release profile of microparticles

A

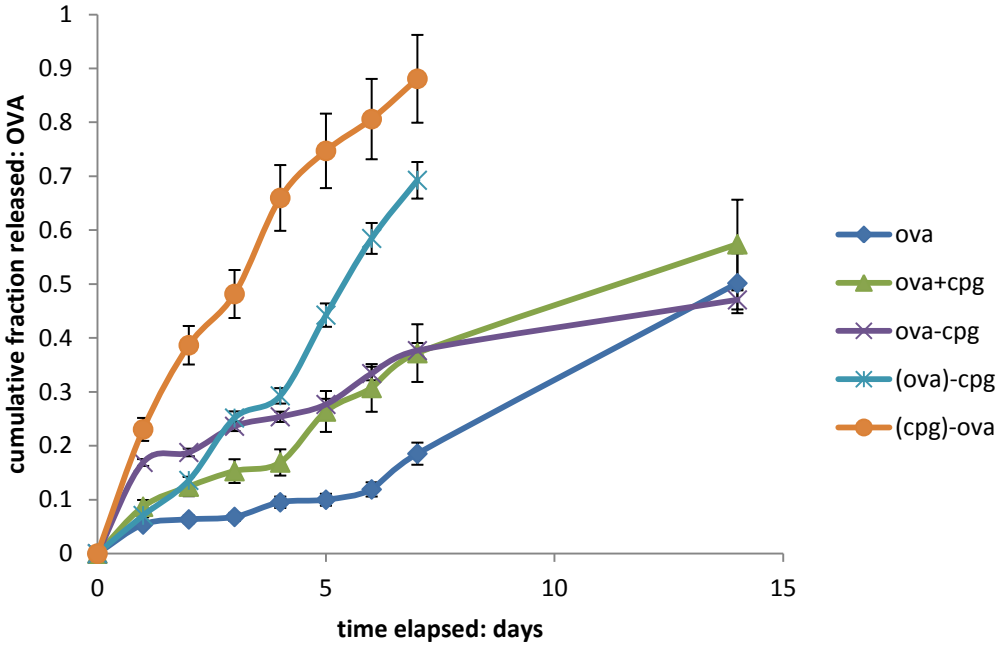

B

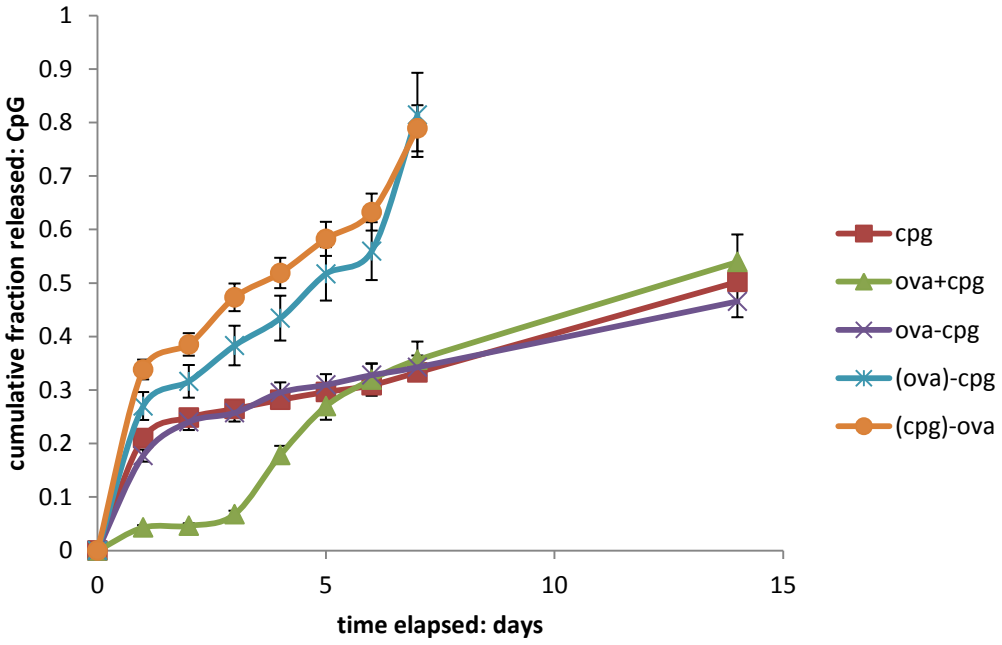

Note: A, release of OVA; B, release of CpG. Mean ±SD, n=3

Figure 4-5: MHC Class I (H2Kb) MHC class II and CD86 expression

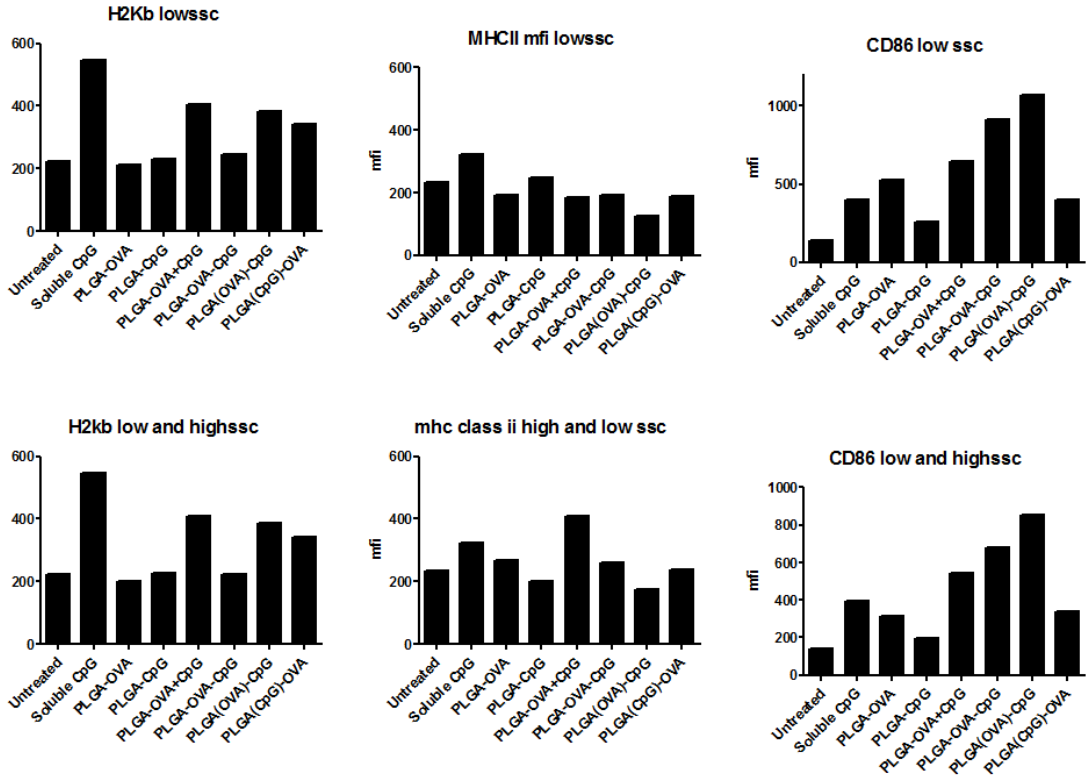

Note: low ssc = DCs that possibly have Not taken up particles based on side scatter values; low and high ssc includes all DCs

Figure 4-6: cell flow cytometry

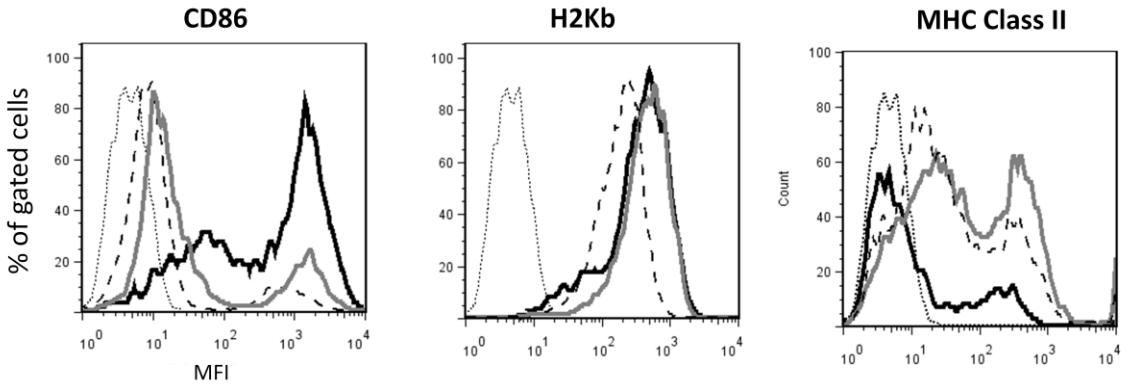

Note: Dotted line = DCs (+ neg cont antibody)
Dashed line = Untreated DCS (+ anti-Marker antigen (indicated))
Thick Grey line = DCs treated with soluble CpG (+ anti-Marker antigen (indicated))
Thick Black line = DCs treated with PLGA (Ova)-CpG (+ anti-Marker antigen (indicated))

Figure 4-7: anti-OVA specific IgG level by ELISA

A

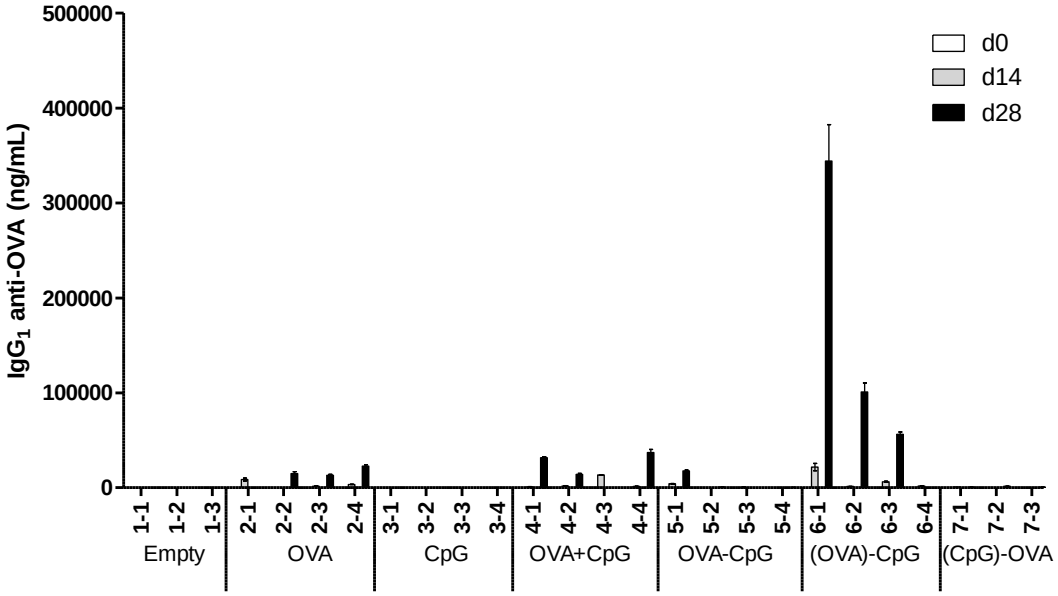

B

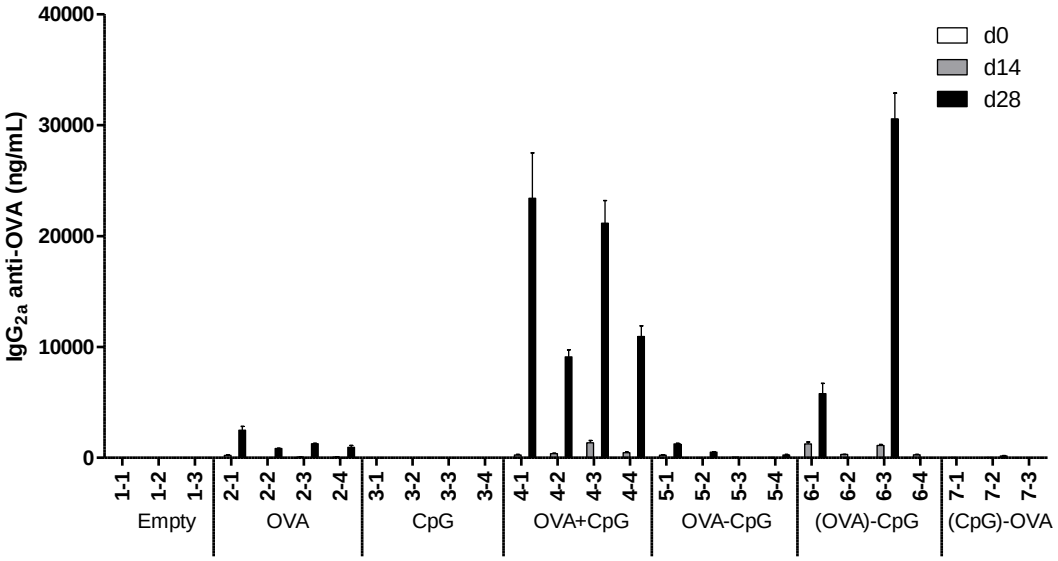

Note: A, IgG1; B, IgG2a

Figure 4-8: anti-OVA specific CD8+ T cells percentage

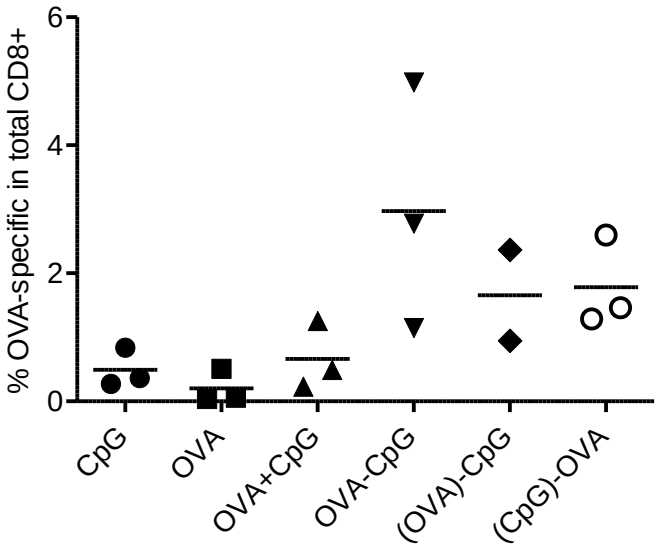

Note: detection by K^b-OVA_{257} tetramer staining and statistical analysis of the frequency of OVA-specific CD8+ splenocytes. Analysis was performed 14 days after immunization of C57BL/6 mice. Data represents values measured in individual mice/group with the line showing the mean for the group.

CHAPTER 5: CONCLUSIONS AND FUTURE WORK

Our research studies focused on the development of carrier systems for gene and vaccine delivery. Cationic polymers were used to condense siRNA and plasmid DNA. Mannose, PEG and PEI were used to build a carrier for siRNA. Mannose served as a cell binding ligand that could induce endocytosis. The use of mannose was expected to result in efficient delivery to DC whose surface presents mannose receptors. The PEG component was selected to provide stealth properties to the complexes formed with polymer and siRNA. The inclusion of PEG helps reduce toxicity of PEI and extends the circulation half life of complexes. An additional advantage of PEGylation is decreased non-specific phagocytosis and increased delivery efficiency. A delivery system composed of these elements has much greater potential for *in vivo* applications. As part of our studies, we aimed to identify the influence of the location of the mannose ligand on the PEGylated PEI constructs on gene silencing and toxicity. For this reason, PEGylated mannosylated PEI was assembled in two different structures. In the first, PEG was used as a spacer between mannose and PEI. In the second, mannose and PEG were attached directly to the PEI. Both constructs were synthesized and tested as an siRNA carrier. ^{1}HNMR and resorcinol assays were conducted to characterize the structure of the polymer and to determine the content of each component. All of the modified PEIs were able to complex and condense siRNA into particles at N/P ratios of 1 and above as determined by gel electrophoresis assays. Only the complexes formed with mannose-PEI conjugates showed some migration at N/P 1, but even these were fully retarded at N/P what limitation do u see to ratios of 3 and above. The size of complexes formed with polymer and siRNA was small enough for efficient uptake by RAW cells, resulting in

efficient delivery of siRNA. The lowest efficiency was observed with mannose-PEI. Mannose-PEG-PEI showed significantly faster delivery of siRNA than mannose-PEI-PEG, with abundant distribution inside the broadest range of cells. Confocal microscopy studies suggested that siRNA delivered using mannose-PEG-PEI allowed for fast escape of siRNA from lysosomes. In these studies, siRNA was distributed in the perinuclear area which allows for siRNA to be readily incorporated in RISC and thereby initiate the RNAi process. The incorporation of siRNA into RISC is known to be a critical step in gene silencing. After validating the various polymers ability to deliver siRNA, gene knockdown was conducted to compare the efficiency of the various carriers. RT-PCR analysis showed that mannosylated pegylated PEI resulted in slightly better but comparable mRNA knockdown efficiencies when compared to PEI. The difference was not significant between mannose-PEG-PEI and mannose-PEI-PEG. Mannosylation did moderately decrease the gene knockdown efficiency and this was found to be broadly correlated with with decreased cell uptake. Characterization of protein levels was determined using the dual luciferase reporter assay. Mannose-PEG-PEI was the most effective material in generating gene knockdown amongst all the modified PEIs tested. At an N/P ratio of 3, PEG-PEI showed better knockdown than mannose-PEG-PEI. PEI showed the highest knockdown at an N/P ratio of 10, which was slightly stronger than mannose-PEG-PEI. However, at an N/P ratio of 3, mannose-PEG-PEI was more efficient at gene knockdown than PEI. When also taking into consideration the toxicity reduction achieved after PEGylation, we expect mannose-PEG-PEI to have more advantages when used *in vivo*. Both mannosylation and PEGylation reduced the toxicity of PEI. Mannose-PEG-PEI showed stronger cellular uptake and greater gene knockdown than mannose-

PEI-PEG. PEG-PEI also showed decreased toxicity relative to PEI alone which is an observation that is consistent with findings in the literature. Toxicity was also correlated to polymer concentration with increasing concentrations increasing toxicity. In summary, we found that both mannose-PEG-PEI and PEG-PEI were promising candidates for siRNA delivery. Further optimization on the degrees of mannosylation and PEGylation could enhance toxicity and gene knockdown further. As reported in previous studies, too high an abundance of ligands conjugated to polymers can reduce binding to cell surface receptors and this could account for the lowered gene knockdown efficiency of mannose-PEI. Optimized degrees of PEGylation could generate an appropriate balance between steric stabilization, strong endocytosis and optimal gene knockdown. In addition, other targeting moieties can be used to replace mannose to further increase the knockdown efficiency and target other cell types. Galactose, transferrin, RGD and TAT peptides are commonly used targeting units in gene delivery and could readily replace mannose in this construct using similar chemistries.

In the next project, dextran-PEI conjugate polymers were developed as a carrier for plasmid DNA that had lower toxicity and improved stability in serum relative to PEI alone. As pointed out earlier, toxicity is a major concern in the application of PEI. Several approaches have been tried to decrease the toxicity of PEI. In addition, PEI-pDNA complexes tend to aggregate in the presence of serum. For these nanoparticles to be applicable to *in vivo* applications, they must be stable in the presence of serum. Aggregation of nanoparticles can cause capillary embolism and decrease the efficiency of transfections. Dextran was selected and used to modify PEI so as to impart properties that include stability in serum and reduced toxicity. The overall structure was developed to be

hydrolysable because of the dextran component. Dextran was oxidized to generate aldehyde groups which are highly reactive with PEI. The success of conjugation was confirmed using ^{1}HNMR and the content of PEI in the conjugates quantified. Conjugate polymers made with PEI 2000 were able to complex and condense plasmid DNA efficiently. However, polymers prepared using the lower Mw PEI 800 were less effective at plasmid DNA complexation. Gel electrophoresis assays showed that DP1 and DP2 were able to fully retard migration of complexes prepared at N/P ratios of 10 and 15, but not at N/P ratios of 5. In contrast, DP3 and DP4 which were made with PEI 2000 showed full retardation at all N/P ratios, suggesting a compact DNA condensing into particles. These findings were consistent with the sizes of complexes determined using zetasizer measurements. DP1 and DP2 produced larger complexes with plasmid DNA at N/P ratios of 5. DP3 and DP4 generated compact complexes suitable for cellular uptake. All the conjugates synthesized were able to provide a net positive charge in complexes. Toxicity studies using the MTS assay showed that dextran modification significantly reduced relative to unmodified PEI 25k. Dextran-PEI was tested as a gene carrier in transfection studies with HEK293 cells. DP3 and DP4 generated slightly lower efficiencies than PEI in serum free culture media. When the media was replaced with media containing serum, DP3 and DP4 showed improved transfection efficiencies that were comparable to PEI 25k. The efficiencies of DP3 and DP4 were further increased and significantly higher than PEI's when incubated in serum containing media for an extended time period of 48 hrs. Similar results were found in COS7 cells transfected with dextran-PEI. The improved efficiency was thought to be related to the improved stability of complexes in serum, as demonstrated by turbidity study results. Intracellular trafficking studies showed that DP3

complexes separated from lysosomes suggesting that the gene cargo had been released into the cytoplasm and provided a strong explanation as to the reasons why dextran-PEI conjugates were generating strong transfection efficiencies. The results generated in this study suggest that dextran-PEI conjugates have strong potential for gene delivery.

Our lab has previously shown that PLGA microparticle have strong potential in gene and vaccine delivery applications. In particular, our lab has previously identified that co-delivery of CpG ODN and antigens generates stronger antigen-specific immune responses than delivery of either component alone or both components delivered in solution. We believed that the sequence of OVA and CpG release could be used to optimize this response even further. In this study, we evaluated several different types of PLGA microparticles. PAMAM coated PLGA microparticles loaded with OVA and CpG were fabricated using the w/o/w double emulsion technique. OVA and CpG was conjugated together using sulfo-MBS and thiol linkage. The conjugate was analyzed using MicroBCA and SDS-PAGE electrophoresis assays. The ratio of CpG conjugated to OVA was determined to be approximately 3.5 to 1. As the Mw of OVA was much larger than CpG, the conjugate of CpG was not affecting the size of OVA significantly. This result was consistence with SDS-PAGE gel results which showed a similar migration of OVA and OVA-CpG bands with relatively close Mw values. In another electrophoresis assay without SDS, the gel was stained using EtBr and visualized under UV. The band of OVA-CpG indicated the existence of CpG in the OVA-CpG conjugate. Neither OVA nor CpG alone was visible on the gel, because OVA was not intercalated with EtBr and CpG was too small and not retained in the gel. Using a zetasizer, the size and zeta potential values of PLGA microparticles were measured. The size of microparticles was in range

that could be efficiently internalized by dendritic cells, and the net negative zeta potential was attributed to the carboxylic end groups on the PLGA.. SEM micrographs confirmed the size of the microparticles. The release studies of CpG and OVA from PLGA microparticles were conducted at room temperature and physiological pHAll formulations showed a sustained release of OVA/CpG over a time course of 14 days. A typical initial burst release of CpG was observed for the first day in all microparticle formualtions except for OVA+CpG co-loaded formulation. Physical adsorption of OVA/CpG was released quickly within 7 days. Typically, at least 50% release of OVA/CpG was released by 14 days, which is appropriate and necessary for vaccine applications. Mice were injected subcutaneously with the various microparticle vaccine formulations. The upregulation of the CD86 marker suggests that microparticles could induce a strong activation and maturation of DC. The upregulation of H2Kb by OVA+CpG, (OVA)-CpG and (CpG)-OVA suggests that these formulations could induce a strong cytotoxic CD8+ T cell response. In contrast, MHC II marker levels that typically correlate to CD4+ T cell responses were not significant. The antigen-specific IgG1 and IgG2a antibody responses indicated that OVA+CpG and (OVA)-CpG microparticles generated the strongest antigen-specifc immune response amongst all the groups tested Tetramer staining showed that OVA-CpG, (OVA)-CpG and (CpG)-OVA microparticles generated the highest antigen-specific cytotoxic CD8+ T cell responses. Based on these results, it was concluded that sequential release of OVA and CpG can be used to enhance the antigen-specific immune response and that this should be taken into consideration in the future design and development of particle based vaccines.

REFERENCES

1. Engelhardt JF, Wilson JM 1992. Gene therapy of cystic fibrosis lung disease. J Pharm Pharmacol 44 Suppl 1:165-167.

2. Boucher RC, Knowles MR, Johnson LG, Olsen JC, Pickles R, Wilson JM, Engelhardt J, Yang Y, Grossman M 1994. Gene therapy for cystic fibrosis using E1-deleted adenovirus: a phase I trial in the nasal cavity. The University of North Carolina at Chapel Hill. Hum Gene Ther 5(5):615-639.

3. Parkman R, Gelfand EW 1991. Severe combined immunodeficiency disease, adenosine deaminase deficiency and gene therapy. Curr Opin Immunol 3(4):547-551.

4. Ramsey WJ, Mullen CA, Blaese RM 1995. Retrovirus mediated gene transfer as therapy for adenosine deaminase (ADA) deficiency. Leukemia 9 Suppl 1:S70.

5. Jolly DJ 1991. HIV infection and gene transfer therapy. Hum Gene Ther 2(2):111-112.

6. Mackiewicz A, Gorny A, Laciak M, Malicki J, Murawa P, Nowak J, Wiznerowicz M, Hawley RG, Heinrich PC, Rose-John S 1995. Gene therapy of human melanoma. Immunization of patients with autologous tumor cells admixed with allogeneic melanoma cells secreting interleukin 6 and soluble interleukin 6 receptor. Hum Gene Ther 6(6):805-811.

7. Anderson WF 1990. September 14, 1990: the beginning. Hum Gene Ther 1(4):371-372.

8. Morgan RA, Dudley ME, Wunderlich JR, Hughes MS, Yang JC, Sherry RM, Royal RE, Topalian SL, Kammula US, Restifo NP, Zheng Z, Nahvi A, de Vries CR, Rogers-Freezer LJ, Mavroukakis SA, Rosenberg SA 2006. Cancer regression in patients after transfer of genetically engineered lymphocytes. Science 314(5796):126-129.

9. Ott MG, Schmidt M, Schwarzwaelder K, Stein S, Siler U, Koehl U, Glimm H, Kuhlcke K, Schilz A, Kunkel H, Naundorf S, Brinkmann A, Deichmann A, Fischer M, Ball C, Pilz I, Dunbar C, Du Y, Jenkins NA, Copeland NG, Luthi U, Hassan M, Thrasher AJ, Hoelzer D, von Kalle C, Seger R, Grez M 2006. Correction of X-linked chronic granulomatous disease by gene therapy, augmented by insertional activation of MDS1-EVI1, PRDM16 or SETBP1. Nat Med 12(4):401-409.

10. Brown BD, Venneri MA, Zingale A, Sergi Sergi L, Naldini L 2006. Endogenous microRNA regulation suppresses transgene expression in hematopoietic lineages and enables stable gene transfer. Nat Med 12(5):585-591.

11. Maguire AM, Simonelli F, Pierce EA, Pugh EN, Jr., Mingozzi F, Bennicelli J, Banfi S, Marshall KA, Testa F, Surace EM, Rossi S, Lyubarsky A, Arruda VR, Konkle B, Stone E, Sun J, Jacobs J, Dell'Osso L, Hertle R, Ma JX, Redmond TM, Zhu X, Hauck B,

Zelenaia O, Shindler KS, Maguire MG, Wright JF, Volpe NJ, McDonnell JW, Auricchio A, High KA, Bennett J 2008. Safety and efficacy of gene transfer for Leber's congenital amaurosis. N Engl J Med 358(21):2240-2248.

12. Hacein-Bey-Abina S, Fischer A, Cavazzana-Calvo M 2002. Gene therapy of X-linked severe combined immunodeficiency. Int J Hematol 76(4):295-298.

13. Hacein-Bey-Abina S, Hauer J, Lim A, Picard C, Wang GP, Berry CC, Martinache C, Rieux-Laucat F, Latour S, Belohradsky BH, Leiva L, Sorensen R, Debre M, Casanova JL, Blanche S, Durandy A, Bushman FD, Fischer A, Cavazzana-Calvo M 2010. Efficacy of gene therapy for X-linked severe combined immunodeficiency. N Engl J Med 363(4):355-364.

14. Teichler Zallen D 2000. US gene therapy in crisis. Trends Genet 16(6):272-275.

15. Renkawitz R, Beug H, Graf T, Matthias P, Grez M, Schutz G 1982. Expression of a chicken lysozyme recombinant gene is regulated by progesterone and dexamethasone after microinjection into oviduct cells. Cell 31(1):167-176.

16. Prayaga SK, Ford MJ, Haynes JR 1997. Manipulation of HIV-1 gp120-specific immune responses elicited via gene gun-based DNA immunization. Vaccine 15(12-13):1349-1352.

17. Horiki M, Yamato E, Noso S, Ikegami H, Ogihara T, Miyazaki J 2003. High-level expression of interleukin-4 following electroporation-mediated gene transfer accelerates Type 1 diabetes in NOD mice. J Autoimmun 20(2):111-117.

18. McConnell MJ, Imperiale MJ 2004. Biology of adenovirus and its use as a vector for gene therapy. Hum Gene Ther 15(11):1022-1033.

19. Miyazawa N, Leopold PL, Hackett NR, Ferris B, Worgall S, Falck-Pedersen E, Crystal RG 1999. Fiber swap between adenovirus subgroups B and C alters intracellular trafficking of adenovirus gene transfer vectors. J Virol 73(7):6056-6065.

20. Meier O, Greber UF 2004. Adenovirus endocytosis. J Gene Med 6 Suppl 1:S152-163.

21. Medina-Kauwe LK 2003. Endocytosis of adenovirus and adenovirus capsid proteins. Adv Drug Deliv Rev 55(11):1485-1496.

22. Thacker EE, Nakayama M, Smith BF, Bird RC, Muminova Z, Strong TV, Timares L, Korokhov N, O'Neill AM, de Gruijl TD, Glasgow JN, Tani K, Curiel DT 2009. A genetically engineered adenovirus vector targeted to CD40 mediates transduction of canine dendritic cells and promotes antigen-specific immune responses in vivo. Vaccine 27(50):7116-7124.

23. Liu Q, Muruve DA 2003. Molecular basis of the inflammatory response to adenovirus vectors. Gene Ther 10(11):935-940.

24. Shayakhmetov DM, Li ZY, Ni S, Lieber A 2004. Analysis of adenovirus sequestration in the liver, transduction of hepatic cells, and innate toxicity after injection of fiber-modified vectors. J Virol 78(10):5368-5381.

25. Farlow SJ, Jerusalmi A, Sano T 2007. Enhanced transduction of colonic cell lines in vitro and the inflamed colon in mice by viral vectors, derived from adeno-associated virus serotype 2, using virus-microbead conjugates bearing lectin. BMC Biotechnol 7:83.

26. Suter DM, Cartier L, Bettiol E, Tirefort D, Jaconi ME, Dubois-Dauphin M, Krause KH 2006. Rapid generation of stable transgenic embryonic stem cell lines using modular lentivectors. Stem Cells 24(3):615-623.

27. Ziske C, Nagaraj S, Marten A, Gorschluter M, Strehl J, Sauerbruch T, Abraham NG, Schmidt-Wolf IG 2004. Retroviral IFN-alpha gene transfer combined with gemcitabine acts synergistically via cell cycle alteration in human pancreatic carcinoma cells implanted orthotopically in nude mice. J Interferon Cytokine Res 24(8):490-496.

28. Gansbacher B 2003. Report of a second serious adverse event in a clinical trial of gene therapy for X-linked severe combined immune deficiency (X-SCID). Position of the European Society of Gene Therapy (ESGT). J Gene Med 5(3):261-262.

29. Lemarchand P, Jaffe HA, Danel C, Cid MC, Kleinman HK, Stratford-Perricaudet LD, Perricaudet M, Pavirani A, Lecocq JP, Crystal RG 1992. Adenovirus-mediated transfer of a recombinant human alpha 1-antitrypsin cDNA to human endothelial cells. Proc Natl Acad Sci U S A 89(14):6482-6486.

30. Ledley FD 1995. Nonviral gene therapy: the promise of genes as pharmaceutical products. Hum Gene Ther 6(9):1129-1144.

31. Lollo CP, Banaszczyk MG, Chiou HC 2000. Obstacles and advances in non-viral gene delivery. Curr Opin Mol Ther 2(2):136-142.

32. Felgner JH, Kumar R, Sridhar CN, Wheeler CJ, Tsai YJ, Border R, Ramsey P, Martin M, Felgner PL 1994. Enhanced gene delivery and mechanism studies with a novel series of cationic lipid formulations. J Biol Chem 269(4):2550-2561.

33. Simoes S, Pires P, da Cruz MT, Duzgunes N, de Lima MC 2003. Gene delivery by cationic liposome-DNA complexes containing transferrin or serum albumin. Methods Enzymol 373:369-383.

34. Schwartz B, Benoist C, Abdallah B, Scherman D, Behr JP, Demeneix BA 1995. Lipospermine-based gene transfer into the newborn mouse brain is optimized by a low lipospermine/DNA charge ratio. Hum Gene Ther 6(12):1515-1524.

35. Abdallah B, Hassan A, Benoist C, Goula D, Behr JP, Demeneix BA 1996. A powerful nonviral vector for in vivo gene transfer into the adult mammalian brain: polyethylenimine. Hum Gene Ther 7(16):1947-1954.

36. Tang MX, Redemann CT, Szoka FC, Jr. 1996. In vitro gene delivery by degraded polyamidoamine dendrimers. Bioconjug Chem 7(6):703-714.

37. Erbacher P, Zou S, Bettinger T, Steffan AM, Remy JS 1998. Chitosan-based vector/DNA complexes for gene delivery: biophysical characteristics and transfection ability. Pharm Res 15(9):1332-1339.

38. Holter W, Fordis CM, Howard BH 1989. Efficient gene transfer by sequential treatment of mammalian cells with DEAE-dextran and deoxyribonucleic acid. Exp Cell Res 184(2):546-551.

39. Midoux P, Mendes C, Legrand A, Raimond J, Mayer R, Monsigny M, Roche AC 1993. Specific gene transfer mediated by lactosylated poly-L-lysine into hepatoma cells. Nucleic Acids Res 21(4):871-878.

40. Emi N, Kidoaki S, Yoshikawa K, Saito H 1997. Gene transfer mediated by polyarginine requires a formation of big carrier-complex of DNA aggregate. Biochem Biophys Res Commun 231(2):421-424.

41. Ihm JE, Han KO, Han IK, Ahn KD, Han DK, Cho CS 2003. High transfection efficiency of poly(4-vinylimidazole) as a new gene carrier. Bioconjug Chem 14(4):707-708.

42. Tavares CR, Vieira M, Petrus JCC, Bortoletto EC, Ceravollo F 2002. Ultrafiltration/complexation process for metal removal from pulp and paper industry wastewater. Desalination 144(1-3):261-265.

43. Nguyen HK, Lemieux P, Vinogradov SV, Gebhart CL, Guerin N, Paradis G, Bronich TK, Alakhov VY, Kabanov AV 2000. Evaluation of polyether-polyethyleneimine graft copolymers as gene transfer agents. Gene Ther 7(2):126-138.

44. Densmore CL, Orson FM, Xu B, Kinsey BM, Waldrep JC, Hua P, Bhogal B, Knight V 2000. Aerosol delivery of robust polyethyleneimine-DNA complexes for gene therapy and genetic immunization. Mol Ther 1(2):180-188.

45. Gebhart CL, Sriadibhatla S, Vinogradov S, Lemieux P, Alakhov V, Kabanov AV 2002. Design and formulation of polyplexes based on pluronic-polyethyleneimine conjugates for gene transfer. Bioconjug Chem 13(5):937-944.

46. Banerjee P, Weissleder R, Bogdanov A, Jr. 2006. Linear polyethyleneimine grafted to a hyperbranched poly(ethylene glycol)-like core: a copolymer for gene delivery. Bioconjug Chem 17(1):125-131.

47. Ahn HH, Lee JH, Kim KS, Lee JY, Kim MS, Khang G, Lee IW, Lee HB 2008. Polyethyleneimine-mediated gene delivery into human adipose derived stem cells. Biomaterials 29(15):2415-2422.

48. Intra J, Salem AK 2008. Characterization of the transgene expression generated by branched and linear polyethylenimine-plasmid DNA nanoparticles in vitro and after intraperitoneal injection in vivo. J Control Release 130(2):129-138.

49. Wightman L, Kircheis R, Rossler V, Carotta S, Ruzicka R, Kursa M, Wagner E 2001. Different behavior of branched and linear polyethylenimine for gene delivery in vitro and in vivo. J Gene Med 3(4):362-372.

50. Godbey WT, Wu KK, Mikos AG 1999. Poly(ethylenimine) and its role in gene delivery. J Control Release 60(2-3):149-160.

51. Boussif O, Lezoualc'h F, Zanta MA, Mergny MD, Scherman D, Demeneix B, Behr JP 1995. A versatile vector for gene and oligonucleotide transfer into cells in culture and in vivo: polyethylenimine. Proc Natl Acad Sci U S A 92(16):7297-7301.

52. Boussif O, Zanta MA, Behr JP 1996. Optimized galenics improve in vitro gene transfer with cationic molecules up to 1000-fold. Gene Ther 3(12):1074-1080.

53. Ferrari S, Moro E, Pettenazzo A, Behr JP, Zacchello F, Scarpa M 1997. ExGen 500 is an efficient vector for gene delivery to lung epithelial cells in vitro and in vivo. Gene Ther 4(10):1100-1106.

54. Sonawane ND, Szoka FC, Jr., Verkman AS 2003. Chloride accumulation and swelling in endosomes enhances DNA transfer by polyamine-DNA polyplexes. J Biol Chem 278(45):44826-44831.

55. Moghimi SM, Symonds P, Murray JC, Hunter AC, Debska G, Szewczyk A 2005. A two-stage poly(ethylenimine)-mediated cytotoxicity: implications for gene transfer/therapy. Mol Ther 11(6):990-995.

56. Hunter AC 2006. Molecular hurdles in polyfectin design and mechanistic background to polycation induced cytotoxicity. Adv Drug Deliv Rev 58(14):1523-1531.

57. Fischer D, Bieber T, Li Y, Elsasser HP, Kissel T 1999. A novel non-viral vector for DNA delivery based on low molecular weight, branched polyethylenimine: effect of molecular weight on transfection efficiency and cytotoxicity. Pharm Res 16(8):1273-1279.

58. Fischer D, von Harpe A, Kunath K, Petersen H, Li Y, Kissel T 2002. Copolymers of ethylene imine and N-(2-hydroxyethyl)-ethylene imine as tools to study effects of polymer structure on physicochemical and biological properties of DNA complexes. Bioconjug Chem 13(5):1124-1133.

59. Godbey WT, Wu KK, Mikos AG 1999. Size matters: molecular weight affects the efficiency of poly(ethylenimine) as a gene delivery vehicle. J Biomed Mater Res 45(3):268-275.

60. Thomas M, Ge Q, Lu JJ, Chen J, Klibanov AM 2005. Cross-linked small polyethylenimines: while still nontoxic, deliver DNA efficiently to mammalian cells in vitro and in vivo. Pharm Res 22(3):373-380.

61. Forrest ML, Koerber JT, Pack DW 2003. A degradable polyethylenimine derivative with low toxicity for highly efficient gene delivery. Bioconjug Chem 14(5):934-940.

62. Petersen H, Fechner PM, Martin AL, Kunath K, Stolnik S, Roberts CJ, Fischer D, Davies MC, Kissel T 2002. Polyethylenimine-graft-poly(ethylene glycol) copolymers: influence of copolymer block structure on DNA complexation and biological activities as gene delivery system. Bioconjug Chem 13(4):845-854.

63. Guillem VM, Tormo M, Revert F, Benet I, Garcia-Conde J, Crespo A, Alino SF 2002. Polyethyleneimine-based immunopolyplex for targeted gene transfer in human lymphoma cell lines. J Gene Med 4(2):170-182.

64. Ouji Y, Yoshida-Terakura A, Hayashi Y, Maeda I, Kawase M, Yamato E, Miyazaki J, Yagi K 2002. Polyethyleneimine/chitosan hexamer-mediated gene transfection into intestinal epithelial cell cultured in serum-containing medium. J Biosci Bioeng 94(1):81-83.

65. Strehblow C, Schuster M, Moritz T, Kirch HC, Opalka B, Petri JB 2005. Monoclonal antibody-polyethyleneimine conjugates targeting Her-2/neu or CD90 allow cell type-specific nonviral gene delivery. J Control Release 102(3):737-747.

66. Kakimoto S, Moriyama T, Tanabe T, Shinkai S, Nagasaki T 2007. Dual-ligand effect of transferrin and transforming growth factor alpha on polyethyleneimine-mediated gene delivery. J Control Release 120(3):242-249.

67. Bromberg L, Raduyk S, Hatton TA, Concheiro A, Rodriguez-Valencia C, Silva M, Alvarez-Lorenzo C 2009. Guanidinylated polyethyleneimine-polyoxypropylene-polyoxyethylene conjugates as gene transfection agents. Bioconjug Chem 20(5):1044-1053.

68. Guo Q, Shi S, Wang X, Kan B, Gu Y, Shi X, Luo F, Zhao X, Wei Y, Qian Z 2009. Synthesis of a novel biodegradable poly(ester amine) (PEAs) copolymer based on low-molecular-weight polyethyleneimine for gene delivery. Int J Pharm 379(1):82-89.

69. Kircheis R, Kichler A, Wallner G, Kursa M, Ogris M, Felzmann T, Buchberger M, Wagner E 1997. Coupling of cell-binding ligands to polyethylenimine for targeted gene delivery. Gene Ther 4(5):409-418.

70. Guo W, Lee RL 1999. Receptor-targeted gene delivery via folate-conjugated polyethylenimine. AAPS PharmSci 1(4):E19.

71. Sagara K, Kim SW 2002. A new synthesis of galactose-poly(ethylene glycol)-polyethylenimine for gene delivery to hepatocytes. J Control Release 79(1-3):271-281.

72. Intra J, Salem AK Rational design, fabrication, characterization and in vitro testing of biodegradable microparticles that generate targeted and sustained transgene expression in HepG2 liver cells. J Drug Target 19(6):393-408.

73. Wolschek MF, Thallinger C, Kursa M, Rossler V, Allen M, Lichtenberger C, Kircheis R, Lucas T, Willheim M, Reinisch W, Gangl A, Wagner E, Jansen B 2002. Specific systemic nonviral gene delivery to human hepatocellular carcinoma xenografts in SCID mice. Hepatology 36(5):1106-1114.

74. Kunath K, Merdan T, Hegener O, Haberlein H, Kissel T 2003. Integrin targeting using RGD-PEI conjugates for in vitro gene transfer. J Gene Med 5(7):588-599.

75. Fire A, Xu S, Montgomery MK, Kostas SA, Driver SE, Mello CC 1998. Potent and specific genetic interference by double-stranded RNA in Caenorhabditis elegans. Nature 391(6669):806-811.

76. Bernstein E, Caudy AA, Hammond SM, Hannon GJ 2001. Role for a bidentate ribonuclease in the initiation step of RNA interference. Nature 409(6818):363-366.

77. Macrae IJ, Zhou K, Li F, Repic A, Brooks AN, Cande WZ, Adams PD, Doudna JA 2006. Structural basis for double-stranded RNA processing by Dicer. Science 311(5758):195-198.

78. Hammond SM, Boettcher S, Caudy AA, Kobayashi R, Hannon GJ 2001. Argonaute2, a link between genetic and biochemical analyses of RNAi. Science 293(5532):1146-1150.

79. Wright CL, Alder-Moore JP 1985. The adjuvant effects of mycoviral dsRNA and polyinosinic:polycytidylic acid on the murine immune response. Biochem Biophys Res Commun 131(2):949-955.

80. Karpala AJ, Doran TJ, Bean AG 2005. Immune responses to dsRNA: implications for gene silencing technologies. Immunol Cell Biol 83(3):211-216.

81. Schomber T, Kalberer CP, Wodnar-Filipowicz A, Skoda RC 2004. Gene silencing by lentivirus-mediated delivery of siRNA in human CD34+ cells. Blood 103(12):4511-4513.

82. Hui EK, Yap EM, An DS, Chen IS, Nayak DP 2004. Inhibition of influenza virus matrix (M1) protein expression and virus replication by U6 promoter-driven and lentivirus-mediated delivery of siRNA. J Gen Virol 85(Pt 7):1877-1884.

83. Schiffelers RM, Ansari A, Xu J, Zhou Q, Tang Q, Storm G, Molema G, Lu PY, Scaria PV, Woodle MC 2004. Cancer siRNA therapy by tumor selective delivery with ligand-targeted sterically stabilized nanoparticle. Nucleic Acids Res 32(19):e149.

84. Kang H, DeLong R, Fisher MH, Juliano RL 2005. Tat-conjugated PAMAM dendrimers as delivery agents for antisense and siRNA oligonucleotides. Pharm Res 22(12):2099-2106.

85. Landen CN, Merritt WM, Mangala LS, Sanguino AM, Bucana C, Lu C, Lin YG, Han LY, Kamat AA, Schmandt R, Coleman RL, Gershenson DM, Lopez-Berestein G, Sood AK 2006. Intraperitoneal delivery of liposomal siRNA for therapy of advanced ovarian cancer. Cancer Biol Ther 5(12):1708-1713.

86. Yuan X, Li L, Rathinavelu A, Hao J, Narasimhan M, He M, Heitlage V, Tam L, Viqar S, Salehi M 2006. SiRNA drug delivery by biodegradable polymeric nanoparticles. J Nanosci Nanotechnol 6(9-10):2821-2828.

87. Haensler J, Szoka FC, Jr. 1993. Polyamidoamine cascade polymers mediate efficient transfection of cells in culture. Bioconjug Chem 4(5):372-379.

88. Qin L, Pahud DR, Ding Y, Bielinska AU, Kukowska-Latallo JF, Baker JR, Jr., Bromberg JS 1998. Efficient transfer of genes into murine cardiac grafts by Starburst polyamidoamine dendrimers. Hum Gene Ther 9(4):553-560.

89. Bielinska AU, Chen C, Johnson J, Baker JR, Jr. 1999. DNA complexing with polyamidoamine dendrimers: implications for transfection. Bioconjug Chem 10(5):843-850.

90. Wang Y, Kong W, Song Y, Duan Y, Wang L, Steinhoff G, Kong D, Yu Y 2009. Polyamidoamine dendrimers with a modified Pentaerythritol core having high efficiency and low cytotoxicity as gene carriers. Biomacromolecules 10(3):617-622.

91. Rudolph C, Lausier J, Naundorf S, Muller RH, Rosenecker J 2000. In vivo gene delivery to the lung using polyethylenimine and fractured polyamidoamine dendrimers. J Gene Med 2(4):269-278.

92. Gebhart CL, Kabanov AV 2001. Evaluation of polyplexes as gene transfer agents. J Control Release 73(2-3):401-416.

93. Tomalia DA, Reyna LA, Svenson S 2007. Dendrimers as multi-purpose nanodevices for oncology drug delivery and diagnostic imaging. Biochemical Society transactions 35(Pt 1):61-67.

94. Eichman JD, Bielinska AU, Kukowska-Latallo JF, Baker JR, Jr. 2000. The use of PAMAM dendrimers in the efficient transfer of genetic material into cells. Pharmaceutical science & technology today 3(7):232-245.

95. Choi JS, Nam K, Park JY, Kim JB, Lee JK, Park JS 2004. Enhanced transfection efficiency of PAMAM dendrimer by surface modification with L-arginine. J Control Release 99(3):445-456.

96. Kim TI, Seo HJ, Choi JS, Jang HS, Baek JU, Kim K, Park JS 2004. PAMAM-PEG-PAMAM: novel triblock copolymer as a biocompatible and efficient gene delivery carrier. Biomacromolecules 5(6):2487-2492.

97. Nam HY, Hahn HJ, Nam K, Choi WH, Jeong Y, Kim DE, Park JS 2008. Evaluation of generations 2, 3 and 4 arginine modified PAMAM dendrimers for gene delivery. Int J Pharm 363(1-2):199-205.

98. Liu XX, Rocchi P, Qu FQ, Zheng SQ, Liang ZC, Gleave M, Iovanna J, Peng L 2009. PAMAM dendrimers mediate siRNA delivery to target Hsp27 and produce potent antiproliferative effects on prostate cancer cells. ChemMedChem 4(8):1302-1310.

99. Perez AP, Romero EL, Morilla MJ 2009. Ethylendiamine core PAMAM dendrimers/siRNA complexes as in vitro silencing agents. Int J Pharm 380(1-2):189-200.

100. Waite CL, Roth CM 2009. PAMAM-RGD conjugates enhance siRNA delivery through a multicellular spheroid model of malignant glioma. Bioconjug Chem 20(10):1908-1916.

101. Devarakonda B, Hill RA, de Villiers MM 2004. The effect of PAMAM dendrimer generation size and surface functional group on the aqueous solubility of nifedipine. Int J Pharm 284(1-2):133-140.

102. Devarakonda B, Hill RA, Liebenberg W, Brits M, de Villiers MM 2005. Comparison of the aqueous solubilization of practically insoluble niclosamide by polyamidoamine (PAMAM) dendrimers and cyclodextrins. Int J Pharm 304(1-2):193-209.

103. Ma M, Cheng Y, Xu Z, Xu P, Qu H, Fang Y, Xu T, Wen L 2007. Evaluation of polyamidoamine (PAMAM) dendrimers as drug carriers of anti-bacterial drugs using sulfamethoxazole (SMZ) as a model drug. Eur J Med Chem 42(1):93-98.

104. Takeda K, Akira S 2001. Roles of Toll-like receptors in innate immune responses. Genes Cells 6(9):733-742.

105. Lien E, Ingalls RR 2002. Toll-like receptors. Critical care medicine 30(1 Suppl):S1-11.

106. Ashkar AA, Rosenthal KL 2002. Toll-like receptor 9, CpG DNA and innate immunity. Current molecular medicine 2(6):545-556.

107. Chuang TH, Lee J, Kline L, Mathison JC, Ulevitch RJ 2002. Toll-like receptor 9 mediates CpG-DNA signaling. Journal of leukocyte biology 71(3):538-544.

108. Vollmer J, Weeratna R, Payette P, Jurk M, Schetter C, Laucht M, Wader T, Tluk S, Liu M, Davis HL, Krieg AM 2004. Characterization of three CpG oligodeoxynucleotide classes with distinct immunostimulatory activities. Eur J Immunol 34(1):251-262.

109. Leifer CA, Kennedy MN, Mazzoni A, Lee C, Kruhlak MJ, Segal DM 2004. TLR9 is localized in the endoplasmic reticulum prior to stimulation. J Immunol 173(2):1179-1183.

110. Li WM, Bally MB, Schutze-Redelmeier MP 2001. Enhanced immune response to T-independent antigen by using CpG oligodeoxynucleotides encapsulated in liposomes. Vaccine 20(1-2):148-157.

111. Diwan M, Tafaghodi M, Samuel J 2002. Enhancement of immune responses by co-delivery of a CpG oligodeoxynucleotide and tetanus toxoid in biodegradable nanospheres. J Control Release 85(1-3):247-262.

112. Shi R, Hong L, Wu D, Ning X, Chen Y, Lin T, Fan D, Wu K 2005. Enhanced immune response to gastric cancer specific antigen Peptide by coencapsulation with CpG oligodeoxynucleotides in nanoemulsion. Cancer Biol Ther 4(2):218-224.

113. Kwon YJ, Standley SM, Goh SL, Frechet JM 2005. Enhanced antigen presentation and immunostimulation of dendritic cells using acid-degradable cationic nanoparticles. J Control Release 105(3):199-212.

114. Zhang XQ, Dahle CE, Baman NK, Rich N, Weiner GJ, Salem AK 2007. Potent antigen-specific immune responses stimulated by codelivery of CpG ODN and antigens in degradable microparticles. J Immunother 30(5):469-478.

115. Zhang XQ, Dahle CE, Weiner GJ, Salem AK 2007. A comparative study of the antigen-specific immune response induced by co-delivery of CpG ODN and antigen using fusion molecules or biodegradable microparticles. J Pharm Sci 96(12):3283-3292.

116. Bozza S, Gaziano R, Lipford GB, Montagnoli C, Bacci A, Di Francesco P, Kurup VP, Wagner H, Romani L 2002. Vaccination of mice against invasive aspergillosis with recombinant Aspergillus proteins and CpG oligodeoxynucleotides as adjuvants. Microbes and infection / Institut Pasteur 4(13):1281-1290.

117. Verthelyi D, Wang VW, Lifson JD, Klinman DM 2004. CpG oligodeoxynucleotides improve the response to hepatitis B immunization in healthy and SIV-infected rhesus macaques. Aids 18(7):1003-1008.

118. Myatt EA, Scarpa I 1992. Effects of Polyethyleneimine Derivatives on 2-Hydroxy-5-Nitrobenzyl Ionization. J Macromol Sci Pure 29(2):153-160.

119. Lee RJ, Wang S, Turk MJ, Low PS 1998. The effects of pH and intraliposomal buffer strength on the rate of liposome content release and intracellular drug delivery. Biosci Rep 18(2):69-78.

120. Lenter MC, Garidel P, Pelisek J, Wagner E, Ogris M 2004. Stabilized nonviral formulations for the delivery of MCP-1 gene into cells of the vasculoendothelial system. Pharm Res 21(4):683-691.

121. Woodle MC, Scaria P, Ganesh S, Subramanian K, Titmas R, Cheng C, Yang J, Pan Y, Weng K, Gu C, Torkelson S 2001. Sterically stabilized polyplex: ligand-mediated activity. J Control Release 74(1-3):309-311.

122. Ogris M, Brunner S, Schuller S, Kircheis R, Wagner E 1999. PEGylated DNA/transferrin-PEI complexes: reduced interaction with blood components, extended circulation in blood and potential for systemic gene delivery. Gene Ther 6(4):595-605.

123. Owens DE, 3rd, Peppas NA 2006. Opsonization, biodistribution, and pharmacokinetics of polymeric nanoparticles. Int J Pharm 307(1):93-102.

124. Diebold SS, Kursa M, Wagner E, Cotten M, Zenke M 1999. Mannose polyethylenimine conjugates for targeted DNA delivery into dendritic cells. J Biol Chem 274(27):19087-19094.

125. Diebold SS, Plank C, Cotten M, Wagner E, Zenke M 2002. Mannose receptor-mediated gene delivery into antigen presenting dendritic cells. Somat Cell Mol Genet 27(1-6):65-74.

126. Monsigny M, Petit C, Roche AC 1988. Colorimetric determination of neutral sugars by a resorcinol sulfuric acid micromethod. Anal Biochem 175(2):525-530.

127. Brus C, Petersen H, Aigner A, Czubayko F, Kissel T 2004. Physicochemical and biological characterization of polyethylenimine-graft-poly(ethylene glycol) block copolymers as a delivery system for oligonucleotides and ribozymes. Bioconjug Chem 15(4):677-684.

128. Larsen C 1989. Dextran prodrugs -- structure and stability in relation to therapeutic activity. Adv Drug Deliv Rev 3(1):103-154.

129. Rosenfeld EL, Lukomskaya IS 1957. The splitting of dextran and isomaltose by animal tissues. Clin Chim Acta 2(2):105-114.

130. Arturson G, Granath K, Grotte G 1966. Intravascular persistence and renal clearance of dextran of different molecular sizes in normal children. Arch Dis Child 41(216):168-171.

131. Arturson G, Wallenius G 1964. The Intravascular Persistence of Dextran of Different Molecular Sizes in Normal Humans. Scandinavian journal of clinical and laboratory investigation 16:76-80.

132. Chang RL, Ueki IF, Troy JL, Deen WM, Robertson CR, Brenner BM 1975. Permselectivity of the glomerular capillary wall to macromolecules. II. Experimental studies in rats using neutral dextran. Biophys J 15(9):887-906.

133. Mehvar R, Robinson MA, Reynolds JM 1994. Molecular weight dependent tissue accumulation of dextrans: in vivo studies in rats. J Pharm Sci 83(10):1495-1499.

134. Arturson G, Granath K 1972. Dextrans as test molecules in studies of the functional ultrastrucutre of biological membranes. Molecular weight distribution analysis by gel chromatography. Clin Chim Acta 37:309-322.

135. Vercauteren R, Bruneel D, Schacht E, Duncan R 1990. Effect of the Chemical Modification of Dextran on the Degradation by Dextranase. J Bioact Compat Polym 5(1):4-15.

136. Vercauteren R, Schacht E, Duncan R 1992. Effect of the Chemical Modification of Dextran on the Degradation by Rat Liver Lysosomal Enzymes. J Bioact Compat Polym 7(4):346-357.

137. Lopata MA, Cleveland DW, Sollner-Webb B 1984. High level transient expression of a chloramphenicol acetyl transferase gene by DEAE-dextran mediated DNA transfection coupled with a dimethyl sulfoxide or glycerol shock treatment. Nucleic Acids Res 12(14):5707-5717.

138. Golub EI, Kim H, Volsky DJ 1989. Transfection of DNA into adherent cells by DEAE-dextran/DMSO method increases drastically if the cells are removed from surface and treated in suspension. Nucleic Acids Res 17(12):4902.

139. Takai T, Ohmori H 1990. DNA transfection of mouse lymphoid cells by the combination of DEAE-dextran-mediated DNA uptake and osmotic shock procedure. Biochim Biophys Acta 1048(1):105-109.

140. Azzam T, Eliyahu H, Shapira L, Linial M, Barenholz Y, Domb AJ 2002. Polysaccharide-oligoamine based conjugates for gene delivery. Journal of medicinal chemistry 45(9):1817-1824.

141. Azzam T, Eliyahu H, Makovitzki A, Linial M, Domb AJ 2004. Hydrophobized dextran-spermine conjugate as potential vector for in vitro gene transfection. J Control Release 96(2):309-323.

142. Eliyahu H, Joseph A, Azzam T, Barenholz Y, Domb AJ 2006. Dextran-spermine-based polyplexes--evaluation of transgene expression and of local and systemic toxicity in mice. Biomaterials 27(8):1636-1645.

143. Sun YX, Zhang XZ, Cheng H, Cheng SX, Zhuo RX 2008. A low-toxic and efficient gene vector: carboxymethyl dextran-graft-polyethylenimine. J Biomed Mater Res A 84(4):1102-1110.

144. Tseng WC, Tang CH, Fang TY 2004. The role of dextran conjugation in transfection mediated by dextran-grafted polyethylenimine. J Gene Med 6(8):895-905.

145. Tseng WC, Fang TY, Su LY, Tang CH 2005. Dependence of transgene expression and the relative buffering capacity of dextran-grafted polyethylenimine. Mol Pharm 2(3):224-232.

146. Sun YX, Xiao W, Cheng SX, Zhang XZ, Zhuo RX 2008. Synthesis of (Dex-HMDI)-g-PEIs as effective and low cytotoxic nonviral gene vectors. J Control Release 128(2):171-178.

147. Zhang XQ, Intra J, Salem AK 2007. Conjugation of polyamidoamine dendrimers on biodegradable microparticles for nonviral gene delivery. Bioconjug Chem 18(6):2068-2076.

148. Zhang XQ, Intra J, Salem AK 2008. Comparative study of poly (lactic-co-glycolic acid)-poly ethyleneimine-plasmid DNA microparticles prepared using double emulsion methods. Journal of microencapsulation 25(1):1-12.

149. Sivori S, Falco M, Della Chiesa M, Carlomagno S, Vitale M, Moretta L, Moretta A 2004. CpG and double-stranded RNA trigger human NK cells by Toll-like receptors: induction of cytokine release and cytotoxicity against tumors and dendritic cells. Proc Natl Acad Sci U S A 101(27):10116-10121.

150. Latz E, Schoenemeyer A, Visintin A, Fitzgerald KA, Monks BG, Knetter CF, Lien E, Nilsen NJ, Espevik T, Golenbock DT 2004. TLR9 signals after translocating from the ER to CpG DNA in the lysosome. Nat Immunol 5(2):190-198.

151. Iwasaki A, Medzhitov R 2004. Toll-like receptor control of the adaptive immune responses. Nat Immunol 5(10):987-995.

152. Lutz MB, Kukutsch N, Ogilvie AL, Rossner S, Koch F, Romani N, Schuler G 1999. An advanced culture method for generating large quantities of highly pure dendritic cells from mouse bone marrow. J Immunol Methods 223(1):77-92.